

AD-A098 567

NAVAL POSTGRADUATE SCHOOL MONTEREY CA
OPTIMIZATION OF A LOW DELTA T RANKINE POWER SYSTEM.(U)
DEC 80 R C SCHAUBEL

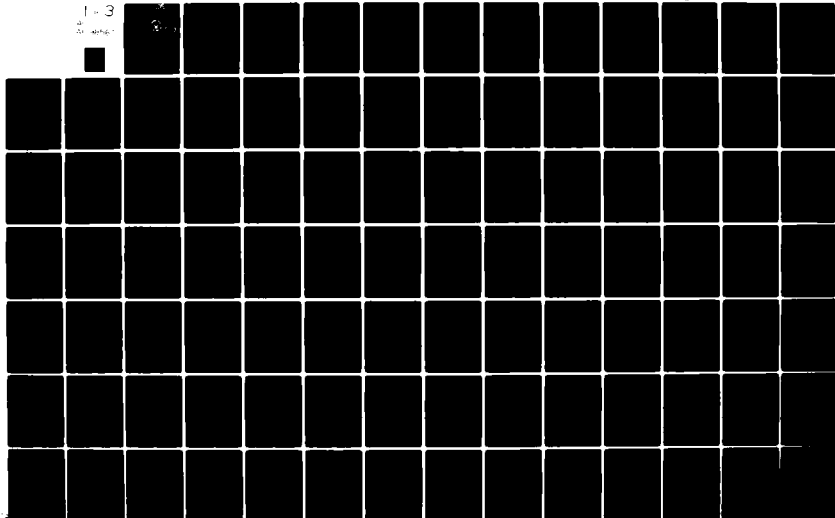
F/G 20/13

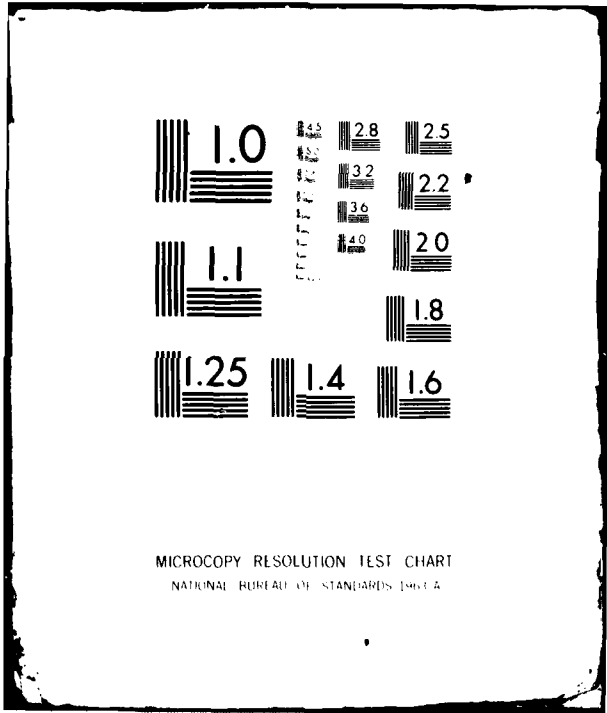
UNCLASSIFIED

1-3

20-1000-1

NL





MICROCOPY RESOLUTION TEST CHART
NATIONAL BUREAU OF STANDARDS-1963-A

LEVEL II

2

BS

**NAVAL POSTGRADUATE SCHOOL
Monterey, California**

AD A 098 567



**DTIC
ELECTE
MAY 06 1981**
S D
E

THESIS

OPTIMIZATION OF A LOW ΔT RANKINE
POWER SYSTEM

by

Raymond C. Schaubel

December 1980

Thesis Advisor:

R. H. Nunn

Approved for public release; distribution unlimited.

DTIC FILE COPY

81 5 04 148

REPORT DOCUMENTATION PAGE		READ INSTRUCTIONS BEFORE COMPLETING FORM
1. REPORT NUMBER	2. GOVT ACCESSION NO.	3. RECIPIENT'S CATALOG NUMBER
	AD-A098567	9
4. TITLE (and Subtitle)	5. TYPE OF REPORT & PERIOD COVERED	
Optimization of a Low AT Rankine Power System.	Master's Thesis, December 1980	
	6. PERFORMING ORG. REPORT NUMBER	
7. AUTHOR(s)	8. CONTRACT OR GRANT NUMBER(s)	
Raymond C. Schaubel	12/236	
9. PERFORMING ORGANIZATION NAME AND ADDRESS		10. PROGRAM ELEMENT, PROJECT, TASK AREA & WORK UNIT NUMBERS
Naval Postgraduate School Monterey, California 93940		
11. CONTROLLING OFFICE NAME AND ADDRESS		12. REPORT DATE
Naval Postgraduate School Monterey, California 93940		11/December 1980
13. MONITORING AGENCY NAME & ADDRESS (if different from Controlling Office)		13. NUMBER OF PAGES
Naval Postgraduate School Monterey, California 93940		235
		15. SECURITY CLASS. (of this report)
		Unclassified
		15a. DECLASSIFICATION/DOWNGRADING SCHEDULE
16. DISTRIBUTION STATEMENT (of this Report)		
Approved for public release; distribution unlimited.		
17. DISTRIBUTION STATEMENT (of the abstract entered in Block 20, if different from Report)		
18. SUPPLEMENTARY NOTES		
19. KEY WORDS (Continue on reverse side if necessary and identify by block number)		
OTEC Rankine COPES/CONMIN		
20. ABSTRACT (Continue on reverse side if necessary and identify by block number)		
The Ocean Thermal Energy Conversion (OTEC) uses the low thermal energy potential available from ocean temperature gradients. A method is presented to analyze such systems and, for this purpose, a comprehensive simulation is developed. The simulation includes parasitic power requirements, losses due to interconnecting lines, and heat exchanger pressure drops. Cost functions are included and numerical optimization is employed to obtain optimal designs based upon minimum cost.		

DD FORM 1473
1 JAN 73

EDITION OF 1 NOV 65 IS OBSOLETE
S/N 0102-014-6001

BLOCK 20. ABSTRACT (Continued)

The analysis is converted to a computer code and coupled to the COPES/CONMIN optimization code to facilitate a fully-automated design where the computer makes the design decisions and performance trade-off studies. The final product is an optimum power system module design for the designated net electrical output required and the specified system and design constraints.

Preliminary results are presented for a range of system power levels. Optimum designs are obtained and compared for systems in which either titanium or aluminum tubes are used in the heat exchangers.

Accession For	
NTIS GRA&I	<input checked="" type="checkbox"/>
DTIC TAB	<input type="checkbox"/>
Unannounced	<input type="checkbox"/>
Justification	
By	
Distribution/	
Availability Codes	
Dist	Avail and/or
	Special
A	

Approved for public release; distribution unlimited.

Optimization of a Low ΔT Rankine
Power System

by

Raymond C. Schaubel
Lieutenant Commander, United States Navy
B.S., United States Naval Academy

Submitted in partial fulfillment of the
requirements for the degree of

MASTER OF SCIENCE IN MECHANICAL ENGINEERING

from the

NAVAL POSTGRADUATE SCHOOL
December 1980

Author

Raymond C. Schaubel

Approved by:

R. A. Merritt

Thesis Advisor

A. J. Underplotts

Co-Advisor

P. J. Marts

Chairman, Department of Mechanical Engineering

William M. Talley

Dean of Science and Engineering

ABSTRACT

The Ocean Thermal Energy Conversion (OTEC) uses the low thermal energy potential available from ocean temperature gradients. A method is presented to analyze such systems and, for this purpose, a comprehensive simulation is developed. The simulation includes parasitic power requirements, losses due to interconnecting lines, and heat exchanger pressure drops. Cost functions are included and numerical optimization is employed to obtain optimal designs based upon minimum cost. The analysis is converted to a computer code and coupled to the COPES/CONMIN optimization code to facilitate a fully-automated design where the computer makes the design decisions and performance trade-off studies. The final product is an optimum power system module design for the designated net electrical output required and the specified system and design constraints.

Preliminary results are presented for a range of system power levels. Optimum designs are obtained and compared for systems in which either titanium or aluminum tubes are used in the heat exchangers.

TABLE OF CONTENTS

I. INTRODUCTION- - - - - 11
A. BACKGROUND- - - - - 11
B. OBJECTIVES- - - - - 13
C. OVERVIEW OF THE OTEC POWER SYSTEM
ANALYSIS- - - - - 14
II. POWER CYCLE DESCRIPTIONS- - - - - 17
A. INTRODUCTION- - - - - 17
B. IDEAL OTEC RANKINE CYCLE- - - - - 17
C. ACTUAL OTEC RANKINE CYCLE - - - - - 19
III. EVAPORATOR AND MOISTURE SEPARATOR - - - - - 22
A. INTRODUCTION- - - - - 22
B. ANALYSIS OF THE EVAPORATOR AND
MOISTURE SEPARATOR- - - - - 24
IV. PARASITIC LOSSES- - - - - 62
A. INTRODUCTION- - - - - 62
B. ANALYSIS OF PARASITIC LOSSES- - - - - 65
V. TURBINE AND ELECTRICAL POWER- - - - - 87
A. INTRODUCTION- - - - - 87
B. ANALYSIS OF THE TURBINE AND ELECTRICAL
POWER REQUIREMENTS- - - - - 89
VI. CONDENSER - - - - - 93
A. INTRODUCTION- - - - - 93
B. ANALYSIS OF THE CONDENSER - - - - - 94
VII. NUMERICAL OPTIMIZATION- - - - - 117
A. INTRODUCTION- - - - - 117

B.	COPEs/CONMIN-	- - - - -	-118
C.	DESIGNATED DESIGN VARIABLES, CONSTRAINTS AND OBJECTIVE FUNCTION-	- - - - -	-122
VIII.	CONCLUSIONS AND RECOMMENDATIONS	- - - - -	-124
A.	CONCLUSIONS	- - - - -	-124
B.	RECOMMENDATIONS	- - - - -	-126
TABLES	- - - - -	- - - - -	-128
APPENDIX A:	SAMPLE INPUT DATA FOR OTEC ANALYSIS	- - - - -	-150
APPENDIX B:	SAMPLE OTEC ANALYSIS OPTIMIZATION OUTPUT DATA	- - - - -	-152
APPENDIX C:	SAMPLE COPEs OPTIMIZATION AND SENSITIVITY ANALYSIS DATA	- - - - -	-157
NOMENCLATURE AND OTEC ANALYSIS CODE-	- - - - -	- - - - -	-160
LIST OF REFERENCES	- - - - -	- - - - -	-231
INITIAL DISTRIBUTION LIST-	- - - - -	- - - - -	-233

LIST OF FIGURES

1. Power System Sequential Analysis - - - - -	16
2. Idealized OTEC Rankine Cycle - - - - -	18
3. Actual OTEC Rankine Cycle- - - - -	20

LIST OF TABLES

1. OTEC Power System Comparison (Titanium Tubed Heat Exchangers) - - - - -128
2. OTEC Power System Comparison (Aluminum Tubed Heat Exchangers) - - - - -134
3. OTEC Heat Exchanger Comparisons (Titanium Tubed) - -140
4. OTEC Heat Exchanger Comparisons (Aluminum Tubed) - -145

PARTIAL LIST OF SYMBOLS

A	heat transfer surface area
A_f	tube bundle frontal area
A_{ff}	free-flow area
C_p	constant pressure specific heat
d	diameter
\dot{E}	power
f	friction factor
F	correction to LMTD
G	mass velocity
g	acceleration of gravity
g_c	conversion factor ($32.2 \text{ lb}_m \cdot \text{ft} / \text{lb}_f \cdot \text{sec}^2$)
h	specific state point enthalpy
\bar{h}	average heat transfer coefficient
K	thermal conductivity
K_m	mean salt water compressibility
L	tube or pipe length
\dot{m}	mass flow rate number
N_t	number of heat exchange tubes
Re	Reynolds number
P	static pressure
\dot{Q}	heat transfer rate
S	specific state point entropy
T	temperature
LMTD	log mean temperature difference

U	overall heat transfer coefficient
v	specific volume
V	velocity
X	quality of working fluid
Z	elevation
ϵ	heat exchange effectiveness
η	efficiency
ρ	density
μ	absolute or dynamic viscosity

I. INTRODUCTION

A. BACKGROUND

Ocean Thermal Energy Conversion (OTEC) is a concept using the low thermal energy potential available from the ocean temperature gradient that exists between warm surface ocean water and cold water in deep ocean regions.

The idea of converting the stored ocean energy to useful power originated with French physicist Jacques d'Arsonval in 1881 [Ref. 1]. It was nearly a half-century later that the technical feasibility of ocean thermal energy conversion could be demonstrated. In 1926, George Claude used an open cycle power system to extract heat from surface water for indirect conversion of the thermal energy of a working fluid. Operating at a low pressure the working fluid was used to drive a turbine providing electrical power generation.

Though Claude's limited power system produced only 22 kilowatts of electricity while requiring approximately 80 kilowatts of power to drive its equipment, it stirred the scientific and research community to consider the attractiveness of ocean thermal energy conversion [Ref. 2].

Claude called for immediate action on his ocean thermal power system, because of the Federal Oil Conservation Board's dire predictions that the United States had only six years of oil production remaining. Obviously the dire predictions ascribed to by the Federal Oil Conservation Board did not

come true, but the oil crisis of that period heightened scientific interest in extracting energy from the ocean.

Now, 55 years later, the United States is faced with an energy crisis because of increasing industrial and social dependence on foreign petroleum. Dwindling supplies and erratic price hikes have rekindled interest in ocean thermal energy conversion, since it utilizes an inexhaustible supply of fuel.

Currently, the United States Department of Energy is attempting to develop the necessary technology and demonstrate the feasibility of large-scale OTEC power systems. However, there are major engineering development problems which must be solved before OTEC can be standardized and become a viable source of electrical power generation.

The single controlling factor which creates troublesome technical encounters is low thermal power system efficiency (one to four percent depending upon parasitic power requirements). Because the heat energy used by OTEC must be extracted from a small ocean temperature difference, extremely large volumes of surface water must pass through a proportionately sized evaporator to provide sufficient indirect heat energy to convert the working fluid into vapor to drive a turbine-generator for electrical power generation. Concurrently, to convert the turbine exhaust to a saturated liquid, completing the closed cycle, a condenser having compatible heat absorption capacity must be employed.

Economic handling of the volume of fluids required for the heat absorption, expansion, and heat rejection phases of the cycle requires close scrutiny of evaporator, turbine, condenser, and pump design to minimize the parasitic losses with respect to the generated electrical output. Because of the low thermal efficiency, relative to nuclear or fossil fuel-fired power plants, the margins for design and operating error in OTEC plants will be narrow.

With the advent of high-speed computers, numerical methods for solving these complex engineering problems with multiple design variables and constraints are now possible. The case for utilizing an optimizing scheme for not just one system component, but rather the complete power generation cycle, can easily be made. In effect, it would serve as a systems analysis tool, to optimize component design and cost, relative to a specific electrical output or to enable comparison and evaluation of competing OTEC designs.

B. OBJECTIVES

The objectives of this work are to develop a computer code for the Ocean Thermal Energy Conversion (OTEC) power system and to couple the analysis to a numerical optimization code to provide an optimum system design capability, considering both performance and economics.

This would create an optimum modular design relative to a specified objective function for a desired net electrical output, such as a 25 MW (net) power system. Such a design

would permit construction of higher capacity power systems using the optimized modules as substations of the total power plant. Cost savings, improved plant performance, redundancy, and reliability could be the immediate beneficiaries of such a venture.

C. OVERVIEW OF THE OTEC POWER SYSTEM ANALYSIS

To analyze the closed-cycle OTEC power system, the fundamental relationships of heat transfer, fluid mechanics and thermodynamics are used to simulate a variety of system component designs, which form the basis of the power system algorithm. The scope of this analysis will be limited to the OTEC power system and sea water systems only. Mooring systems, power delivery, hull, and cold pipe design will not be addressed.

The performance analysis will be divided into four sequential sections as shown in Figure 1, and discussed in detail in subsequent chapters of this thesis.

Input parameters (design constants) for the power cycle analysis will include:

- . Required net electrical output.
- . Salt water inlet temperature to the evaporator and condenser.
- . Length of hot and cold salt water pipes.
- . Heat exchanger tubing material (aluminum or titanium).
- . Heat exchanger tube orientation and profile.
- . Pump mechanical and motor efficiencies.

- . Turbine mechanical efficiency.
- . Generator mechanical and electrical efficiency.
- . Biofouling control factor.
- . Piping absolute roughness.
- . Projected annual inflation rate for aluminum heat exchanger retubing.

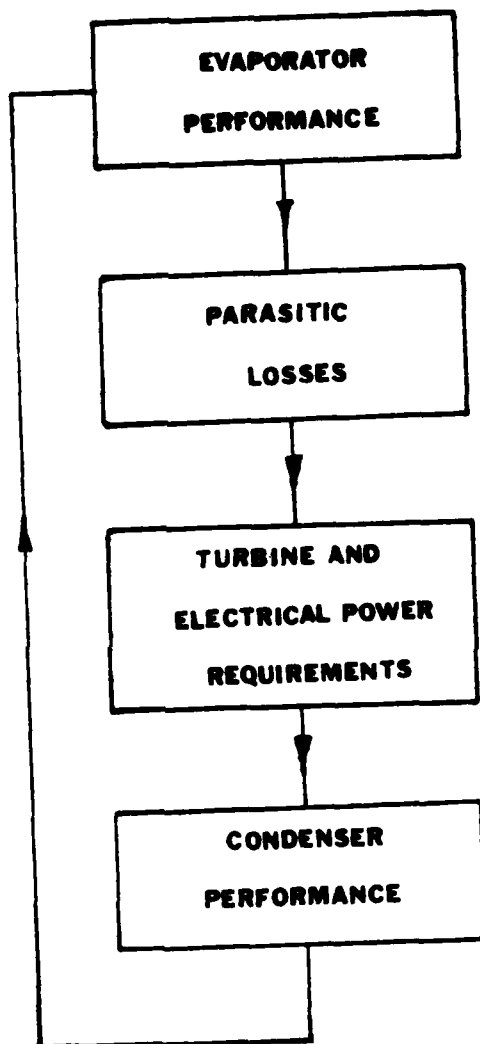


Figure 1. Power System Sequential Analysis

II. POWER CYCLE DESCRIPTIONS

A. INTRODUCTION

This chapter will provide a brief description of the OTEC power system. First, looking at the ideal Rankine cycle, the fundamental thermodynamic concepts will be enumerated. Then the deviations from the ideal cycle will be presented, creating the configuration assumed for the present cycle analysis which will be amplified in detail by follow-on chapters.

B. IDEAL OTEC RANKINE CYCLE

The closed-cycle OTEC concept is based upon a Rankine power cycle that is driven by the low thermal energy potential available from the ocean temperature gradient that exists between warm surface water and cold deep water in ocean regions. The power cycle consists of a working fluid circulation pump, evaporator (heat absorption), turbine (expansion), and condenser (heat rejection), as shown in Figure 2. The majority of current OTEC designs are based upon ammonia as the working fluid -- a design decision that is adopted for this analysis.

Figure 2 also illustrates an ideal OTEC Rankine cycle, plotted on temperature-entropy coordinates. In the ideal cycle, the low pressure working fluid (state point 1) is isentropically pumped to the evaporator operating pressure (state point 2). The working fluid (ammonia) is then

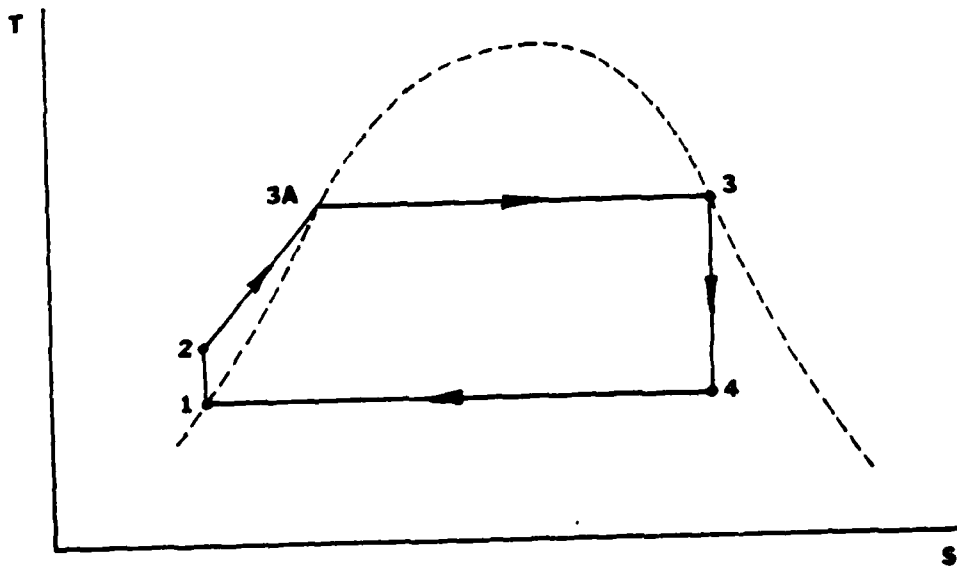
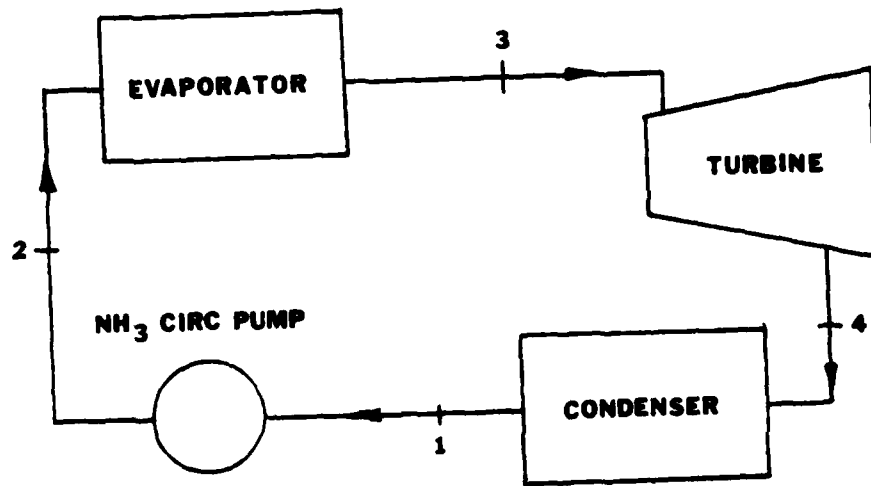


Figure 2. Idealized OTEC Rankine Cycle

converted to a saturated vapor in the evaporator by indirect heat energy exchange from warm surface ocean water (state point 3). Mechanical power is generated by isentropic expansion of the saturated ammonia vapor through the turbine (state point 4).

After exiting the turbine, the wet, low-pressure vapor is converted to a saturated liquid in the condenser by indirect heat absorption from cold ocean water (state point 1), returning the cycle back to the working fluid circulation pump.

C. ACTUAL OTEC RANKINE CYCLE

In actuality there are numerous deviations from the ideal cycle which must be considered in this analysis. These are:

- (1) Turbine, generator and pump efficiencies.
- (2) Pressure drops in evaporator and condenser (tube-side and shellside).
- (3) Pressure drop across moisture separator.
- (4) Elevation change and frictional losses in piping: (a) re-flux pump piping, (b) piping from circulation pump to evaporator.
- (5) Evaporator outlet quality (85 to 95%).
- (6) Moisture separator outlet quality (99 to 99.5%).

The deviations from the ideal Rankine cycle described above are depicted in the flow diagram and temperature-entropy plot of Figure 3. In the actual OTEC Rankine cycle, the low pressure working fluid (state point 1) is pumped up to the evaporator operating pressure by the ammonia circulation pump with an adiabatic efficiency (state point 2). The working

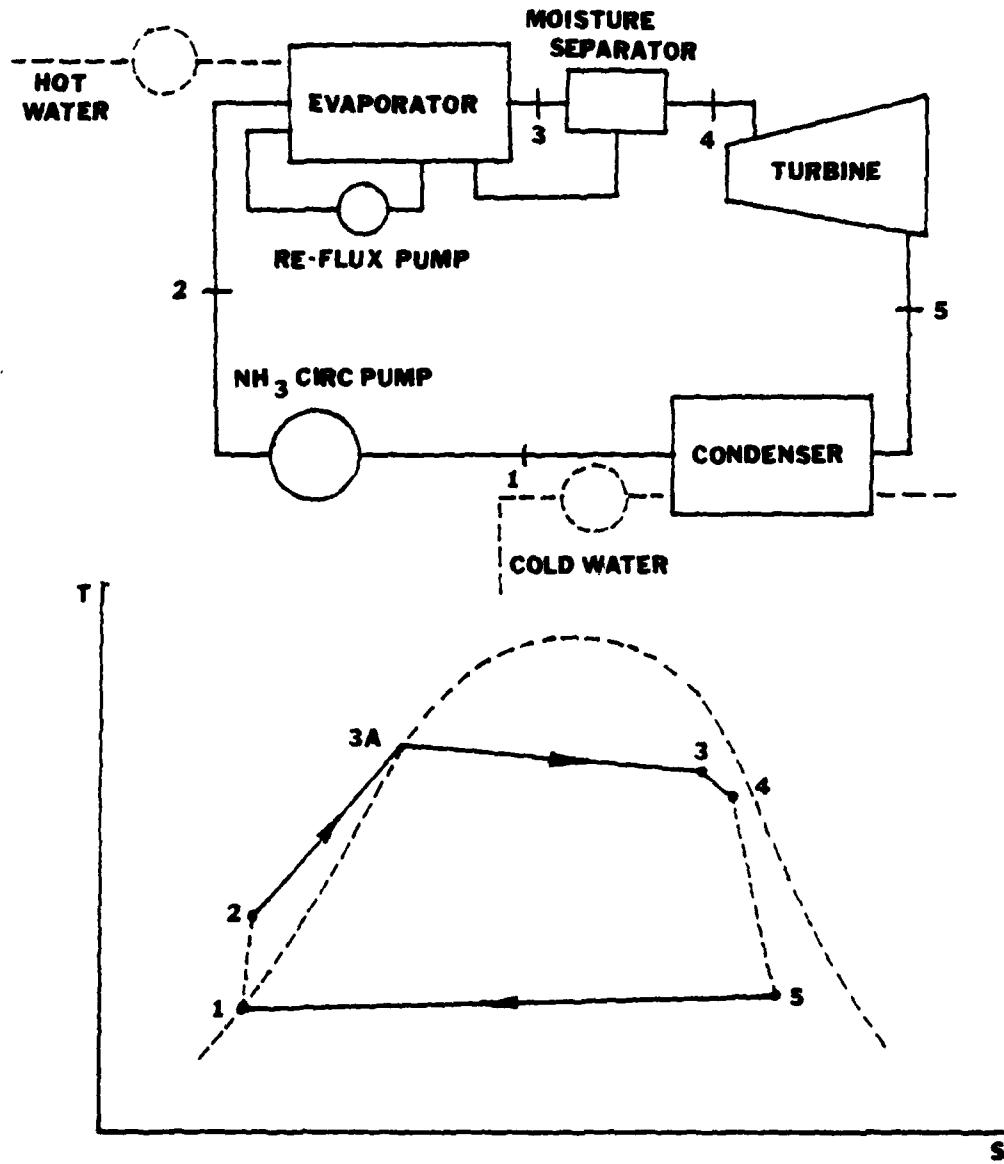


Figure 3. Actual OTEC Rankine Cycle

fluid (ammonia) is then converted to a wet vapor with an evaporator outlet quality (85-95%) acting under a shellside pressure drop (state point 3). Evaporator outlet vapor then passes through a moisture separator to improve vapor quality (99-99.5%) creating a pressure drop (state point 4). Mechanical power is generated by the expansion of the moisture separator outlet vapor through the turbine with an adiabatic efficiency (state point 5). After exiting the turbine, the wet, low pressure vapor is converted to a saturated liquid in the condenser acting under a shellside pressure drop (state point 1), returning the cycle to the working fluid circulation pump.

This figure forms the thermodynamic basis for the OTEC power system analysis which follows.

III. EVAPORATOR AND MOISTURE SEPARATOR

A. INTRODUCTION

Several heat exchanger concepts have been proposed for closed-cycle OTEC systems. Among these designs are:

- . Conventional shell and tube heat exchanger.
- . Plate type heat exchanger.

Within these basic concepts, variations in design have been proposed, including:

- . Orientation of tubes (horizontal or vertical).
- . Heat exchanger tube material (i.e., titanium, aluminum).
- . Method of tube enhancement (i.e., fluted, porous coatings).
- . Location of tube enhancement (i.e., internal and/or external).
- . Location of the vapor separator (i.e., internal or external).
- . Location of the heat exchangers relative to the sea surface.
- . Method of biofouling control.

The analysis to be presented for the evaporative heat exchanger will be based on the following design characteristics:

- . Single-pass shell and tube heat exchanger.
- . Internal vapor separator with a gravity drain to evaporator inlet.
- . Horizontal orientation of tubes with an equilateral triangle or square tube profile.
- . Smooth plain-tube configuration (no enhancements).

- . Tube material (titanium or aluminum based on a 30-year life-cycle criterion).
- . Biofouling control based upon an achievable fouling factor.
- . Heat exchanger centerline located on sea surface.

As an overview of the evaporator-moisture separator analysis, the following major steps in the algorithm are listed in order of their execution (numbers in parentheses refer to equations developed in the subsequent analysis):

- . Specification of system constants (see I.C.).
- . Initialization of design variables (D.V.).
 - .. Tube length.
 - .. SW velocity through hot pipe.
 - .. Inner diameter of hot pipe.
 - .. Tube outer diameter.
 - .. SW velocity through evaporator tubes.
 - .. Inner diameter of NH₃ piping.
 - .. Inner diameter of NH₃ re-flux piping.
 - .. Tube profile pitch ratio.
- . Salt water mass flow rate (1).
- . Total number of tubes (2).
- . Total heat transfer surface area (3).
- . Assume an initial salt water bulk temperature (6), and ammonia heat transfer coefficient (9).
- . Overall heat transfer coefficient (4).
- . Number of transfer units (11).
- . Heat exchanger effectiveness (13).
- . Salt water outlet temperature (15).

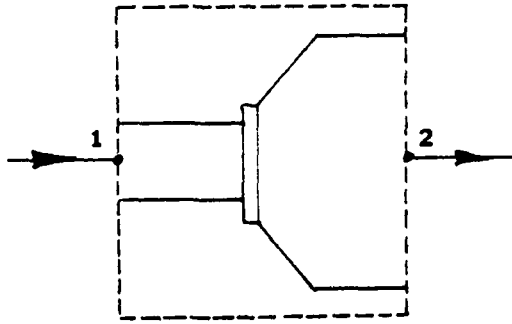
- . Revised bulk temperature (16); iterate with (6).
- . Amount of heat absorption (17).
- . Log mean temperature difference (18).
- . Film temperature (19).
- . Initial ammonia mass flow rate (21) without the effects of moisture separator.
- . Initially assume state point 1 thermodynamic properties are ideal (21).
- . Thermodynamic pump work (23).
- . Tube profile, flow parameters across the tube bank (24, etc.).
- . Tube sheet diameter (30).
- . Evaporator shellside pressure drop for two phase flow (33).
- . Moisture separator pressure drop (38).
- . Properties at state points 3 and 4 (39-41).
- . Revised ammonia mass flow rate and velocity (50) includes the effects of the moisture separator; iterate with (31).
- . Revised ammonia heat transfer coefficient (51, etc.); iterate with (9).
- . Heat exchanger cost analysis.

In the following section, the basic steps summarized above will be described in detail.

B. ANALYSIS OF THE EVAPORATOR AND MOISTURE SEPARATOR

1. Salt Water Mass Flow rate, \dot{m}_{sw}

The salt water mass flow rate through the hot pipe must be equivalent to the flow rate through the evaporator (assuming no leakage)



$$\dot{m}_1 (\text{HOT PIPE}) = \dot{m}_2 (\text{EVAPORATOR})$$

and

$$\dot{m} = \rho_{sw} A V \quad (1)$$

where A = cross-sectional area of the hot pipe.
 V = salt water velocity through hot pipe.
 ρ_{sw} = density of salt water evaluated for an average hot pipe salt water temperature.

As previously stated, the diameter of the hot pipe and salt water velocity are among the initializing conditions of the optimization and will be treated as design variables.

2. Total Number of Evaporator Tubes, N_t

Using equation (1), it follows that

$$\dot{m}_1 = \rho_{sw} \frac{\pi d_i^2}{4} V_t N_t \quad (2)$$

where ρ_{sw} = salt water density evaluated at the average bulk temperature initially assumed as the hot pipe salt water temperature.

d_i = tube inner diameter.

N_t = the number of tubes required to maintain the mass flow rate for an average salt water velocity per tube.

The total number of tubes can be determined by solving Eq. (2) for N_t .

The diameter of the tube and average salt water velocity per tube are initialized for the analysis and will be treated as design variables by the optimization code.

3. Total Evaporator Heat Transfer Surface Area (Outer), A_t

Having determined the number of evaporator tubes, the total heat transfer surface area can be determined using initializing values of outer tube diameter and tube length.

For tubes without extended surfaces

$$A_t = \pi d_o L_t N_t \quad (3)$$

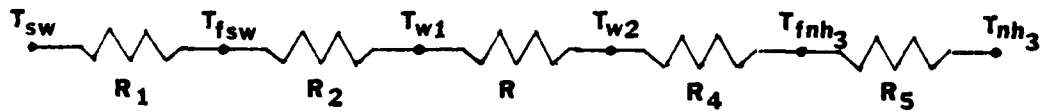
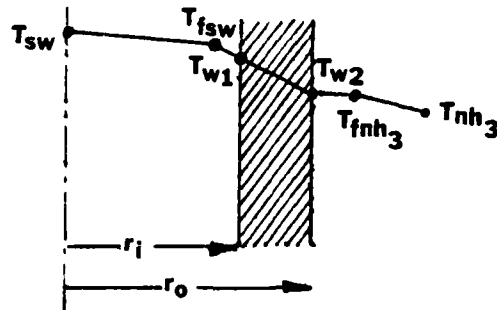
As previously, the outer tube diameter and tube length are initializing conditions and will be treated as design variables.

4. Overall Heat Transfer Coefficient, U

The quantity "U" provides a measure of the total thermal resistance in the flow path, based on either inside or outside surface area.

This analysis will be based on the value of U for the outside surface area derived from Eq. (3).

Using a resistance analysis, assuming one dimensional (radial) heat flow,



the overall heat transfer coefficient may be expressed as

$$U_o = \frac{1}{\frac{A_o}{\eta_o h_{sw} A_i} + \frac{A_o}{A_i} R_{fsw} + \frac{d_o \ln d_o / d_i}{2K} + R_{fNH_3} + \frac{1}{\eta_o h_{NH_3}}} \quad (4)$$

- where
- h_{sw} = tubeside heat transfer coefficient.
 - R_{fsw} = salt water fouling heat transfer resistance.
 - K = thermal conductivity of the tube material.
 - d_o, d_i = outer and inner tube diameter.
 - R_{fNH_3} = ammonia fouling heat transfer resistance (assumed to be negligible).
 - η_o, η_i = outer and inner total fin efficiency (for plain tube analysis, total fin efficiency equals 1).
 - A_o = total outer surface area (including fin and bare tube).

A_i = total inner surface area (including fin and bare tube).¹

$$\eta_i = 1 - \frac{A_{fni}}{A_i} (1 - \eta_{fi})$$

$$\eta_o = 1 - \frac{A_{fno}}{A_o} (1 - \eta_{fo})$$

- where
- A_{fni} = total inner fin surface area.
 - A_i = total inner surface area (including fin and bare tube).
 - A_{fno} = total outer fin surface area.
 - A_o = total outer surface area (including fin and bare tube).
 - η_{fi} = fin efficiency of single internal fin.
 - η_{fo} = fin efficiency of single external fin.
- a. Tubeside Reynolds Number, Re_d

Since the heat transfer coefficient correlations for the evaporator and condenser are dependent on tubeside flow, Reynolds number must be calculated.

The tube Reynolds number is defined as

$$Re_d = \frac{\rho_{sw} v_{sw} d_i}{\mu_{sw}} \quad (5)$$

¹Note that this analysis will hereafter consider smooth plain tube configurations only.

where μ_{sw} = dynamic viscosity of salt water.

ρ_{sw} = density of salt water.

Initially, properties are evaluated for

$$T_{BULK} = T_{SW} (INLET) \quad (6)$$

Reynolds numbers greater than 2300 will be indicative of turbulent flow [Ref. 3]. Transition flow was considered laminar for numerical evaluation.

b. Salt Water Heat Transfer Coefficient, h_{sw}

The simple empirical relation proposed by Sieder and Tate [Ref. 3], expressed as

$$Nu_d = 1.86 (Re_d Pr)^{1/3} \left(\frac{d_i}{L_t} \right)^{1/3} \left(\frac{\mu}{\mu_w} \right)^{0.14} \quad (7)$$

was used for laminar heat transfer in tubes as defined by Eq. (5).

Nusselt and Prandtl numbers, Nu_d and Pr , are defined as

$$Nu_d = \frac{h_{sw} d_i}{k_{sw}}$$

$$Pr = \frac{c_{p_{sw}} \mu_{sw}}{k_{sw}}$$

where μ_{sw} , $c_{p_{sw}}$ and k_{sw} (dynamic viscosity, specific heat, and thermal conductivity) of salt water are evaluated at salt water bulk temperature.

The effect of the viscosity ratio term in Eq. (7)

$$\left(\frac{\mu}{\mu_w}\right)^{0.14}$$

where μ_w is salt water viscosity evaluated at tube wall temperature, is considered negligible and will hereafter be dropped from the expression of Eq. (7).

Relation (7) is based upon the following assumptions:

- . fully developed flow in smooth tubes.
- . fluid properties are evaluated at the bulk fluid temperature.

and is valid for the following condition

$$Re_d Pr \frac{d}{L} > 10$$

For fully developed turbulent flow in a tube as defined by Eq. (5), the Dittus-Boelter correlation [Ref. 3] expressed as

$$Nu_d = 0.023 Re_d^{0.8} Pr^{0.4} \quad (8)$$

was used. Nusselt and Prandtl numbers, Nu_d and Pr , are previously defined by Eq. (9).

Relation (8) is based upon the following assumptions:

- . fully developed flow in smooth tubes.
- . fluid properties are evaluated at the bulk fluid temperature

and is valid for the following conditions:

- . Prandtl numbers ranging from 0.6 to 100.
- . moderate temperature differences between the wall and fluid conditions.

c. Salt Water Fouling Heat Transfer Resistance

In this document, it will be assumed that the fouling resistance coefficient for tubeside salt water can be maintained at .00025 (hr.ft²F°/BTU) using one of the following techniques:

- . Chlorination.
- . MAN Brush System.
- . Amertap.
- . Chemical cleaning

Pressure drops associated with cleaning techniques will not be considered in this analysis. Piping losses will be a function of tube length, inner diameter, salt water velocity and the absolute roughness of the tubing design material only.

d. Ammonia Shellside Heat Transfer Coefficient, h_{NH_3}
Initially, h_{NH_3} will be assumed

$$h_{NH_3} = 1000 \text{ (BTU/hr.ft}^2\text{.F}^\circ\text{)} \quad (9)$$

since its value cannot be directly calculated during this phase of the analysis.

Using the thermal resistance expressed as

$$R_1 = \frac{d_o}{k_i h_{sw} d_i}$$

$$R_2 = \frac{d_o}{\lambda_i h_{fsw} d_i}$$

$$R_3 = \frac{d_o \ln d_o/d_i}{2k}$$

$$R_5 = \frac{1}{\lambda_o h_{NH_3}}$$

an initial value for the overall heat transfer coefficient may be calculated.

$$U_o = \frac{1}{R_1 + R_2 + R_3 + R_5} \quad (10)$$

5. NTU-effectiveness Relations

The NTU-effectiveness relationships will be used to determine the evaporator outlet salt water temperature. Currently, all salt water properties have been based upon the initial assumption that

$$T_{BULK} = T_{Hi} \text{ (SW INLET TO EVAP)}$$

The expression for the number of transfer units (NTU) which is a measure of the size of the heat exchanger is given by

$$NTU = U_o A_t / C_{min}$$

where C_{min} is defined as capacity rate of the single phase flow in an evaporative or condensing two phase flow regime.

$$C_{min} = \dot{m}_{sw} C_{p_{sw}} \quad (11)$$

Evaporator effectiveness can then be expressed as

$$\epsilon = 1 - e^{(-NTU)} \quad (12)$$

for two phase flow regardless of the flow geometry.

Using the definition of effectiveness

$$\text{Effectiveness} = \frac{\text{actual heat transfer}}{\text{maximum possible heat transfer}} \quad (13)$$

$$\epsilon = \frac{\dot{Q}}{\dot{Q}_{max}} = \frac{\Delta T_{min}}{\Delta T_{max}} = \frac{T_{Hi} - T_{Ho}}{T_{Hi} - T_{Ci}} \quad (14)$$

The expression for ΔT_{min} represents the single phase (salt water) flow and T_{Ci} represents ammonia inlet temperature to evaporator taken at state point 3A.

6. Evaporator Salt Water Outlet Temperature and Bulk Temperature

Using the relationships of Eqs. (12) and (14), the following expression may be formulated for salt water outlet temperature

$$T_{Ho} = T_{Hi} - (T_{Hi} - T_{Ci})(1 - e^{(-NTU)}) \quad (15)$$

Concurrently, a revised evaporator average salt water temperature can be expressed as

$$T_{BULK} = (T_{H_L} + T_{H_0})/2 \quad (16)$$

Using the revised value for average salt water temperature, iterate with equation (1) until the revised and current values of bulk temperature satisfy a specified convergence criterion.

7. Amount of Heat Absorption, \dot{Q}

Using the results of Eq. (16) and (12), the amount of heat absorption by the evaporator may be expressed as

$$\dot{Q} = C_{min} (T_{H_L} - T_{H_0}) \quad (17)$$

8. Log Mean Temperature Difference, LMTD

The NTU-effectiveness method can be used to determine the mean effective temperature difference (LMTD) across the evaporator (heat exchanger).

Using Eq. (17) and the definition of

$$\dot{Q} = U_o A_e F LMTD$$

with $\dot{Q}_{max} = C_{min} \Delta T_{max}$

the log mean temperature difference across the evaporator may be expressed as

$$LMTD = \frac{C_{min}(1 - e^{(-NTU)}) (T_{Hi} - T_{Ci})}{U_o A_t F} \quad (18)$$

where $T_{Ci} = T_{NH_3}$ evaluated at state point 3.

F = correction factor on $LMTD$, equal to 1 for two phase flow.

9. Film Temperature for Property Evaluation, T_f

In order to evaluate the shellside ammonia heat transfer coefficient, working fluid properties (i.e., viscosity, specific heat, etc.) must be evaluated at the film temperature to validate critical heat transfer expressions.

By modifying the expression in Eq. (10) multiplying by a single tube outer area, a value for single tube conductance can be expressed as

$$U_o A = \frac{A}{R_1 + R_2 + R_3 + R_5}$$

Subsequently, the average amount of heat transferred per tube would equate to

$$\dot{Q} = U_o A (T_{BULK} - T_3)$$

where $T_3 = T_{NH_3}$ evaluated at state point 3.

Again using the resistance analysis in Section 3, shellside wall temperature may be derived from

$$T_{W2} = T_{BULK} - \dot{Q} \left(\frac{R_1 + R_2 + R_3}{A} \right)$$

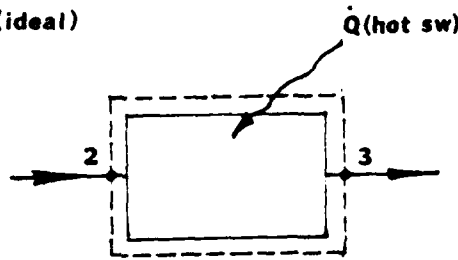
Knowing shellside wall temperature and the free-stream temperature, film temperature can be derived from their arithmetic mean.

$$T_f = \frac{T_{w_2} + T_3}{2} \quad (19)$$

10. Ammonia Mass Flow Rate, \dot{m}_{NH_3}

According to first law of thermodynamics for steady state, steady-flow conditions in the evaporator:

EVAPORATOR (ideal)



$$\dot{m}_{NH_3} h_2 + \dot{Q} = \dot{m}_{NH_3} h_3 \quad (20)$$

from which the ammonia mass flow rate, \dot{m}_{NH_3} , may be determined if the enthalpies at state points 2 and 3 are known.

If we initialize the lower and upper bounds of the analysis in terms of pressure P_1 and P_3 , respectively, and initially assume that a saturated vapor leaves the evaporator, the following relations may be expressed

$$\begin{aligned}
 h_1 = h_f \Big|_{P_1} & \quad T_1 = T_{SAT} \Big|_{P_1} \\
 h_3 = h_g \Big|_{P_3} & \quad T_3 = T_{SAT} \Big|_{P_3}
 \end{aligned}
 \tag{21}$$

where h_1 = represents enthalpy at state point 1 at the suction inlet to the working fluid circulation pump.

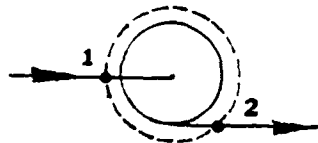
h_3 = represents enthalpy at (ideal)/state point 3 as a saturated vapor.

T_1, T_3 = represent the respective saturation temperatures.

v_1 = represents the specific volume at state point 1.

To summarize, the upper and lower pressure bounds of the system (P_1 and P_3) will be initialized in the analysis and treated as design variables by the optimization code. Temperature at state point 3 is initially assumed to be a saturated vapor (ideal T_3); however, the working fluid is subject to a shellside pressure drop as it passes across the evaporator with an outlet quality of 90-95%. Properties at state point 3 (actual) will be assessed in follow-on sections.

AMMONIA CIRC PUMP



$$\dot{m}_{NH_3} h_1 + \dot{W}_{CP} = \dot{m}_{NH_3} h_2 \quad (22)$$

Assuming steady state, steady-incompressible flow, the change in kinetic and potential energies, and heat losses are negligible for isentropic conditions, and the isentropic pump work can be expressed as

$$\dot{W}_{CPs} = v_1 (P_2 - P_1) \quad \text{where } P_2 = P_{2s}$$

After the isentropic pump work is calculated, the actual (adiabatic) pump work may be determined using pump efficiency, η_p .

$$\dot{W}_{CP} = \frac{\dot{W}_{CPs}}{\eta_p} \quad (23)$$

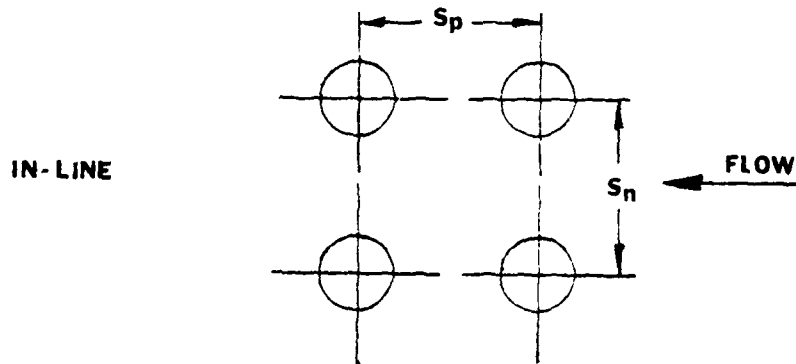
Actual outlet enthalpy at state point 2 may be determined using the results of Eq. (23) with Eq. (22) knowing the enthalpy at state point 1 from Eq. (21).

Using the results of Eqs. (21) and (22), the mass flow rate in Eq. (20) may be calculated as the average shell-side mass flow rate for the working fluid (ammonia).

11. Tube Profile, Flow across Tube Bank, and Tube Sheet Diameter

Since the heat-exchanger arrangements (evaporator and condenser) involve multiple rows of tubes, the geometric arrangement of the tube profiles is important in the determination of the heat transfer coefficient, the tube sheet diameter and the shell side pressure drop associated with two-phase flow (homogeneous model) [Ref. 4].

The following geometric arrangements are used:



where S_n = pitch ratio \times outer tube diameter, equal to S_p .

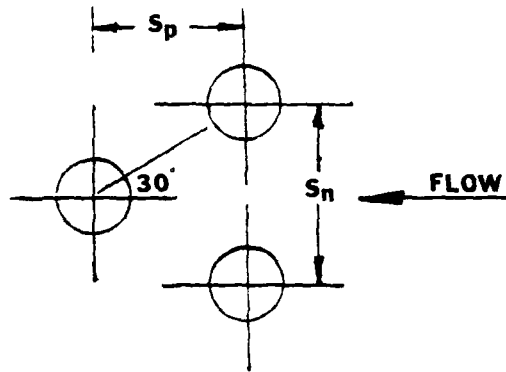
P_R = pitch ratio; the distance between tube centers with respect to outer tube diameter.

A_p = tube profile area (centerline to centerline) per tube.

$$S_n = P_R d_o \quad (24)$$

$$A_p = S_n^2 \quad (25)$$

STAGGERED



$$S_n = 2 P_R d_o \sin 30^\circ \quad (26)$$

$$S_p = P_R d_o \cos 30^\circ \quad (27)$$

Therefore, the tube profile area (centerline to centerline) per tube is equal to

$$A_p = S_n S_p \quad (28)$$

The ratio of minimum flow area to the frontal area can be expressed as

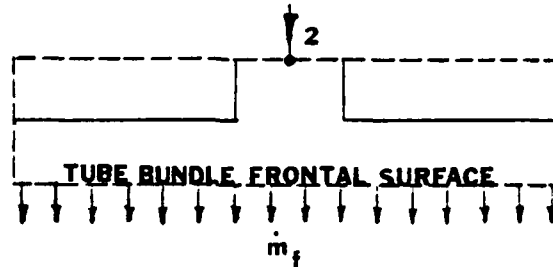
$$\frac{A_{ff}}{A_f} = \frac{S_n - d_o}{S_n} \quad (29)$$

Using the selected tube profile geometry, either in-line or staggered, and knowing the required number of tubes by equation (2), the tube sheet diameter for heat exchanger design can be assessed as follows:

$$N_t A_p = \frac{\pi T_{SD}^2}{4} \quad (30)$$

where T_{SD} = tube sheet diameter.

To estimate the shellside ammonia flow velocity the following control volume is introduced (ammonia circulation piping and the top portion of the evaporator).



If the mass flow rate remains unchanged across any boundary (continuity),

$$\dot{m}_2 = \dot{m}_f$$

Furthermore, if we assume the evaporator has the means to evenly distribute liquid droplets across the top of the tube bundle (spray nozzles and baffling), the following expressions can be applied to estimate the mean droplet velocity approaching the bundle:

Let $(A_f)_{LIQ} = A_f \eta$

where η = percent of tube frontal area which is occupied by droplets.

The mass flow rates are

$$\dot{m}_2 = \rho A_p V_p$$

$$\dot{m}_f = \rho (A_f)_{LIG} V_f$$

where A_p = ammonia pipe cross-sectional area.

V_p = average ammonia velocity in the pipe.

Therefore

$$V_f = \frac{A_p}{(A_f) \eta_1} V_p$$

and since

$$\eta_1 \approx \frac{A_p}{A_f}$$

it follows that the average velocity of ammonia through the circulation pipe is equivalent to the average velocity of ammonia at the tube frontal area boundary.

$$V_p = V_f \quad (31)$$

Thus the assumption that $\eta_1 = A_p/A_f$ is equivalent to the assumption of constant liquid kinetic energy in the transition from the pipe exit to the bundle entrance. Considering the minimum free-flow area for shellside flow passage, A_{ff} can be derived from Eqs. (29) and (30):

$$A_f = T_{SD} L_t$$

$$A_{ff} = A_f \left(\frac{S_{ri} - d_o}{S_{ri}} \right) \quad (32)$$

where A_f = represents the flow frontal area.

L_t = tube length.

Using the calculated values of Eqs. (32) and (20), the mass velocity for the minimum free-flow area can be expressed

$$G = \dot{m}_{NH_3} / A_{ff}$$

where \dot{m}_{NH_3} represents the average ammonia mass flow rate.

12. Pressure Drop of Two-Phase Flow across a Bank of Tubes, ΔP

This portion of the analysis will use an analytical model for two-phase pressure drops applicable for a fog or spray flow pattern occurring at high void fractions -- the homogeneous model [Ref. 4].

The model asserts that if the pressure drop in the two-phase flow for a liquid-vapor mixture is relatively small compared to the absolute pressure, the flow is considered incompressible. Subsequently, the density of each phase is practically constant. During the process of phase change, the phase and velocity distributions are changed, and so is the momentum of the flow. Therefore, the pressure drop of a vertical two-phase flow consists of three components: friction loss, momentum change, and elevation pressure drop arising from the effects of the gravitational force field.

The local pressure gradient for a two-phase flow may be expressed as

$$\Delta P_{TOT} = \Delta P_{FRICTION} + \Delta P_{MOMENTUM} + \Delta P_{ELEVATION} \quad (33)$$

For a given channel length, L_c , the pressure drop components can be represented by

$$\Delta P_{\text{FRICTION}} = \frac{f G^2 \bar{v}}{D_e 2 g_c} L_c \quad (34)$$

$$\Delta P_{\text{MOMENTUM}} = \frac{G^2 \bar{v}}{g_c}$$

$$\Delta P_{\text{ELEVATION}} = \frac{g}{\bar{v} g_c} L_c$$

and the total pressure drop, ΔP_{EVAP} , is given by the sum of these expressions

where f = single-phase friction factor by Jakob expressed in Eqs. (35) and (36).

L_c = channel flow length, defined for horizontal tubed evaporators as $L_c = \Gamma_{SD}$ (tube sheet diameter).

D_e = equivalent diameter of flow channel, defined by $D_e = Pr d_o - d_o$.

\bar{v} = mean specific volume defined by

$$\bar{v} = v_f \left[1 + \frac{\chi}{v_f} (v_g - v_f) \right]$$

where χ = quality of mixture (state point 3).

v_f = specific volume of liquid (state point 1).

v_g = specific volume of vapor (state point 3).

The basic assumptions of the homogeneous model (fog flow model) [Ref. 4] are:

- (1) equal linear velocities of vapor and liquid,
- (2) thermodynamic equilibrium between the two phases, and
- (3) a suitably defined single-phase friction factor is applicable to the two-phase flow.

Using assumption (3) and the correlations by Jakob [Ref. 3], a suitable single-phase friction factor can be calculated from previously defined tube profile relationships: for staggered tube arrangements:

$$f = \left\{ 0.25 + \frac{0.118}{\left[(S_n - d_o) / d_o \right]^{1.28}} \right\} Re_{max}^{-0.16} \quad (35)$$

and for in-line tube arrangements:

$$f = \left\{ 0.044 + \frac{0.02 S_n / d_o}{\left[(S_n - d_o) / d_o \right]^{0.43 + 1.13 d_o / S_n}} \right\} Re_{max}^{-0.15} \quad (36)$$

where Reynolds number (max) is determined from the shellside ammonia flow and the nozzling effect of the tube geometry as expressed by

$$V_{max} = V_f \left(\frac{S_n}{S_n - d_o} \right)$$

where V_f = the ammonia velocity at the tube frontal area boundary determined by equation (31).

Reynolds number for maximum shellside flow can be calculated using the following expression

$$Re_{max} = \frac{\rho V_{max} d_o}{\mu_f} \quad (37)$$

Eq. (37) and tube profile data can then be used to evaluate the single-phase friction factor, required for Eq. (34). All other components of the total pressure drop Eq. (33) can be determined from previously calculated data.

13. Pressure Drop Across the Moisture Separator. $\Delta P_{m.sep}$

This portion of the analysis will simulate the use of a cyclone separator to improve the evaporator outlet vapor quality. The flow pattern in a cyclone separator is complex and simplifying assumptions are inadequate to allow the calculation of the corresponding pressure drop, which can vary from 1 to 20 inlet velocity heads [Ref. 5]. Therefore, the worst case condition will be applied with an approximation for the fluid flow inlet area to the separator banks.

By approximating the inlet area as a fraction of the evaporator frontal area

$$A_{INLET} = 0.1 T_{SD} L_t$$

the inlet fluid velocity can then be determined using the working fluid mass flow rate, Eq. (20).

$$\dot{m}_{NH_3} = \rho A_{INLET} V$$

where ρ = density of ammonia at state point 3.

Therefore, if the pressure drop across the moisture separator is equal to 20 times the inlet velocity head,

$$\Delta P_{IN.SEP} = 20 \rho \frac{V^2}{2g_c} \quad (38)$$

14. Enthalpy at State Points 3 and 4

Since Eq. (33) represents the pressure drop across the evaporator shellside, the actual pressure at state point 3 or evaporator outlet may be determined from

$$P_{3(NEW)} = P_3 - \Delta P_{EVAP} \quad (39)$$

where P_3 was previously described as the pressure for a saturated vapor.

Similarly the actual pressure at state point 4, the moisture separator outlet, may be expressed as

$$P_4 = P_{3(NEW)} - \Delta P_{IN.SEP} \quad (40)$$

Operating under the dome of the Temperature-Entropy diagram, the following properties are defined

$$\begin{aligned} h_{3f(NEW)} &= h_f \Big|_{P_{3(NEW)}} & h_{4f} &= h_f \Big|_{P_4} \\ h_{3g(NEW)} &= h_g \Big|_{P_{3(NEW)}} & h_{4g} &= h_g \Big|_{P_4} \end{aligned} \quad (41)$$

The subscript (NEW) representing a revised property will hereafter be dropped from the expressions in Eq. (41).

Assuming an evaporator outlet quality of 90-95%, and a moisture separator outlet quality of 99-99.5%, enthalpies at state points 3 and 4 may be determined using the relationships of Eqs. (41)

$$\begin{aligned}h_3 &= h_{3f} + X_3 (h_{3g} - h_{3f}) \\h_4 &= h_{4f} + X_4 (h_{4g} - h_{4f})\end{aligned}\tag{42}$$

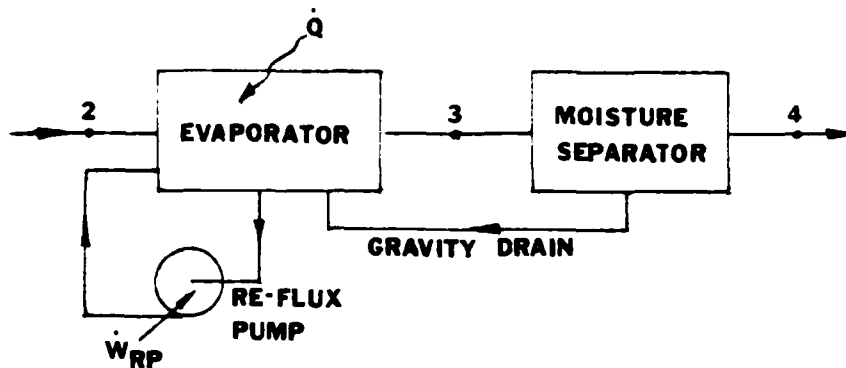
15. Revised Ammonia Mass Flow Rate and Velocity

Till now, we assumed that the shellside mass flow rate was given in accordance with the ideal system defined by Eq. (20); however, in actuality this is not the case.

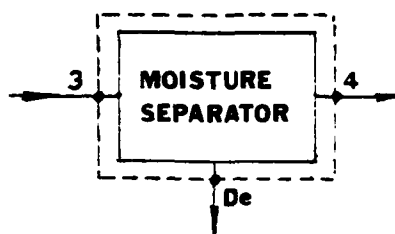
The diagrammatic representation that follows better illustrates the heat absorption phase of the OTEC power system and will provide the basis for the analysis and optimization.

Note, as in the previous control volume analysis, the following conditions are assumed.

- . Steady state.
- . Steady-incompressible flow.
- . Change in potential and kinetic energies is negligible.



Analyzing the moisture separator as a separate control volume,



If we assume that there is no carry-over of vapor in the separator drain, then

$$x_3 \dot{m}_3 = x_4 \dot{m}_4$$

and

$$\dot{m}_3 = \frac{x_4}{x_3} \dot{m}_4 \quad (43)$$

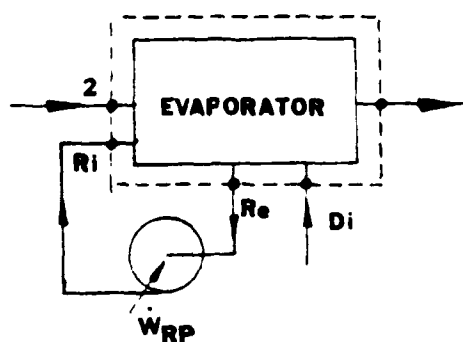
However, for reasons of flow continuity, the mass flow rate through the separator drain must be included in the control volume analysis; therefore

$$\dot{m}_3 = \dot{m}_4 + \dot{m}_{DE} \quad (44)$$

Substituting Eq. (43) into (44) and solving for \dot{m}_{De} , the following expression can be derived

$$\dot{m}_{De} = \left(\frac{X_4}{X_3} - 1 \right) \dot{M}_4 \quad (45)$$

Looking at the evaporator as a separate control volume,



the energy balance is

$$\dot{Q} + \dot{m}_2 h_2 + \dot{m}_{Re} h_{Re} + \dot{m}_D h_{Dc} = \dot{m}_3 h_3 + \dot{m}_{Re} h_{Re}$$

Assuming the change in enthalpy across the re-flux pump and the difference between the separator drain outlet and evaporator inlet are negligible, the energy balance becomes

$$\dot{Q} + \dot{m}_2 h_2 + \dot{m}_{De} h_{De} = \dot{m}_3 h_3 \quad (46)$$

where $\dot{m}_{D2} = \dot{m}_4 \left(\frac{P_2 - P_4}{P_2} \right)$ fluid drained from the separator is

assumed to be a saturated liquid.

Furthermore, a mass balance of the evaporator control volume can be expressed as

$$\dot{m}_2 + \dot{m}_{R2} + \dot{m}_{D2} = \dot{m}_3 + \dot{m}_{R2} \quad (47)$$

where $\dot{m}_{R2} = \dot{m}_{R1}$.

Solving Eq. (47) for the mass flow rate at state point 3 and substituting into Eq. (46) with Eq. (45) yields the following expression

$$\dot{m}_2 \left(1 + \frac{P_2 - P_4}{P_2} \right) \dot{m}_4 \dot{m}_{D2} = \dot{m}_2 \frac{P_4}{P_3} \dot{m}_3 \quad (48)$$

In addition, a mass balance for steady-state, steady-flow indicates that the mass flow rates at state points 2 and 4 are equal and therefore

$$\dot{m}_4 = \dot{m}_2 \quad (49)$$

Using Eqs. (48) and (49), the revised mass flow rate at state point 2 may be determined. Concurrently, the revised average ammonia velocity acting on the tube profile geometry may be determined from this revised mass flow rate.

Using the revised ammonia velocity acting on the tube profile geometry and iterating from Eq. (31) until

an acceptable convergence criterion is achieved provides the pressure drops across the evaporator and moisture separator, and the properties at state points 3 and 4 for a given film temperature. The result is more representative of the heat absorption phase in the OTEC power cycle than is the commonly used ideal analysis.

In addition, solving for the revised temperature at state point 3,

$$T_3 = T_{SAT} \Big|_{P_3} \quad (50)$$

and iterating through Eq. (18) revises the film temperature and subsequent working fluid properties.

16. Revised Shellside Ammonia Heat Transfer Coefficient

In the search for acceptable correlations to predict the average evaporative heat transfer coefficient, two analytical treatments were found that lent themselves to OTEC power system conditions.

The first of these correlations seeks to predict thin film evaporation heat transfer coefficient for horizontal tubes [Ref. 6]. Owens [Ref. 6] uses (1) the similarity between evaporation and condensation, (2) the correlation forms of local evaporation heat transfer coefficients for water on a vertical tube developed by Chun and Seban, and (3) the dependence of heat transfer on the vertical spacing of the tubes as was experimentally demonstrated by Liu, to arrive at the following correlations for non-boiling thin film evaporation:

for laminar flow

$$\bar{h} = 2.2 \left(\frac{H}{d_o} \right)^{0.1} \left(\frac{\mu_f}{g \rho_f^2 k_f^3} \right)^{-1/3} \left(\frac{4\Gamma}{\mu_f} \right)^{-1/3} \quad (51)$$

for turbulent flow

$$\bar{h} = 0.185 \left(\frac{H}{d_o} \right)^{0.1} \left(\frac{\mu_f}{g \rho_f^2 k_f^3} \right)^{-1/3} \left(\frac{C_p \mu_f}{k_f} \right)^{0.5} \quad (52)$$

where $\frac{H}{d_o}$ = vertical spacing with respect to tube outer diameter.

Γ = tube flow rate per unit length.

The laminar-turbulent transition point is defined by the intersection of Eqs. (51) and (52)

$$Re_{TR} = 1000 \left(\frac{C_p \mu_f}{k_f} \right)^{-1.5}$$

The pseudo-Reynolds number for horizontal vertical falling film evaporation is defined by Ref. 7.

$$Re = \frac{4\Gamma}{\mu_f}$$

The second correlation combines boiling and evaporation of liquid films on horizontal tubes, applicable for vertical banks of plain and enhanced tubes [Ref. 8].

The overall model for a single tube is expressed as

$$\bar{h} = h_b + h_d \frac{L_d}{L} + h_c \left(1 - \frac{L_d}{L}\right) \quad (53)$$

where h_b = Rohsenow pool boiling correlation over the entire tube length given by

$$h_b = \frac{\Delta u_f h_{fg}}{C_{sf} \sqrt[3]{\frac{\sigma_f \Delta T}{\rho_f}}} \left(\frac{C_{pf}}{h_{fg} Pr} \right) \Delta T^2 \quad (54)$$

with C_{sf} = function of the fluid-surface combination.

ΔT = wall temperature minus free stream saturation temperature.

σ_f = surface tension

h_d = heat transfer coefficient in the developing region.

$$h_d = \frac{3}{2} C_p \frac{\Gamma}{L_d}$$

$$L_d = \frac{\Gamma^{4/3}}{4\pi \rho \alpha} \left(\frac{3 \mu_f}{\rho_f^2} \right)^{1/3}$$

and h_c = fully developed heat transfer coefficient given for laminar flow by

$$h_c = 0.321 \left(\frac{2^2}{k^3 \mu_f} \right)^{-1/3} \left(\frac{4\Gamma}{\mu_f} \right)^{-0.22} \quad (55)$$

and, for turbulent flow,

$$h_c = 3.8 \times 10^{-3} \left(\frac{2^{-2}}{N^3 y} \right)^{-1/3} \left(\frac{4\Gamma}{\mu_f} \right)^{0.4} \left(\frac{2'}{\alpha} \right)^{0.65} \quad (56)$$

where L = circumferential length of heated surface.

α = thermal diffusivity.

L_d = developing length around tube circumference.

Γ = flow rate per unit axial length of tube.

To apply Eq. (51) for a vertical bank of tubes, L is expressed as

$$L = N_t \pi d_o / 2$$

The laminar-turbulent transition point is defined by the intersection of Eqs. (55) and (56)

$$Re_{TR} = 5800 \left(\frac{2'}{\alpha} \right)^{-1.06}$$

As before, the pseudo-Reynolds number is defined by Ref. 7

$$Re = \frac{4\Gamma}{\mu_f} \quad (57)$$

After using Eq. (57) to establish which flow regime the system is operating in, the revised heat transfer coefficient for non-boiling thin film evaporation or nucleate

boiling may be calculated and then iterated with the initial assumption for the shellside heat transfer coefficient, Eq. (9). This will have a convergence effect on variables which are a function of the shellside heat transfer coefficient, moving them closer to actual OTEC system performance characteristics.

The user should be aware that the predictions for the OTEC power system using ammonia have been for the case where no boiling occurs in the film. This condition is dictated by industrial preference for plain tube heat exchangers to minimize fouling and the characteristic of ammonia to wet surfaces well, flooding out nucleation sites. A number of enhancement techniques have been developed to create nucleate boiling, including a variety of tube configurations and surface preparations; however, a preference for them has not materialized. The nucleate boiling development in Eq. (51) which would be indicative of tube enhancement is provided for information only and will not be included in the optimization or summary of conclusions.

Having described the methods used to predict the shellside heat transfer coefficient, we can complete this chapter of the OTEC power system analysis by constructing the heat exchanger cost analysis.

17. Evaporator Cost Analysis

At the request of TRW, Wyatt Industries, a large exchanger fabricator, prepared cost estimates for three different sizes of vertically configured evaporators and condensers, based upon initial design specifications prepared

by TRW. Based upon these estimates, TRW developed sets of equations that represent the costs of various heat exchanger component parts for shell diameters ranging from 10-35 ft and 35-50 ft [Ref. 9].

The following are the TRW evaporator cost (\$) equations as a function of outer tube diameter (inch), total number of tubes and tube-sheet diameter (ft) for tube-sheet diameters of 10-35 ft.

. Drilling time/tube sheet thickness

$$t_d = 0.66 (d_o - 0.5) \quad (58)$$

. Thickness of the tube sheet

$$t_{TS} = 0.56 T_{SD}^{0.68} \quad (59)$$

. Tube sheet labor cost

$$C_{TSL} = 156695 (N_t / 9630) (t_d / 0.66) (t_{TS} / 4) \quad (60)$$

. Tube sheet material cost

$$C_{TSM} = 189.486 T_{SD}^{2.3} \quad (61)$$

. Tube installation cost

$$C_{TI} = 34 N_t d_o^{0.7} \quad (62)$$

. Heat exchanger shell cost

$$C_{HXS} = 177265 \left(\frac{L_t + 6}{31} \right) (T_{SD} / 18)^2 \quad (63)$$

. Ammonia distribution plate and battles cost

$$C_{DPB} = 93865.75 (N_t/9630) (t_d/0.66) (T_{SD}/18)^2 \quad (64)$$

. Bustle, flanges channels and flow plates cost

$$C_{BFCF} = 308550 (T_{SD}/18)^2 \quad (65)$$

. Tube material cost

$$C_{TM} = (E1 L_t + E2) N_t \frac{d_o}{1.5} \quad (66)$$

where $E1$ = curve fit of tube cost per foot.

$E2$ = tube machining cost if required

. Heat exchanger head costs

$$C_{HXX} = 53240 (T_{SD}/18)^3 \quad (67)$$

. Water inlet, nozzles and supports cost

$$C_{WNS} = 220310.75 (T_{SD}/18)^2 \quad (68)$$

. Tube welding costs (Titanium tubes)

for $N_t \leq 36000$

$$C_{TW} = 14.73 N_t^{1.03} (d_o/1.5)^{0.7} \quad (69)$$

for $N_t > 36000$

$$C_{TW} = 0.8797 N_t^{1.3} (d_o/1.5)^{0.7}$$

The sum of cost Eqs. (60) through (69) would equal the cost to fabricate one OTEC evaporator with a tube sheet diameter of 10-35 feet (all the preceding component costs have been adjusted for current pricing at a 10% annual rate of inflation).

If our analysis is based on a 30-year life-cycle criterion, no adjustments are necessary to any component cost equation if titanium tubing is used due to its anti-corrosive qualities; however, using aluminum tubing (i.e., Al-5052), the expense of retubing must be considered to meet the criterion of a 10-year life cycle for aluminum tubing. This implies Eq. (61) and (66) must be modified to reflect the costs of retubing at the 10 and 20-year point in the cycle.

. Aluminum tube installation cost

$$C_{ATI} = C_{TI} [1 + (1+i)^{10} + (1+i)^{20}] \quad (70)$$

where i = projected inflationary rate (input by customer)

. Aluminum tube material cost

$$C_{ATM} = C_{TM} [1 + (1+i)^{10} + (1+i)^{20}] \quad (71)$$

For tube sheet diameters of 35-50 ft the following cost relationships apply [Ref. 9]:

. Equations for drilling time/tube sheet thickness (58), thickness of tube sheet (59), and tube material costs remain unchanged.

. Tube sheet labor and material cost (titanium)

$$C_{TSL} = 55.189 N_t^{0.741} T_{SD}^{0.68} t_d \quad (72)$$

$$C_{TSM} = 29.566 T_{SD}^{2.014} t_d \quad (73)$$

. Tube sheet labor and material cost (aluminum)

$$C_{TSL} = 73.181 N_t^{0.741} T_{SD}^{0.68} t_d \quad (74)$$

$$C_{TSM} = 354.3 T_{SD}^{1.61} t_{TS} \quad (75)$$

. Tube installation costs

$$C_{TI} = 36.542 N_t d_o^{0.7} \quad (76)$$

. Heat exchanger shell cost

$$C_{HXS} = 12.544 (L_t + 6) T_{SD}^{2.06} \quad (77)$$

. Ammonia distribution plate and baffle costs

$$C_{DPB} = 158.094 T_{SD}^{1.82} + 72.419 N_t^{0.873} t_d \quad (78)$$

. Bustle, flanges, channels, and flow plate costs

$$C_{BFCF} = 472.977 T_{SD}^{2.12} \quad (79)$$

. Heat exchanger head cost

$$C_{HXH} = 1725.31 T_{SD}^{1.45} \quad (80)$$

. Water inlet, nozzles and support cost

$$C_{WINS} = 7445.297 T_{SD}^{1.1} \quad (81)$$

. Tube welding costs (titanium tubes)

for $N_t \leq 36000$

$$C_{TW} = 14.73 N_t^{1.03} (d_o/1.5)^{0.7} \quad (82)$$

for $N_t > 36000$

$$C_{TW} = 0.8797 N_t^{1.03} (d_o/1.5)^{0.7}$$

As indicated previously, the cost to fabricate one OTEC evaporator with a tube sheet diameter 35 to 50 ft is equal to the sum of component costs Eqs. (72) through (85) (all the preceding component costs have been adjusted for current pricing at a 10% annual rate of inflation).

For an analysis based on a 30-year system life-cycle criterion, the additional costs for aluminum retubing must be considered and Eqs. (70) and (71) apply.

IV. PARASITIC LOSSES

A. INTRODUCTION

This chapter describes in detail the programming analysis for parasitic losses which include: (1) pumping and pipe requirements for both cold and hot salt water systems, (2) pumping and pipe requirements for the working fluid (ammonia) circulation and re-flux systems, and (3) turbine generator losses due to inefficiencies. Hotel requirements have not been incorporated into the analysis, but could be included for the final design analysis.

Pumping power requirements will be determined through the use of the general energy equation between the inlet and outlet of the system control volume [Ref. 3].

$$\int_0^i \frac{dP}{\rho} + \frac{V_i^2}{2} + g Z_i = \frac{V_o^2}{2} + g Z_o + \dot{W}_s + (LOSSES)_{i \rightarrow o}$$

To determine the pumping power \dot{W}_s the following effects will be evaluated:

1. Density head.
2. Friction losses.
 - . Intake piping.
 - . Heat exchanger tubing.
 - . Exit piping (if employed).
3. Thermodynamic pressure head.
4. Elevation head.

5. Minor losses.

- . Intake piping inlet configuration (contraction).
- . Intake piping screen (obstruction).
- . Flow through valves, elbows, etc.
- . Outlet piping (expansion).
- . Inlet to heat exchanger tubing (contraction).
- . Outlet from heat exchanger tubing (expansion).
- . Outlet of exit piping (if employed).

In the above pump head evaluations, the following inputs are specified:

- . Pipe lengths (hot, cold, ammonia circulation and re-flux piping).
- . Inner pipe diameters (initialized and treated as a design variable by the optimization code).
- . Absolute roughness corresponding to piping/tubing material (designer specified).
- . Fluid velocity. (initialized and treated as a design variable by the optimization code).
- . Pump mechanical and electrical efficiencies.

As an overview of the parasitic pump loss analysis, the following major steps in the algorithm are listed in order of their execution:

- . Hot pipe salt water pump.
 - .. Inlet piping friction losses (86).
 - .. Minor piping losses due to inlet screen (87) and plenum design to evaporator core (88).
 - .. Evaporator core minor losses (89, 90) and tubeside friction losses.
 - .. Total pressure losses (92) and pumping head (93).
 - .. Pumping power requirements (95).

- .. Pump cost analysis (96).
- . Cold pipe salt water pump.
 - .. Initialize cold pipe inner diameter and SW velocity (design variables).
 - .. Minor losses due to inlet ducting (97) and plenum design to condenser core (98).
 - .. Inlet piping friction losses (99).
 - .. Condenser core minor losses (100, 101) and tubeside friction losses (103).
 - .. Density head (104).
 - .. Total pressure losses (105).
 - .. Pumping power requirement (107).
 - .. Pump cost analysis (108).
- . Ammonia circulation pump.
 - .. Piping friction (109) and minor losses due to valving/elbows (110).
 - .. Pressure drop across evaporator shellside (112).
 - .. Thermodynamic head (113).
 - .. Elevation head (114).
 - .. Total pressure losses (115).
 - .. Pumping power requirement (116).
 - .. Pump cost analysis (118).
- . Ammonia re-flux pump.
 - .. Piping friction (119) and minor losses due to valving/elbows (120).
 - .. Thermodynamic head due to pressure drop of saturated liquid ammonia across evaporator shellside (122).
 - .. Elevation head (123).
 - .. Total pressure losses (124).

- .. Pumping power requirements (126).
- .. Pump cost analysis (127).
- . Parasitic pump losses.

In the following section, the basic steps summarized above will be described in detail.

B. ANALYSIS OF PARASITIC LOSSES

1. Hot Pipe Salt Water Pump, P_{HP}

The pressure losses due to piping friction and associated minor losses will be determined using the Darcy-Weisbach correlation [Ref. 10].

$$\Delta P = \sum_{i=1}^n \rho \frac{K_i V^2}{2g_c} \quad (83)$$

where K_i describes the resistance coefficient.
 V = fluid velocity.

$$K_i = f \frac{L}{D} \quad (84)$$

where f = friction factor.
 $\frac{L}{D}$ = equivalent length in pipe diameters.

In order to determine the friction factor, the pipe flow Reynolds number must be calculated.

$$Re_d = \frac{\rho_{sw} V_{sw} d_i}{\mu_{sw}}$$

where ρ_{sw}, μ_{sw} = properties of salt water at the hot pipe inlet temperature (assumed constant throughout the pipe).

v_{sw}, d_i = salt water velocity and inner pipe diameter (initialized and treated as design variables by the optimization code); velocity assumed constant over pipe length.

Pipe flow Reynolds number greater than 2300 will be considered turbulent.

for laminar flow

$$f = \frac{64}{Re_d} \quad (85)$$

for turbulent flow

$$f = \frac{1.325}{\left[\ln \left(\frac{\epsilon}{3.7 d_i} + \frac{5.74}{Re_d^{0.4}} \right) \right]^2} \quad (86)$$

where ϵ = absolute roughness corresponding to piping material selected.

Eq. (86) yields a friction factor within one percent of the Colebrook equation and is valid for the following conditions [Ref. 9].

$$10^{-6} \leq \frac{\epsilon}{D} \leq 10^{-2}$$

$$5000 \leq Re_d \leq 10^8$$

Considering the resistance coefficient for pipe minor losses

- . Assume the inlet duct is the same size as the pipe inner diameter, but it is screened

$$K = 1.5 \quad (87)$$

- . Assume piping enters evaporator through an area which is abruptly changed [Ref. 11]

$$K = \left[1 - \left(d_i / T_{so} \right)^2 \right]^2 \quad (88)$$

where T_{so} = evaporator tube sheet diameter (assume tube sheet diameter is twice as large as the inner pipe diameter).

Summing the results of Eqs. (84), (87), and (88) to determine the total resistance coefficient, the pressure losses due to piping can then be determined using Eq. (83).

If a variety of valves or fittings are to be included with Eq. (84), Ref. 11 provides a representative listing of equivalent length-to-pipe-diameter values.

To analyze the pressure drop across the evaporator tubeside, we again use the Darcy-Weisbach correlation, but for different design assumptions.

- . Assume inlets to evaporator tubing are well rounded [Ref. 11]

$$K = 0.5 \quad (89)$$

. Assume outlets of evaporator tubing expand to an infinite reservoir [Ref. 10]

$$K = 1.0 \quad (90)$$

Using the Reynolds number in the previous chapter, Eq. (5), the corresponding friction factor Eq. (85) or (86), and resistance coefficient can be determined

$$K_{CORE} = f \frac{L_t}{d_i} \quad (91)$$

where L_t, d_i = evaporator tube length and inner tube diameter and are initialized and treated as design variables by the optimization code.

Summing the results of the resistance coefficient in Eqs. (89), (90) and (91), the pressure losses due to the evaporator design may be determined using the Darcy-Weisbach correlation Eq. (83).

The results of the piping losses and core design losses are equivalent to the hot pipe salt water pumping system requirements

$$\Delta P_{pump} = \Delta P_{PIPE SYSTEM} + \Delta P_{EVAP DESIGN} \quad (92)$$

converting to pumping head

$$H = \frac{g_c}{\rho_{sw} g} \Delta P_{pump} \quad (93)$$

Pumping power in terms of horsepower can be determined using the following expression

$$P_{HP} = \frac{\dot{m}_{sw}}{\eta_p} \left(\frac{g H}{g_c} \right) \quad (94)$$

where η_p = pump mechanical efficiency (designer input).

\dot{m}_{sw} = salt water mass flow rate determined in previous chapter, Eq. (2).

To equate parasitic pump losses to power input, Eq. (94) is converted to the motor load requirement in terms of megawatts electrical.

$$P_{HP(MW)} = \frac{P_{HP}}{\eta_M} \times \text{CONVERSION FACTOR} \quad (95)$$

where η_M = pump motor efficiency (designer input).

Because of the high salt water flow rates and relatively low pumping heads, good engineering design would dictate the use of axial flow (propeller) type pumps.

Using the algorithm developed by TRW [Ref. 9] from data provided by Johnston Pump Co., and Process Equipment Co. (distributors of Ingersoll Rank and Johnston Pumps), the cost of salt water pumps can be expressed as

$$C_{pump} = \left[(D/1000)^{0.75} + 50 \right] 1.21 \times 10^3 \quad (96)$$

where

$$D = \frac{\pi d_i^2}{4} V_{sw}$$

where d_i, V_{sw} = inner hot pipe diameter, salt water velocity (initialized for analysis and treated as design variables by the optimization code).

The above algorithm is valid for the following conditions

- . vertical, wet pit, propeller type pumps with cast iron steel columns with protective epoxy coating, stainless steel shaft and bronze impeller.
- . pump size from 155,000 through 750,000 GPM with total dynamic heads of 8 through 12 feet.

Eq. (96) has been adjusted for current pricing at a 10% annual rate of inflation.

2. Cold Pipe Salt Water Pump, Per

Using Reynolds number

$$Re_d = \frac{\rho_{sw} V_{sw} d_i}{\mu_{sw}}$$

where ρ_{sw}, μ_{sw} = properties of salt water at the cold pipe inlet temperature (assumed constant throughout the pipe).

V_{sw}, d_i = salt water velocity and inner pipe diameter (initialized and treated as design variable by the optimization code), velocity assumed constant over pipe length.

Pipe flow characteristics and friction factor can be identified. A pumping analysis will be developed for the cold pipe pump using the Darcy-Weisbach correlation, similar to the development in the preceding section.

Considering the resistance coefficient for minor pipe losses

- . Assume the inlet duct is well rounded [Ref. 11].

$$K_{\text{INLET}} = 0.5 \quad (97)$$

- . Assume piping enters condenser through an area which is abruptly changed [Ref. 10].

$$K_{\text{PLENUM}} = \left[1 + (d_i / T_{SD})^2 \right]^2 \quad (98)$$

where T_{SD} = condenser tube sheet diameter (assume tube sheet diameter is twice as large as the inner pipe diameter).

- . Assume one ninety-degree elbow is required in system [Ref. 11].

$$\frac{L}{D} = 30$$

Summing the results of Eqs. (84), (97), and (98), the total resistance coefficient can be expressed as

$$K = f \left(\frac{L_P}{d_i} + \frac{L}{D} \right) + K_{\text{INLET}} + K_{\text{PLENUM}} \quad (99)$$

where L_p = length of cold pipe.

d_i = inner diameter of cold pipe.

Pressure losses due to piping can then be determined using the Darcy-Weisbach, Eq. (83).

In analyzing the pressure drop across the condenser tubeside, the Darcy-Weisbach correlation is used again, but for different design assumptions.

- . Assume inlets to evaporator tubing are well rounded.

$$K = 0.5 \quad (100)$$

- . Assume outlet of condenser tubing expands to an infinite reservoir.

$$K = 1.0 \quad (101)$$

Defining Reynolds number for condenser tubeside flow, while assuming

$$T_{BULK} = T_{COLD(INLET)} \quad (102)$$

$$Re_d = \frac{\rho_{sw} V_{sw} d_i}{\mu_{sw}}$$

where ρ_{sw}, μ_{sw} = properties evaluated at condenser tubeside bulk temperature (initially assumed equal to cold pipe inlet temperature).

V_{sw, d_i} = average salt water velocity through tubing, inner condenser tube diameter (both are initialized and treated as design variables by the optimization code).

The corresponding friction factor, Eq. (85) or (86), and resistance coefficient can be determined

$$K_{CORE} = f \frac{L_t}{d_i} \quad (103)$$

where L_t, d_i , the condenser tube length and inner tube diameter are initialized and treated as design variables by the optimization code.

Summing the results of the resistance coefficient in Eqs. (100), (101), and (103), the pressure losses due to the condenser design may be determined using the Darcy-Weisbach correlation, Eq. (83).

A complete analysis of cold pipe losses must also include the effect of density head and a corresponding increase in pumping power requirements.

For most engineering problems involving the flow of liquids through a pipe, where the temperature change in the pipe is small, the density of the fluid is considered to be a constant and the fluid is termed "incompressible." However, the flow problem in OTEC cold pipe systems is unique. We can continue to assume that there is negligible change in the fluid temperature, virtually unaffected by the ocean thermal gradients, because of the system's characteristic high mass

flow rates. However, the height of the water column (1500 to 3000 feet) inside the pipe requires the effect of fluid compressibility to be taken into consideration.

The effect of an increase in density with depth can be expressed by the integral

$$\int_i^e \frac{dP}{\rho g}$$

with a density head defined as²

$$H_p = z_e - z_i + \int_i^e \frac{dP}{\rho g}$$

Integrating the pressure-density variation, the density head reduces to [Ref. 12]

$$H_p = z_e - z_i + \frac{1}{\rho_0 g} (P_e - P_i) \left[1 - \frac{K_m}{2} (P_e + P_i) \right]$$

where K_m = mean compressibility of salt water, f(salinity, temperature and pressure).

ρ_0 = reference density at which K_m is evaluated.

Considering pressure at any depth obtained from the integral,

$$P = -g \int_i^e \rho(z) dz$$

the density head can be rewritten as follows

$$H_p = (z_e - z_i) - \frac{1}{\rho_0} \int_{z_i}^{z_e} \rho(z) dz \left\{ 1 - \frac{K_m}{2} \int_0^{z_i + z_e} \rho g dz \right\}$$

²Note that z is measured as positive upward so that ocean depth values (z_e, z_i) are negative and $(z_e - z_i)$ is a positive quantity.

Rigorous procedures for calculating the density profile which is a function of temperature, salinity and pressure may be found in Ref. 13; however, they will not be discussed in this document.

For the purposes of simplification, the following solution technique was developed:

(1) If the liquid in the pipe is taken to have a constant density with respect to pressure, the compressibility approaches zero; the density head can then be expressed as

$$H_p = (z_2 - z_1) - \frac{1}{\rho_i} \int_{z_1}^{z_2} \rho(z) dz$$

(2) Converting the geometric term for elevation to an equivalent integral expression

$$z_2 - z_1 = \frac{1}{\rho_i} \int_{z_1}^{z_2} \rho_i dz$$

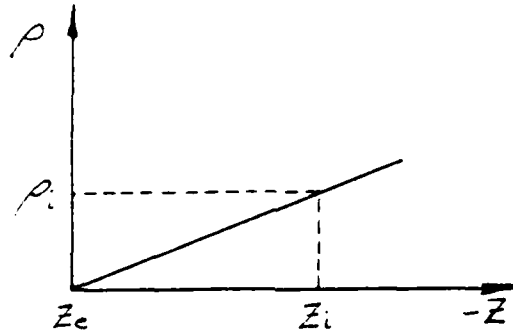
The reference density is taken to be the inlet value so that

$$\rho_i = \rho_0$$

and the density head can be rewritten as follows

$$H_p = \frac{1}{\rho_i} \int_{z_1}^{z_2} (\rho_i - \rho(z)) dz$$

(3) Assuming a linear distribution of density with depth, due to temperature variations, as illustrated below



the following linear expression for density with respect to depth may be formulated, where $z_e=0$ for convenience.

$$\rho_i - \rho = (\rho_i - \rho_e) \left(1 - \frac{z}{z_i}\right)$$

(4) Applying the equation developed in section 3 to the density head integral above and integrating over the range of values for sea water depth (z), the following equation is derived as a linear approximation to the density variation of sea water with respect to depth

$$H_p = \left(\frac{\rho_i - \rho_e}{\rho_i}\right) \left(-\frac{z_i}{2}\right)$$

where ρ_i, ρ_e = curve fit evaluations of density for specified depths of sea water. Data extracted from Ref. 14.

The results of the piping losses, core design losses, and density head are equivalent to the cold pipe salt water pumping system requirements

$$\Delta P_{\text{pump}} = \Delta P_{\text{PIPE SYSTEM}} + \Delta P_{\text{COND DESIGN}} + \Delta P_{\text{DENSITY}} \quad (105)$$

Using Eq. (93), Eq. (105) can be converted to a pumping head. Similarly, pumping power in terms of horsepower can be determined using Eq. (44).

$$P_{CP} = \frac{\dot{m}_{SW}}{\eta_P} \left(\frac{gH}{g_c} \right)$$

where

$$\dot{m}_{SW} = \rho_{SW} \left(\frac{\pi d_i}{4} \right)^2 V_{SW} \quad (106)$$

and ρ_{SW} = density of salt water evaluated for a constant inlet temperature.

$V_{SW, di}$ = cold pipe salt water velocity, and inner diameter (initialized and treated as design variables by the optimization code). Note salt water velocity through cold pipe is considered to be constant.

Pumping power can then be expressed in terms of megawatts electrical

$$P_{CP(MW)} = \frac{P_{CP}}{\eta_M} \times \text{CONVERSION FACTOR} \quad (107)$$

where η_M = pump motor efficiency (designer input).

Using the same arguments for the selection of an axial flow (impeller type) pump, as used for the hot pipe salt water pump, the pump cost algorithm developed by TRW can be applied to the cold pipe salt water pump assuming

the required conditions are validated.

$$C_{\text{pump}} = \left[(D/1000) 0.75 + 50 \right] 1.21 \times 10^3 \quad (108)$$

Equation (108) has been adjusted for current pricing at a 10% annual rate of inflation.

3. Ammonia Circulation Pump. P_{CIRC}

The function of the ammonia circulation pump is to circulate and lift saturated liquid ammonia from the condenser hot well at state point 1 and increase its pressure to exceed the operating conditions in the evaporator at state point 2.

In order to evaluate these characteristics, the following pumping elements will be included in the analysis:

- . Piping losses (friction and minor).
- . Heat exchanger shellside pressure drop.
- . Thermodynamic pressure head.
- . Elevation head.

As in the preceding analysis, Reynolds number is used to determine pipe flow characteristics

$$Re_d = \frac{\rho V d_i}{\mu}$$

where ρ, μ = saturated liquid properties of ammonia for the temperature at state point 1 (assume any temperature increase from pump work is negligible).

d_i = inner pipe diameter (initialized and treated as a design variable by the optimization code).

V = ammonia flow velocity determined from the preceding chapter, Eq. (50).

The ammonia pipe friction factor can then be determined from Eqs. (85) or (86), and the piping friction resistance coefficient can be expressed as

$$k = f \frac{L}{d_i} \quad (109)$$

where L = ammonia circulation pipe length (designer input).

Considering the resistance coefficient for minor pipe losses, assume there are four ninety-degree elbows in the system

$$K = 4 \frac{L}{D} \quad (110)$$

where $\frac{L}{D}$ = equivalent length in pipe diameters for a standard elbow [Ref. 11].

Summing the results of Eqs. (109) and (110), piping losses (friction and minor) can be determined using the Darcy-Weisbach equation (83).

$$\Delta P_{PIPE} = \rho \left[f \frac{L}{d_i} + 4 \frac{L}{D} \right] \frac{V^2}{2g_c} \quad (111)$$

The heat exchanger shellside pressure drop is also included in the pumping head requirement because it serves as a resistance to flow.

Pressure drop across the evaporator shellside was determined using the two-phase flow model (homogeneous) expressed by Eq. (33)

$$\Delta P_{EVAP} = \Delta P_{FRICTION} + \Delta P_{MOMENTUM} + \Delta P_{ELEVATION} \quad (112)$$

Since the pump is required to lift the working fluid to a higher elevation and increase its operating pressure, the following elements must be included in the analysis:

. Thermodynamic head

$$\text{where } \Delta P_{THERMO} = P_2 - P_1 \quad (113)$$

represents the difference in thermodynamic operating pressure between state point 2 and state point 1.

. Elevation head

$$\text{where } \Delta P_{ELEVATION} = Z_2 - Z_1 \quad (114)$$

Z_1 = datum.

Z_2 = elevation of the evaporator inlet above datum (taken to be equal to evaporator tube sheet diameter plus 25).

represents the lift head required to move the working fluid to a higher elevation.

The results of piping losses (111), evaporator pressure drop (112), the thermodynamic head (113) and elevation head (114) are equivalent to the ammonia circulation pump system requirements.

$$\Delta P_{\text{pump}} = \Delta P_{\text{PIPE}} + \Delta P_{\text{EVAP}} + \Delta P_{\text{THERMIC}} + \Delta P_{\text{ELEVATION}} \quad (115)$$

Using Eq. (93) with ammonia properties, Eq. (115) can be converted to pumping head and finally expressed as pumping power (horsepower).

$$P_{\text{CIRC}} = \frac{\dot{m}_{\text{NH}_3}}{\eta_p} \left(\frac{gH}{g_c} \right) \quad (116)$$

where \dot{m}_{NH_3} = mass flow rate of ammonia determined by Eq. (20) of the previous chapter.

η_p = pump mechanical efficiency (designer input).

Pumping power can then be expressed in terms of megawatts electrical

$$P_{\text{CIRC(MW)}} = \frac{P_{\text{CIRC}}}{\eta_M} \times \text{CONVERSION FACTOR} \quad (117)$$

where η_M = pump motor efficiency (designer input).

Because of high pumping head and moderate flow rates, good engineering design would dictate the use of a single suction centrifugal flow type pump.

Using the algorithm developed by Westinghouse Electric Co. [Ref. 15] from data provided by Bingham Pump Division, Portland, Oregon, the cost of the ammonia circulation pump can be expressed as

$$C_{\text{pump}} = \left(\frac{\dot{m}_{\text{NH}_3} v_f}{20100} \right)^{0.64} 1.21 \times 10^5 \quad (118)$$

where \dot{m}_{NH_3} = mass flow rate of ammonia (lb_m/hr)

v_f = specific volume of saturated liquid ammonia at state point 1 (ft³/lb_m)

Eq. (118) has been adjusted for current pricing at a 10% annual rate of inflation.

4. Ammonia Re-flux Pump, P_{RE-FLUX}

The function of the re-flux pump is to recycle ammonia droplets which are not evaporated in the heat absorption process. Saturated liquid at approximately the heat exchanger's operating pressure is lifted from the evaporator drain to the ammonia feed inlet, for redistribution as droplets across the evaporator tube bundle. (Drainage mass flow rate is assumed to be equal to 30% of the evaporator inlet feed mass flow rate.)

In order to evaluate these characteristics, the following pump elements will be analyzed:

- . Piping losses (friction and minor).

- . Thermodynamic pressure head.
- . Elevation head.

As in the preceding analysis, Reynolds number is used to determine pipe flow characteristics

$$Re_d = \frac{\rho V d_i}{\mu}$$

where ρ, μ = saturated liquid properties of ammonia for the average pressure across the evaporator.

d_i = inner pipe diameter (initialized and treated as a design variable by the optimization code).

V = ammonia flow velocity determined from the evaporator drainage mass flow rate assumed equal to 30% of the evaporator inlet feed mass flow rate (assume velocity constant throughout the pipe).

The re-flux pipe friction factor can be determined from Eqs. (85) or (86), and the piping resistance coefficient can be expressed as

$$K = f \frac{L}{d_i} \quad (119)$$

where L = ammonia re-flux pipe length (designer input).

Once again, considering the resistance coefficient for minor pipe losses assume there are four ninety-degree elbows in the system

$$K = 4 \frac{L}{D} \quad (120)$$

where $\frac{L}{D}$ = equivalent length in pipe diameters from a standard elbow.

Summing the results of Eqs. (119) and (120), piping losses (friction and minor) can be determined using the Darcy-Weisbach, equation (83)

$$\Delta P_{PIPE} = \rho \left[f \frac{L}{d_i} + 4 \frac{L}{D} \right] \frac{V^2}{2 g_c} \quad (121)$$

In order to determine the thermodynamic pressure head, the pressure drop across the evaporator for the saturated ammonia liquid must be analyzed. Since the saturated vapor and liquid are in thermodynamic equilibrium, the results of Eq. (112) apply. Therefore

$$\Delta P_{LIQ} = P_3 - P_2$$

Therefore, the thermodynamic pressure head is equal to the pressure drop across the evaporator for the saturated ammonia liquid.

$$\Delta P_{THERMO} = \Delta P_{LIQ} \quad (122)$$

Finally, the elevation head is equal to the elevation of the evaporator feed inlet with respect to datum, the drain outlet.

Therefore,

$$\Delta P_{ELEV} = Z_2 - Z_1 \quad (123)$$

where Z_1 = datum, drain outlet.

Z_2 = elevation of the evaporator inlet above datum
(taken to be equal to the evaporator tube
sheet diameter plus 10).

The results of piping losses (121), the thermodynamic pressure head (122), and elevation head (123) are equivalent to the ammonia re-flux pump system requirements.

$$\Delta P_{PUMP} = \Delta P_{PIPE} + \Delta P_{ELEVATION} + \Delta P_{THERMO} \quad (124)$$

As before, using Eq. (93), Eq. (124) can be converted to a pump head and finally expressed in terms of pumping power (horsepower).

$$P_{RE-FLUX} = \frac{\dot{m}_R}{\eta_p} \left(\frac{gH}{g_c} \right) \quad (125)$$

where \dot{m}_R = drainage mass flow rate.

η_p = pump mechanical efficiency (designer input).

Pumping power can be expressed in terms of megawatts electrical

$$P_{RE-FLUX(MW)} = \frac{P_{RE-FLUX}}{\eta_M} \times \text{CONVERSION FACTOR} \quad (126)$$

where $\eta_{(M)}$ = pump motor efficiency (designer input).

Using the same arguments for the selection of a centrifugal pump, the pump cost algorithm developed by Westinghouse can also be applied to the ammonia re-flux pump.

$$C_{pump} = \left(\frac{\dot{m}_R v_f}{80100} \right)^{0.64} 1.21 \times 10^5 \quad (127)$$

where \dot{m}_R = mass flow rate of evaporator drainage ammonia (lb_m/hr)

v_f = specific volume evaluated at the average evaporator pressure (ft³/lb_m)

Eq. (127) has been adjusted for current pricing at a 10% annual rate of inflation.

5. Parasitic Pump Losses

Parasitic pump losses is the summation of electrical auxiliary pumping requirements (hotel and maintenance loads not included) determined by Eqs. (95), (107), and (126).

$$P_{LOSS} = P_{HP} + P_{CP} + P_{CIRC} + P_{RE-FLUX} \quad (128)$$

V. TURBINE AND ELECTRICAL POWER

A. INTRODUCTION

The turbine generator is one of the critical elements of the OTEC power system. Its energy conversion efficiency and efficiency of design have a major effect on the overall system performance. To illustrate this point, Ref. 16 reported that a three-point change in turbine efficiency from 85 to 88% results in a 3.6% increase in gross power, and a 5% increase in net power developed.

This chapter will describe the analysis to evaluate the expansion turbine thermodynamic properties and generator output. The use of these properties will determine the internal turbine efficiency and outlet quality subject to design and thermodynamic constraints. The relationship between the condenser operating pressure (design variable) and the turbine outlet quality will be used to initialize the heat rejection characteristics of the condenser.

General literature on turbomachinery designed for OTEC closed cycle systems indicates that a turbine having the following characteristics

- . Double flow, axial inflow,
- . Four stages of expansion,
- . Operating at 1800 RPM,

provides the optimum aerodynamic design [Ref. 16]. However, it is not the intent of this thesis to analyze the geometry

and performance parameters of the turbine. Turbine geometry such as

- . Specific speed and specific diameter,
- . Wheel diameter,
- . Rotational speed,
- . Blade height,
- . Blade stresses,

should be treated as a separate systems problem using optimization to improve state-of-the-art design.

Parasitic losses due to the following generator turbine inefficiencies will be evaluated in this section.

- . Generator mechanical and electrical.
- . Turbine mechanical.

As an overview of the turbine-generator analysis, the following major steps of the algorithm are listed in order of their execution:

- . Gross electrical output with no parasitic losses (129).
- . Enthalpy at state point 5 (130).
- . Turbine outlet quality (131).
- . Entropy at state point from a specified outlet quality (132).
- . Quality and enthalpy at state point 5s (133, 134).
- . Internal (adiabatic) turbine efficiency (135).
- . Turbine cost analysis (137).
- . Generator cost analysis (138).

In the following section, the basic steps summarized above will be described in detail.

B. ANALYSIS OF THE TURBINE AND ELECTRICAL POWER REQUIREMENTS

1. Gross Electrical Output and Inefficiency Losses

If the net electrical output required is indicated by (in terms of megawatts), the gross electrical load at the turbine shaft can be expressed as

$$\dot{E}_g = \frac{\dot{E}}{\eta_{TM} \eta_{GEN}} + P_{LOSS} \quad (129)$$

where P_{LOSS} = parasitic pump losses determined by Eq. (128).

η_{TM} = turbine mechanical efficiency (designer input).

η_{GEN} = generator mechanical and electrical efficiency (designer input).

The loss of electrical output due to generator-turbine inefficiencies is equal to

$$\dot{E}_{LOSS} = \dot{E} \left(\frac{1}{\eta_{TM} \eta_{GEN}} \right)$$

2. Turbine Efficiency

The power developed across the turbine is

$$\dot{E}_g = \dot{m} (h_5 - h_4)$$

where \dot{m} = mass flow rate of ammonia given by Eq. (48).

h_4 = enthalpy at state point 4, Eq. (42).

From this, the enthalpy at state point 5 can be calculated.

If we initialize the operating pressure of the condenser in terms of P_5 , the following relations may be expressed

$$h_{5g} = h_g \Big|_{P_5} \quad h_{5f} = h_f \Big|_{P_5} \quad (130)$$

Therefore, it follows that the turbine outlet quality, x_5 , can be determined from

$$h_5 = h_{5f} + x_5 (h_{5g} - h_{5f}) \quad (131)$$

Having established the moisture separator outlet pressure and temperature, Eqs. (40) and (41), the entropy at state point 4 can be determined for a known separator outlet quality (designer input) using the following relations

$$\begin{aligned} S_{4f} = S_f \Big|_{T_4} \quad S_{4g} = S_g \Big|_{T_4} \\ S_4 = S_{4f} + x_4 (S_{4g} - S_{4f}) \end{aligned} \quad (132)$$

For isentropic turbine work,

$$S_4 = S_{5s} \quad (133)$$

the quality at state point 5s may be determined using the following relations

$$\begin{aligned} S_{5g} = S_g \Big|_{T_5} \quad S_{5f} = S_f \Big|_{T_5} \\ S_{5s} = S_{5f} + x_{5s} (S_{5g} - S_{5f}) \end{aligned} \quad (134)$$

Having determined the quality at state point 5s, the enthalpy can now be determined.

$$h_{5s} = h_{5f} + X_{5s} (h_{5g} - h_{5f}) \quad (135)$$

Using the results of Eqs. (41), (130), and (132), the internal turbine efficiency (adiabatic) can be determined, expressed by

$$\eta_T = \frac{h_4 - h_5}{h_4 - h_{5s}} \quad (136)$$

To ensure a realistic selection of internal efficiency, the following constraints are attached to the optimization code

- $h_5 < h_{5g}$
- $X_{5s} < X_5$
- $\eta_T \leq 90\%$

3. Turbine Cost Analysis

The ammonia turbine cost is based on an algorithm developed by Westinghouse to estimate manufacturing costs [Ref. 15].

$$C_{TURB} = 2.42 \times 10^6 \left(0.375 + \dot{E}_g / 136000 N_f \right) F_f \quad (137)$$

where \dot{E}_g = gross electrical output in KW.
 N_f = 2 (for a double flow turbine).
 F_f = flow price factor (1.0 for single-flow, 1.447 for double-flow).

The above algorithm is valid for the following conditions:

- . Double flow, axial inflow.
- . Multi-stage.
- . Operating at 1800 RPM.

The generator cost will be based on an algorithm developed by TRW from data provided by selected manufacturers,

$$C_{GEN} = (0.023 \dot{E}_g + 0.3) 1.21 \times 10^6 \quad (138)$$

and is valid for the following conditions

- . 1800 RPM rotor speed.
- . power factor 0.8.

Eqs. (137) and (138) have been adjusted for current pricing at a 10% annual rate of inflation.

VI. CONDENSER

A. INTRODUCTION

As indicated in the introduction to Chapter III, several heat exchanger concepts have been proposed for the closed-cycle OTEC system, with variations in their design.

The analysis to be presented for the condensing heat exchanger will be based upon the following design characteristics:

- . Single-pass shell and tube heat exchanger.
- . Horizontal/vertical orientation of tubes with an equilateral triangle or square tube profile.
- . Smooth plain-tube configuration (no enhancements).
- . Tube material (titanium or aluminum based on a 30-year life-cycle criterion).
- . Biofouling control based upon an achievable fouling factor.
- . Heat exchanger centerline located on sea surface.

As an overview of the condenser analysis, the following major steps in the algorithm are listed in order of their execution:

- . Initialization of design variables (DV).
 - .. Tube length.
 - .. SW velocity through condenser tubes.
 - .. Outer tube diameter.
 - .. Tube profile pitch ratio.
- . Amount of heat rejection (139).
- . Tubeside bulk temperature (142).

- . Total number of tubes (143).
- . Log mean temperature difference (144).
- . Conductance (146).
- . Number of transfer units (145).
- . Heat exchanger effectiveness (147).
- . Initially assume a value for ammonia heat transfer coefficient (151).
- . Single tube conductance (148).
- . Average heat rejection per tube (152).
- . Film temperature (153).
- . Revised ammonia heat transfer coefficient (154, etc.); iterate with (151).
- . Tube profile, flow parameters across the tube bank (158, etc.).
- . Tube sheet diameter (163).
- . Condenser shellside pressure drop for two-phase flow (166).
- . Revised properties at state point 1 (171, 172); iterate with (21).
- . Overall heat transfer coefficient (173).
- . Total heat transfer surface area (174).
- . Revised condenser tube length (175).
- . Heat exchanger cost analysis.

In the following section, the basic steps summarized above will be described in detail.

B. ANALYSIS OF THE CONDENSER

1. Amount of Heat Rejection, \dot{Q}

Using the calculated value for enthalpy at state point 5, equation (131) from the previous chapter, the ideal

values at state point 1, Eq. (21), and the steady-state mass flow rate of ammonia, Eq. (48), the amount of heat rejected by the condenser can be expressed as

$$\dot{Q} = \dot{m}_{NH_3} (h_5 - h_1) \quad (139)$$

2. Tubeside Bulk Temperature

As in condenser tubeside Reynolds number, salt water properties will be evaluated at bulk temperature, initially assumed equal to the cold pipe inlet temperature.

Using this premise, the condenser salt water capacity rate can be evaluated

$$\dot{C}_{min} = \dot{m}_{cp} c_{p,sw} \quad (140)$$

where $c_{p,sw}$ = specific heat of salt water initially evaluated at the cold pipe inlet temperature.

\dot{m}_{cp} = mass flow rate of salt water through the cold pipe previously evaluated by Eq. (107).

Using the results of Eqs. (139) and (140), and the known cold pipe inlet temperature, the condenser salt water outlet temperature may be evaluated from the basic expression

$$\dot{Q} = \dot{C}_{min} (T_{c_o} - T_{c_i}) \quad (141)$$

where T_{c_o}, T_{c_i} = condenser salt water outlet and inlet temperatures, respectively.

Having determined the condenser salt water outlet temperature, the revised bulk temperature can be expressed as

AD-A098 567

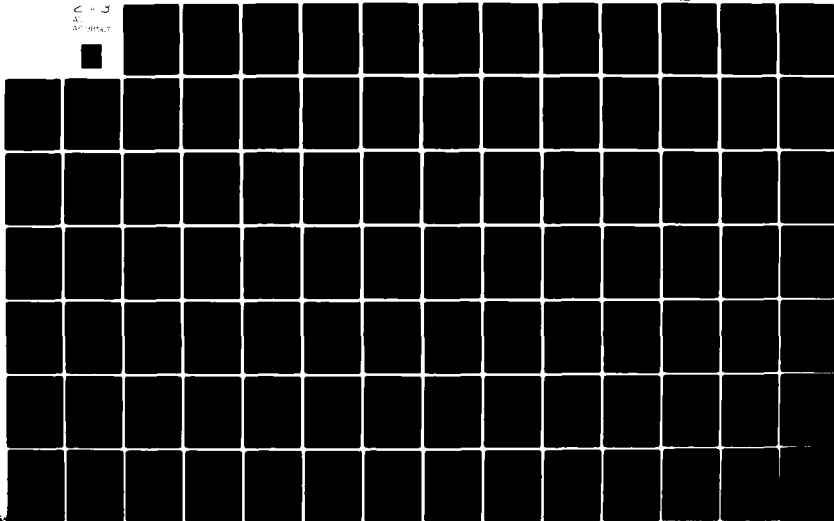
NAVAL POSTGRADUATE SCHOOL, MONTEREY, CA
OPTIMIZATION OF A LOW DELTA T RANKINE POWER SYSTEM. (U)
DEC 80 R C SCHAUBEL

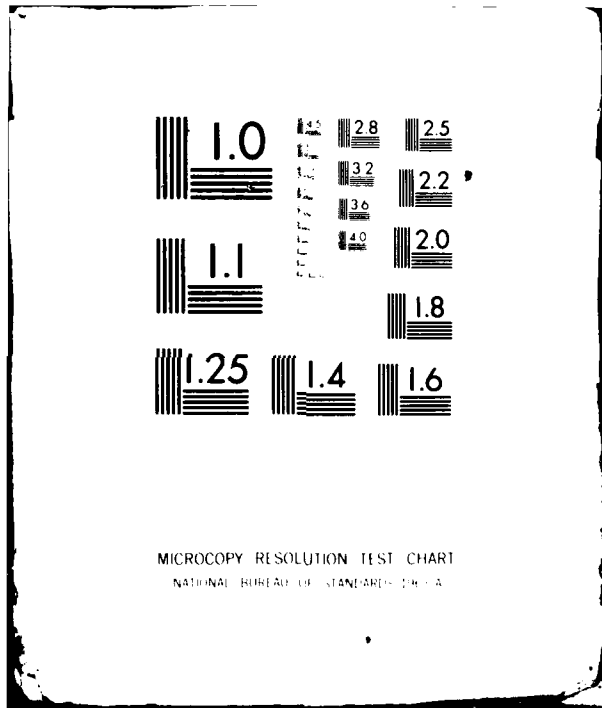
F/G 20/13

UNCLASSIFIED

NL

C-3
A
A098567





MICROCOPY RESOLUTION TEST CHART
NATIONAL BUREAU OF STANDARDS-1963-A

$$T_B = \frac{T_{c_o} + T_{c_i}}{2} \quad (142)$$

Using the revised condenser bulk temperature and iterating with Eq. (102) corrects the operating temperature for salt water properties which are essential to the analysis.

3. Total Number of Condenser Tubes, N_t

Since the mass flow rate of salt water through the cold pipe is equivalent to the mass flow rate through the condenser, according to the law of continuity,

$$\dot{m}_{cp} = \dot{m}_{COND}$$

it follows that the number of condenser tubes for a specified tube diameter, can be evaluated using the following expression:

$$\dot{m} = \rho_{sw} \frac{\pi d_i^2}{4} V_t N_t \quad (143)$$

where ρ_{sw} = average salt water density evaluated at bulk temperature.

d_i = inner tube diameter (initialized and treated as a design variable by the optimization code).

V_t = average salt water velocity through the condenser (initialized and treated as a design variable by the optimization code).

4. Log Mean Temperature Difference, LMTD

Using the result of Eq. (141), the known pipe salt water inlet temperature, and the inlet temperature of ammonia evaluated at state point 5, the LMTD of the condenser may be expressed as

$$LMTD = \frac{T_{c_o} - T_{c_i}}{\ln\left(\frac{T_s - T_{c_i}}{T_s - T_{c_o}}\right)} \quad (144)$$

5. NTU-Effectiveness Relations

The number of transfer units which is a measure of the condenser size can be determined from the basic expression

$$NTU = \frac{U_o A_o}{C_{min}} \quad (145)$$

where the conductance ($U_o A_o$) of the heat exchanger is a function of the heat absorbed and the LMTD.

$$\dot{Q} = (U_o A_o) LMTD \quad (146)$$

The condenser effectiveness can then be expressed as

$$\epsilon = 1 - e^{(-NTU)} \quad (147)$$

for a two-phase flow, regardless of the flow geometry.

6. Single-Tube Conductance, $U_o A_o$.

Using the resistance analysis derived in Chapter III, Section 4 for an initialized tube length

$$L = L_i$$

the heat exchanger conductance for a single tube can be expressed as

$$U_o A_o = \frac{1}{\eta_i h_{sw} A_i + \frac{1}{A_i} R_{fsw} + \frac{\ln d_o/d_i}{2\pi K L} + \frac{1}{A_o} R_{fNH_3} + \frac{1}{\eta_o h_{NH_3} A_o}} \quad (148)$$

where h_{sw} = tubeside heat transfer coefficient.

R_{fsw} = salt water fouling heat transfer resistance.

K = thermal conductivity of the tube material.

A_o, A_i = total outer and inner tube surface areas (including fin and bare tube); tube length is initialized and treated as a design variable by the optimization code).

R_{fNH_3} = ammonia fouling heat transfer resistance

η_o, η_i = outer and inner total fin efficiency

a. Tubeside Reynolds Number

Since the salt water heat transfer correlation is dependent on tubeside flow, Reynolds number must be evaluated

$$Re_d = \frac{\rho_{sw} V_{sw} d_i}{\mu_{sw}}$$

where ρ_{sw}, μ_{sw} = salt water density and viscosity are evaluated for the fluid's bulk temperature.

d_i, V_{sw} = inner diameter and average salt water tube velocity.

Reynolds numbers greater than 2300 will be indicative of turbulent flow [Ref. 3].

b. Salt Water Heat Transfer Coefficient, h_{sw}

Once again the empirical relationship proposed by Sieder and Tate [Ref. 3] will be used for laminar heat transfer in tubes and as defined by

$$Nu_d = 1.86 (Re_d Pr)^{1/3} \left(\frac{d_i}{L}\right)^{1/3} \left(\frac{\mu}{\mu_w}\right)^{0.14}$$

Nusselt and Prandtl numbers are defined as

$$Nu_d = \frac{h_{sw} d_i}{k_{sw}} \quad (149)$$

$$Pr = \frac{c_{p_{sw}} \mu_{sw}}{k_{sw}} \quad (150)$$

where dynamic viscosity, specific heat, and thermal conductivity of salt water are evaluated at the salt water bulk temperature.

The effect of the viscosity ratio in the Sieder-Tate equation is considered negligible, and will hereafter be dropped from the expression. The assumptions and validity condition associated with the Sieder-Tate equation were stated in Chapter III, Section 4, and will not be repeated here.

For fully developed turbulent flow, again the Dittus-Boelter correlation [Ref. 3] was used.

$$Nu_d = 0.023 Re_d^{0.8} Pr^{0.3}$$

Nusselt and Prandtl numbers are previously defined by Eqs. (149) and (150). Assumptions and conditions for validity were stated in Chapter III, Section 4.

c. Salt Water Fouling Heat Transfer Resistance

As indicated previously, it will be assumed that the fouling resistance for tube side salt water can be maintained at $.00025 \text{ (hr. ft}^2\text{F/BTU)}$.

d. Ammonia Shellside Heat Transfer Coefficient, h_{NH_3}

Initially, h_{NH_3} will be assumed

$$h_{NH_3} = 1000 \text{ (BTU/hr.ft}^2\text{F)} \quad (151)$$

since its value cannot be directly calculated during this phase of the analysis.

Using the following single-tube thermal resistance

$$R_1 = \frac{1}{\eta_i h_{sw} \pi d_i L}$$

$$R_2 = \frac{1}{\eta_i h_{fsw} \pi d_i L}$$

$$R_3 = \frac{\ln d_o/d_i}{2\pi KL}$$

$$R_5 = \frac{1}{\eta_o h_{NH_3} \pi d_o L}$$

an initial value for single tube conductance (outer tube surface) may be calculated

$$U_o A_o = \frac{1}{R_1 + R_2 + R_3 + R_5}$$

7. Film Temperature for Property Evaluation, T_f

In order to evaluate the shellside ammonia heat transfer coefficient, working fluid properties must be evaluated at the film temperature.

This can be accomplished by using the results of the single tube conductance, the tube side bulk temperature and the working fluid saturation temperature, expressed in the following equation for single tube heat transfer rate (average).

$$\dot{Q} = U_o A_o (T_5 - T_{BULK}) \quad (152)$$

Again using the resistance analysis as in Chapter III, the shellside wall temperature may be expressed as

$$T_{W_2} = T_{BULK} + \dot{Q} (R_1 + R_2 + R_3)$$

Knowing the shellside wall temperature and the free-stream temperature, the film temperature can be derived from their arithmetic mean

$$T_f = \frac{T_{W_2} + T_5}{2} \quad (153)$$

For purposes of this calculation, saturated temperature conditions at state point 5 are taken to represent

free-stream conditions, when in fact the two-phase process will experience a pressure drop and a corresponding drop in temperature.

8. Revised Shellside Ammonia Heat Transfer Coefficient,

$$\bar{h}_{NH_3}$$

This analysis will include correlations for both horizontal and vertical heat exchangers.

In the horizontal-tubed condenser, Nusselt's correlation was used as a predictor [Refs. 7 and 17], for laminar flow

$$\bar{h} = 0.95 \left(\frac{K_f^3 \rho_f^2 g L}{\mu_f w} \right)^{1/3} \quad (154)$$

where w = estimate of ammonia mass flow rate across each tube.

K_f, ρ_f, μ_f = properties evaluated at film temperature.

L = tube length (initialized and treated as a design variable by the optimization code).

This correlation is probably conservative, since it does not consider turbulence due to high vapor velocity or splashing of condensate [Ref. 7].

For turbulent flow, Nusselt's correlation is increased by 10% as recommended by Jakob [Ref. 17]

$$\bar{h} = 1.045 \left(\frac{K_f^3 \rho_f g L}{\mu_f w} \right)^{1/3} \quad (155)$$

The laminar-turbulent transition point is defined by a Reynolds number of 2100, where the pseudo-Reynolds number for film-type condensation on horizontal tubes is defined as [Ref. 7]

$$Re = \frac{2\Gamma}{\mu_f}$$

where Γ = mass flow rate of condensate per tube over its length.

In the vertical tubed condenser, both Nusselt's and Kirkbride's correlations were used as predictors [Ref. 7].

For laminar flow, Nusselt's correlation is increased by a factor of 1.28 as recommended by McAdams [Ref. 7]:

$$\bar{h} = 1.28 \left[1.47 \left(\frac{\mu_f}{K_f^3 \rho_f^2 g} \right)^{-1/3} \left(\frac{4\Gamma}{\mu_f} \right)^{-1/3} \right] \quad (156)$$

where Γ = mass flow rate of condensate per tube over its diameter.

For turbulent flow, Kirkbride's correlation is applied

$$\bar{h} = 0.0077 \left(\frac{\mu_f^2}{K_f^3 \rho_f^2 g} \right)^{-1/3} \left(\frac{4\Gamma}{\mu_f} \right)^{0.4} \quad (157)$$

The laminar-turbulent transition point is defined by a Reynolds number of 1800, where the pseudo-Reynolds number for film-type condensation on vertical tubes is defined as [Ref. 7]

$$Re = \frac{4\Gamma}{\mu_f}$$

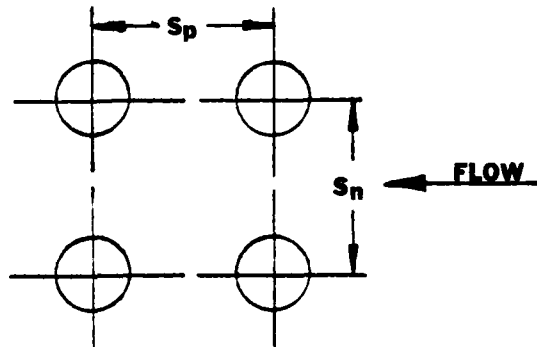
After using the pseudo-Reynolds number to establish the flow in which regime the system is operating, the revised heat transfer coefficient for film-type condensation may be calculated and then iterated with the initial assumption for the shellside heat transfer coefficient, Eq. (151). Once again this will have a convergence effect on variables in which the shellside heat transfer coefficient is a function, moving closer to actual OTEC system operating point characteristics.

9. Tube Profile, Flow across Tube Bank, and Tube Sheet Diameter

Since the condenser tube bundle involves multiple rows of tubes, the geometry of the tube profile arrangement is important to determine the shellside heat transfer coefficient, the tube sheet diameter and the shellside pressure drop associated with the "homogenous" two-phase flow model [Ref. 4].

Using the same arrangements shown in Chapter III, Section 2,

IN-LINE



$$S_n = P_R d_o \quad (158)$$

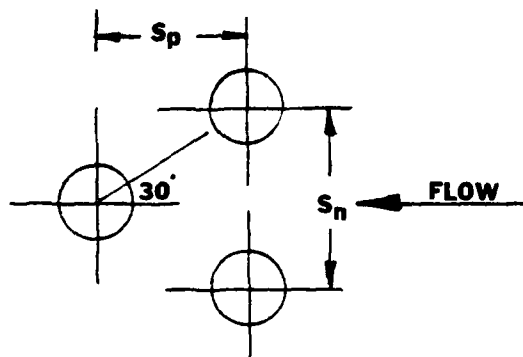
$$A_p = S_n^2 \quad (159)$$

where S_n = pitch ratio x outer tube diameter.

P_R = pitch ratio (initialized and treated as a design variable for the optimization code).

A_p = tube profile area per tube

STAGGERED



where

$$S_n = 2 P_R d_o \sin 30^\circ \quad (160)$$

$$S_p = P_R d_o \cos 30^\circ \quad (161)$$

$$A_p = S_n S_p \quad (162)$$

the ratio of minimum flow area to the frontal area can be expressed as

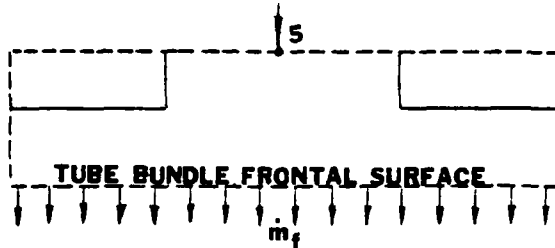
$$\frac{A_{ff}}{A_f} = \frac{S_n - d_o}{S_n} \quad (163)$$

Using the selected tube profile geometry and knowing the number of condenser tubes by Eq. (143), the tube sheet diameter for the condenser design can be evaluated from the following expression

$$N_t A_p = \frac{\pi T_{SD}^2}{4} \quad (164)$$

where T_{SD} = Tube sheet diameter.

To analyze the shellside ammonia flow velocity, the following control volume is introduced (turbine generator discharge and top portion of the condenser).



Since the mass flow rate remains unchanged across any boundary

$$\dot{m}_5 = \dot{m}_f$$

Furthermore, if we assume the condenser has the capability to evenly distribute vapor across the tube bundle (distribution baffles), the following development applies to the vapor coverage:

Let $(A_f)_{VAP} = A_f \eta$

where η = percent of tube frontal area which is covered by vapor.

$$\dot{m}_5 = \rho_s A_s V_s$$

$$\dot{m}_f = \rho_f A_f V_f \eta$$

where A_5 = condenser inlet cross-sectional area.

V_5 = turbine discharge ammonia velocity.

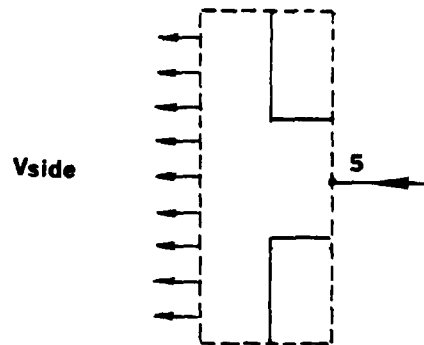
Therefore

$$V_f = \frac{\rho_5 A_5}{\rho_f A_f \eta} V_5$$

If $\eta = \rho_5 A_5 / A_f \rho_f$, it follows that the turbine discharge velocity is equal to the average velocity of ammonia at the tube frontal area boundary. A determination of the distribution fraction η requires a detailed knowledge of the design of the turbine/condenser interface. In the absence of this information it is assumed that

$$V_f = V_5$$

A similar argument could be presented for a vertical tubed condenser where turbine discharge is admitted to a distribution ring that bands the condenser tube bank. Exhaust vapor would travel radially through the tube bundle and then collect at the bottom after vertical film-condensation.



Again, in the absence of a detailed design, it is assumed that

$$V_{SIDE} = V_5$$

Considering the minimum free-flow area for a horizontal tubed condenser, A_{ff} can be derived using Eq. (163) and the projected frontal area.

$$A_f = T_{SD} L_t$$

$$A_{ff} = A_f \left(\frac{S_n - d_o}{S_n} \right) \quad (165)$$

where A_f = the flow frontal area.

L_t = tube length.

For vertical condensers

$$A_f = \pi T_{SD} \times \text{FRONTAL LENGTH OF VAPOR INLET FLOW}$$

Using the previously calculated value of the ammonia flow rate and Eq. (165), mass velocity for the minimum free flow area can be expressed as

$$G = \frac{\dot{m}_4}{A_{ff}} \quad (166)$$

10. Pressure Drop of Two-Phase Flow across a Bank of Tubes, ΔP

The pressure drop in the two-phase flow condensing heat exchanger will be determined using the homogeneous model introduced in Chapter III. The model will consist of three components -- friction loss, momentum change, and elevation pressure drop arising from the effects of gravity.

The local pressure drop for a two-phase flow may be expressed as

$$\Delta P_{\text{COND}} = \Delta P_{\text{FRICTION}} + \Delta P_{\text{MOMENTUM}} + \Delta P_{\text{ELEVATION}} \quad (167)$$

For a given channel length, L_c , the pressure drop components can be expressed by

$$\Delta P_{\text{FRICTION}} = \frac{f G^2 \bar{v}}{D_e 2 g_c} L_c \quad (168)$$

$$\Delta P_{\text{MOMENTUM}} = \frac{G^2 \bar{v}}{g_c} \quad (169)$$

$$\Delta P_{\text{ELEVATION}} = \frac{g}{\bar{v} g_c} L_c \quad (170)$$

where f = single phase friction factor by Jakob expressed in Eq. (35) or (36).

G = mass flow velocity determined from Eq. (166).

L_c = channel flow length, defined for horizontal tubed condensers as $L_c = T_{SD}$ (tube sheet diameter) and for vertical tubed condensers as $L_c = L_t$ (tube length).

D_e = equivalent diameter of flow channel, defined by

$$D_e = P_R d_o - d_o$$

\bar{v} = mean specific volume defined by

$$\bar{v} = v_f \left[1 + \frac{x}{v_f} (v_g - v_f) \right]$$

where X = quality of mixture (state point 5).

v_f = specific volume of liquid (state point 1)

v_g = specific volume of vapor (state point 5).

All components of the pressure drop model Eqs. (168, 169, and 170) can be determined using the preceding information.

11. Revised Properties at State Point 1

Since Eq. (167) represents the pressure drop across the condenser shellside, the actual pressure at state point 1 or condenser outlet may be determined from

$$P_{1(NEW)} = P_1 - \Delta P_{COND} \quad (171)$$

where P_1 is previously described as the condenser operating pressure for the ideal cycle.

Operating on the saturated liquid line on the Temperature-Entropy diagram, the following properties are defined:

$$h_{1(NEW)} = h_f \Big|_{P_{1(NEW)}} \quad T_{1(NEW)} = T_{SAT} \Big|_{P_{1(NEW)}} \quad (172)$$

The subscript (NEW) representing a revised property will hereafter be dropped from the expression in Eq. (172).

Until now, we assumed the condenser outlet temperature and pressure were designed to operate as an ideal system, without a pressure drop. Therefore, using the revised temperature at state point 1 and iterating over the range from Eq. (21) until an acceptable convergence criterion is achieved, all the preceding variables as function of T_1

will be reevaluated to complete the closed-loop cycle of the simulated OTEC power system.

12. Overall Heat Transfer Coefficient, U_o

The quantity "U" represents a measure of the total thermal resistances in the flow path. Therefore, using the tube conductance expressed in Eq. (148) which is divided by the outer heat transfer surface area of a single tube, the overall heat transfer coefficient for the condenser can be determined.

The thermal resistances are now expressed as

$$R_1 = \frac{d_o}{\eta_i h_{sw} d_i}$$

$$R_2 = \frac{d_o}{\eta_i h_{fsw} d_i}$$

$$R_3 = \frac{d_o \ln d_o/d_i}{2K}$$

$$R_5 = \frac{1}{\eta_o h_{NH_3}}$$

and the overall heat transfer coefficient for the condenser may be calculated using

$$U_o = \frac{1}{R_1 + R_2 + R_3 + R_5} \quad (173)$$

13. Total Condenser Heat Transfer Surface Area, A_t

Having determined the corrected number of condenser transfer units (145), salt water capacity rate (140) and overall heat transfer rate (173), the total condenser heat transfer area can be calculated from the NTU expression

$$NTU = \frac{U_o A_t}{C_{min}} \quad (174)$$

14. Revised Condenser Tube Length

Using the total heat transfer surface area calculated from Eq. (174) and the total number of condenser tubes (143), the revised condenser tube length can be determined from the basic expression

$$A_t = N_t \pi d_o L_t (REVISED) \quad (175)$$

At this time, it is necessary to iterate the condenser design until the two values (initial and revised) of the tube length converge. This iteration may be accomplished by the COPES routine if the following constraint is defined

$$L_{DIFF} = L_t (REVISED) - L_t (INITIAL)$$

Minimization of this difference will cause continual adjustment of the required tube length, already treated as a design variable by the optimization code.

15. Condenser Heat Exchanger Cost Analysis

As indicated in Chapter III, TRW developed sets of equations to represent the costs of various heat exchanger component parts for shall diameters ranging from 10-35 feet and 35-50 feet [Ref. 9].

The following are the TRW component cost equations for the condensing heat exchanger. Prior equation reference numbers will be substituted where equalities exist with the evaporative heat exchanger component cost expressions.

for tube sheet diameter 10-35 feet

. Drilling time/tube sheet thickness. (58)

. Thickness of the tube sheet. (59)

. Tube sheet labor cost. (60)

. Tube sheet material cost. (61)

. Tube installation cost. (62)

. Heat exchanger drill cost. (63)

. Ammonia distribution plate and baffles cost.

$$C_{DPB} = 1.539 \times 10^{-2} t_d N_t T_{SD}^{2.0} \quad (176)$$

. Bustle, flanges, channels and flow plate cost.

$$C_{BFCF} = 1185.286 T_{SD}^{2.0} \quad (177)$$

. Tube material cost.

$$C_{TM} = (C_1 L_t + C_2) N_t d_o / 1.5 \quad (178)$$

where C_1 = curve fit of tube material cost
per foot.

C_2 = tube machining cost if required.

. Heat exchanger header cost. (67)

. Water inlet, nozzles and support cost.

$$C_{WINS} = 10106.475 T_{SD} \quad (179)$$

. Tube welding costs (Titanium tubes). (69)

The sum of the preceding costs would equal the cost to fabricate one OTEC condenser with a tube sheet diameter of 10-35 feet (all the preceding component costs have been adjusted for current pricing at a 10% annual rate of inflation).

If our analysis is based on a 30-year life-cycle criterion, no adjustments are necessary to any component cost equation if titanium tubing is selected. However, using Al 5052-0, the expense of retubing must be considered to meet the 30-year life-cycle criterion, as in the case of the evaporation. For convenience, and possible subsequent modification, these considerations are repeated here.

Based upon the utility of Al 5052-0, two complete condenser retubings will be required to meet the basic 30-year criterion. This implies Eqs. (62) and (178) must be modified to reflect the costs of retubing at the 10 and 20 year point in the cycle.

. Aluminum tube installation cost.

$$C_{ATI} = C_{TI} [1 + (1+i)^{10} + (1+i)^{20}] \quad (180)$$

where i = projected annual inflationary
rate (input by customer).

. Aluminum tube material cost.

$$C_{ATM} = C_{TM} [1 + (1+i)^{10} + (1+i)^{20}] \quad (181)$$

for tube sheet diameter 35-50 feet.

. Drilling time/tube sheet thickness (58)

. Thickness of the tube sheet. (59)

. Tube sheet labor and material costs
(titanium). (72, 73)

. Tube sheet labor and material costs
(aluminum). (74, 75)

. Tube installation cost. (76)

. Tube material cost. (178)

. Heat exchanger shell cost. (77)

. Ammonia distribution plate and
baffles cost.

$$C_{DPB} = 9.825 N_t^{0.479} t_d^{2.184} \quad (182)$$

. Bustle, flanges, channels and
flow plate.

$$C_{BFCF} = 382.824 T_{SD}^{2.184} \quad (183)$$

. Heat exchange head cost.

$$C_{HXH} = 939.62 T_{SD}^{1.43} \quad (184)$$

. Water inlet, nozzles, and supporters
cost.

$$C_{WINS} = 7453.6 T_{SD}^{1.056} \quad (185)$$

. Tube welding cost (titanium tubes). (82)

As indicated previously, the cost to fabricate one OTEC condenser with a tube sheet diameter of 35 to 50 feet is equal to the sum of component costs (note, all the preceding component costs have been adjusted for current pricing at a 10% annual inflation rate).

For an analysis based on a 30-year life-cycle criterion, the additional costs for replacing aluminum tubing must be considered and Eqs. (180) and (181) apply.

VII. NUMERICAL OPTIMIZATION

A. INTRODUCTION

Nearly all design processes attempt the minimization or maximization of some parameter or design objective. For the design to be acceptable, it must satisfy a set of constraints which impose limits or bounds on design parameters.

For the stated problem a computer program can be written to perform the basic analysis of the proposed design. If any parameters fall outside the prescribed bounds, the design engineer changes the parameters and re-runs the program. In effect, the computer code provides the analysis with the engineering making the actual design decisions.

A logical extension to the computer-aided approach is a fully automated design, where the computer also makes the actual design decisions and performs trade-off studies. The COPES program provides this automated design and trade-off capability by the use of the optimization program COPES/CONMIN [Ref. 18]. COPES is an acronym for Control Program for Engineering Synthesis, and CONMIN is an acronym for CONstrained function MINimization. Subsequently, a FORTRAN analysis program simulating a closed-cycle OTEC power system can be coupled to the COPES program for automated design, using some basic programming guidelines [Ref. 18].

B. COPES/CONMIN

There are many numerical optimization schemes available to the engineer. Methods employed by these schemes fall into four basic categories: random search, sequential unconstrained minimization, optimality criteria, and direct constrained optimization. The optimization program, selected for automated design analysis of the simulated OTEC power system, is based upon direct constrained optimization.

Before any discussion of the optimization technique, basic definitions are summarized for convenient reference [Ref. 19]:

- . Design variables - those parameters which the optimization program is permitted to change in order to improve the program.
- . Objective function - the parameter which is to be minimized or maximized during the optimization process.
- . Inequality constraint - one-sided conditions which must be satisfied for an acceptable design.
- . Equality constraint - condition which must be equaled for the design to be acceptable.

. Side constraints - upper and lower bounds in a design variable.

Assuming that the FORTRAN analysis program has been developed and a particular objective function has been selected, the general optimization problem can be stated as [Ref. 20]:

Find the vector of design variables, \bar{X} , to

$$\text{Minimize } F(\bar{X}) \quad (186)$$

Subject to the constraints:

$$G_j(\bar{X}) \leq 0 \quad j=1, NCON \quad (187)$$

$$H_j(\bar{X}) = 0 \quad j=1, NEQ \quad (188)$$

$$VLB_i \leq \bar{X}_i \leq VUB_i \quad i=1, NDV \quad (189)$$

where \bar{X} = the vector containing the set of independent design variables.

$F(\bar{X})$ = the objective function to be minimized.

$G_j(\bar{X})$ = inequality constraint (NCON is the number of such constraints).

$H_j(\bar{X})$ = equality constraint (NEQ is the number of such constraints).

VLB_i/VUB_i = lower and upper bounds, respectively, on the design variables.

If all inequalities of Eqs. (187) and (189) are satisfied, the design is said to be feasible if any constraint is not satisfied, the design is infeasible. If the objective function

is a minimum and the design is feasible, it is said to be the optimal design.

In order to start the optimization algorithm, the initial set of design variables, \bar{X} , must be specified. It is desirable, but not essential, that the initial design variables provide a feasible solution. The optimization algorithm will then proceed in an iterative fashion using the following relationship

$$\bar{X}^{q+1} = \bar{X}^q + \alpha * \bar{S}^q$$

where q = the iteration number.

α = scalar quantity which defines the move in the search direction.

\bar{S} = vector search direction which will reduce the objective function (useable direction) without violating constraints (feasible direction).

To solve this problem, the optimization program COPES/CONMIN is used [Ref. 18]. CONMIN uses the Fletcher-Reeves algorithm for locally unconstrained problems [Ref. 20] and Zoutendijk's method of feasible directions (modified to improve efficiency and reliability and to deal with designs which do not initially satisfy all the constraints) for locally constrained problems [Ref. 21].

However, CONMIN does not handle equality constraints directly, but rather by means of penalty parameters. To achieve this, the objective function is augmented as follows

[Ref. 19]:

$$F'(\bar{x}) = F(\bar{x}) - K \sum_{j=1}^{NEQ} H_j \quad (190)$$

and the equality condition of Eq. (188) is treated as an inequality constraint

$$H_j(\bar{x}) \leq 0 \quad j=1, NEQ$$

The penalty function approach effectively satisfies the equality constraint while maintaining the rapid convergence characteristics of the CONMIN program.

The numerical optimization problems of equations (186) through (190) are very general, allowing for any number of design variables and constraints. In assessing the value of optimization, the automated design provides a very attractive approach to numerical optimization; however, there are both advantages and limitations to these techniques [Ref. 20].

Advantages:

- . Reduction in design time.
- . Systematic design procedure.
- . Applicable to a wide variety of design variables and constraints.
- . Virtually always yields some design improvement.
- . Not biased by engineering experience.
- . Requires a minimal amount of man-machine interface.

Limitations:

- . Computer times may increase dramatically as the number of design variables increases. A practical limit imposed by the current state of the art for most problems is 30 design variables.

- . Optimization techniques have no stored experience to draw upon; the validity of the result is limited to the validity of the analysis program.
- . The results of the optimization are as correct as the analysis program is theoretically precise.
- . Optimization algorithms used here cannot deal with discontinuous functions.
- . The optimization program will not always obtain a global design optimum and may require restarting from several different points to acquire reasonable assurance of obtaining the global optimum.
- . The analysis program must be properly structured to couple with the COPES/CONMIN optimization code.

C. DESIGNATED DESIGN VARIABLES, CONSTRAINTS AND OBJECTIVE FUNCTION

To assist in the interpretation of the enclosed OTEC power system FORTRAN analysis, the following summary identifies the design variables, constraint functions and objective function used in the analysis and subsequently operated upon by the COPES/CONMIN optimization code. These parameters are all contained in a labeled COMMON block in the computer code, referred to here as "GLOBAL COMMON." Specific GLOBAL COMMON location numbers and upper/lower bounds for operating parameters summarized below can be located in Appendix C.

Design Variables

- . Inner cold pipe diameter
- . Inner hot pipe diameter
- . Inner ammonia circ pipe diameter
- . Inner ammonia re-flux pipe diameter

- . Evaporator operating pressure
- . Condenser operating pressure
- . Outer condenser tube diameter
- . Outer evaporator tube diameter
- . Evaporator tube length
- . Condenser tube length
- . Condenser tube salt water velocity
- . Cold pipe salt water velocity
- . Evaporator tube salt water velocity
- . Hot pipe salt water velocity
- . Evaporator tube profile pitch ratio
- . Condenser tube profile pitch ratio

Constraint Functions

- . Operating system pressure ratio
- . Upper temperature bound of ammonia
- . Lower temperature bound of ammonia
- . Satisfactory enthalpy at state point 5
- . Satisfactory quality at state point 5
- . Satisfactory condenser tube length
- . Internal turbine efficiency
- . Evaporator tube sheet diameter
- . Condenser tube sheet diameter

Objective Function

- . Cost of major power system components

VIII. CONCLUSIONS AND RECOMMENDATIONS

A. CONCLUSIONS

1. The use of an analysis code for OTEC power systems coupled to COPES/CONMIN optimization code provides a powerful tool to design an optimum power system for the desired net electrical output, measured against the objective function. Such a design could permit construction of higher capacity systems using the optimized modules as substations of the total power plant.

2. The analysis code coupled to COPES/CONMIN provides an excellent vehicle to evaluate proposed designs relative to a true optimum. Tables 1 through 4 illustrate the result of preliminary calculations using the analysis code with an objective function to minimize system cost. From these, the following conclusions can be drawn concerning horizontally oriented aluminum (Al-5052) and titanium-tubed heat exchanger power systems:

a. The cost/KW output is nearly constant over the range of optimum designs for both titanium and aluminum tube heat exchangers.

b. During testing for feasible plant designs in increments of 5 MW (net) electrical output, it was observed that a higher megawatt output plant could be achieved with titanium-tubed heat exchangers than for aluminum (Al-5052). For titanium-tubed heat exchangers, a 25 MW (net) power

system is a feasible design; however, aluminum-tubed systems could not provide a feasible design for the same output. Titanium tubed plants failed to produce a feasible design for a 30 MW (net) output power system. In both cases of infeasible design, the constraint which was consistently violated was turbine internal efficiency, set at 90% for current state-of-the-art design.

c. The energy conversion and efficiency of design of a turbine-generator has a major effect on the overall system performance as indicated in paragraph b above.

d. The cost/KW output for titanium-tubed heat exchangers is one third the cost/KW output for aluminum-tubed heat exchangers using a 30-year life-cycle criterion, with a 10% annual inflation rate and retubing at 10 and 20 year marks with AL-5052 tubing.

e. Aluminum-tubed heat exchangers have larger tube bundle volumes, with volumetric differences between aluminum and titanium varying from 26.1 to 11.8% for evaporators and 23.2 to 7.4% for condensers over the range of net power levels considered. In both cases volumetric differences diminish as the system's net electrical output increases to 20 megawatts.

f. COPES/CONMIN has provided optimum designs for each incremental output power level. By manipulating the specified design variables, subject to imposed constraints, COPES/CONMIN has created designs whose geometry and operating

parameters cannot be scaled on the basis of net power output (10 MW). Therefore, designs for component geometry at increasing power levels based upon such simplistic scaling criteria will not achieve an optimum design with respect to the cost objective function.

B. RECOMMENDATIONS

1. Evaluate additional objective functions including:

- a. Minimize heat exchanger volumes.
- b. Minimize parasitic power losses.
- c. Maximize thermodynamic efficiency.
- d. Maximize net electrical output.

2. Perform a sensitivity analysis on power system design variables to evaluate their influence on component and system performance. This allows the designer to prioritize system components which can provide improvement in the objective function for a corresponding improvement in component design.

3. Considerable uncertainties are associated with the expressions used to estimate component performances (two-phase pressure drops, film coefficients, etc.). The code should be tested to determine the sensitivity of system design to these uncertainties.

4. Expand the code to include the use of enhanced heat transfer techniques and evaluate the influence of increased piping friction factors on pumping power requirements.

5. Evaluate proposed OTEC designs using proposed system parameter inputs, comparing both the basic analysis and the optimization output.

6. Select other analytical expressions for heat transfer coefficients to validate the performance and output of the existing code.

7. Evaluate the effect of a smaller thermal difference seen by the power system and its influence on a feasible design for a specific net electrical output.

8. Evaluate the cost aspects of using variable-pitch pumps versus fixed-blade for a variable thermal gradient environment.

9. Evaluate and verify the influence of incremental improvements (percent) in turbine internal/adiabatic efficiency with respect to gross and net electrical outputs and compare with the results reported in Ref. 16.

TABLE 1: OTEC Power System Comparisons (Titanium Tubed Heat Exchangers)

EVAPORATOR	10 MW	15 MW	20 MW	25 MW
HT ABSORB (BTU/HR)	1.44 E09	2.01 E09	2.80 E09	3.46 E09
SW FLOW (LB _m /HR)	2.27 E08	3.34 E08	4.14 E08	4.86 E08
NH ₃ FLOW (LB _m /HR)	2.73 E06	3.78 E06	5.29 E06	6.53 E06
OPER PRESS (LB _f /IN ²)	129.	130.0	127.7	127.1
OVL HT COEF (BTU/ HR·FT ² ·F)	623.19	612.97	601.47	595.73
HT SURFACE (FT ²)	387,598	572,405	743,093	922,075
TUBE OUTER DIA (IN)	0.947	0.952	0.945	0.929
TUBE WALL THICK (IN)	0.025	0.025	0.025	0.025
TUBE PROFILE - STAGGERED EQUILATERAL TRIANGLE				
PITCH RATIO	1.4	1.4	1.47	1.52
TUBE LENGTH (FT)	43.66	42.18	42.27	42.56
TUBE SHEET DIA (FT)	21.96	27.21	32.45	36.76
TOT NR OF TUBES	35,806	54,449	71,034	89,105

TABLE 1. OTEC Power System Comparisons (Continued)

CONDENSER	10 MW	15 MW	20 MW	25 MW
HT REJECT (BTU/HR)	1.39 E09	1.94 E09	2.71 E09	3.34 E09
SW FLOW (LB _m /HR)	2.23 E08	3.35 E08	4.72 E08	5.69 E08
NH ₃ FLOW (LB _m /HR)	2.73 E06	3.79 E06	5.29 E06	6.53 E08
OPER PRESS (LB _f /IN ²)	88.16	88.15	87.46	87.49
OVL HT COEF (BTU/ HR·FT ² ·F)	454.4	446.8	438.4	435.7
HT SURFACE (FT ²)	552,314	762,190	1,168,239	1,483,762
TUBE OUTER DIA (IN)	0.935	0.972	0.957	0.940
TUBE WALL THICK (IN)	0.025	0.025	0.025	0.025
TUBE PROFILE - STAGGERED EQUILATERAL TRIANGLE				
PITCH RATIO	1.4	1.4	1.48	1.51
TUBE LENGTH (FT)	58.57	57.42	58.32	59.09
TUBE SHEET DIA. (FT)	22.48	27.194	35.16	39.734
TOT NR OF TUBES	38,524	52,179	79,956	102,054

TABLE 1: OTEC Power System Comparisons (Continued)

PIPING SYSTEMS	10 MW	15 MW	20 MW	25 MW
SW HOT PIPE (300 FT LENGTH)				
INNER DIA (FT)	17.20	20.08	21.86	23.30
SW VEL (FT/SEC)	4.26	4.6	4.80	4.97
PRESS DROP (LB_f/IN^2)	0.280	0.322	0.348	0.371
SW COLD PIPE (3000 FT LENGTH)				
INNER DIA (FT)	16.1	18.62	21.35	22.97
SW VEL (FT/SEC)	4.94	5.33	5.72	5.95
PRESS DROP (LB_f/IN^2)	0.49	0.508	0.526	0.539
NH ₃ CIRC PIPE (150 FT LENGTH)				
INNER DIA (FT)	2.0	2.0	2.0	2.0
PRESS DROP (LB_f/IN^2)	8.46	9.87	11.33	12.53
NH ₃ RE-FLUX PIPE (50 FT LENGTH)				
INNER DIA (FT)	2.0	2.0	2.0	2.0
PRESS DROP (LB_f/IN^2)	8.46	9.87	11.33	12.53

TABLE 1: OTEC Power System Comparisons (Continued)

PUMP SYSTEMS	10 MW	15 MW	20 MW	25 MW
EVAP SW PUMP (EFFICIENCY 85 PCT)				
HEAD (FT)	11.0	9.89	9.42	9.26
CAPACITY (GAL/MIN)	444,338	653,260	808,625	930,352
COND SW PUMP (EFFICIENCY 85 PCT)				
HEAD (FT)	22.23	20.75	20.04	20.03
CAPACITY (GAL/MIN)	452,026	652,119	920,116	1,107,382
NH ₃ CIRC PUMP (EFFICIENCY 75 PCT)				
HEAD (FT)	200.9	217.33	214.93	220.52
CAPACITY (GAL/MIN)	8709.3	12,101.7	16,880.2	20,586.8
NH ₃ RE-FLUX PUMP (EFFICIENCY 75 PCT)				
HEAD (FT)	32.4	38.02	43.53	48.13
CAPACITY (GAL/MIN)	2684.3	3732.4	5201.4	6424.3

TABLE 1: OTEC Power System Comparisons (Continued)

EFFICIENCY OF OPERATION	10 MW	15 MW	20 MW	25 MW
TURBINE-GENERATOR (TURB MECH 99.8 PCT, GEN MECH AND ELECT 96.6 PCT)				
TURB INTERNAL (PCT)	87.16	89.88	88.22	89.80
OUTLET QUALITY (PCT)	96.6	96.77	96.9	96.9
POWER REQUIREMENTS (MEGAWATTS)				
TURB EFFIC LOSSES	0.373	0.559	0.745	0.932
EVAP SW PUMP	1.131	1.496	1.762	2.034
COND SW PUMP	2.334	3.143	4.283	5.151
NH ₃ CIRC PUMP	0.281	0.412	0.583	0.738
NH ₃ RE-FLUX PUMP	0.014	0.022	0.035	0.048
TURB-GEN GROSS	14.132	20.633	27.409	33.904
PCT PARASITIC POWER	26.6	24.6	24.31	23.51
THERMO CYCLE EFFIC (PCT)	2.45	2.65	2.53	2.56

TABLE 1: OTEC Power System Comparisons (Continued)

COMPONENT COSTS (\$)	10 MW	15 MW	20 MW	25 MW
EVAPORATOR	5,134,322.	8,223,672.	11,501,680.	13,026,794.
CONDENSER	5,952,658.	8,667,154.	13,011,939.	16,558,713.
GEN-TURBINE	1,495,085.	1,578,776.	1,666,011.	1,749,636.
GENERATOR	756,287.	937,205.	1,125,782.	1,306,554.
EVAP SW PUMP	463,736.	653,333.	794,355.	922,944.
COND SW PUMP	470,714.	652,298.	895,505.	1,065,449.
NH ₃ CIRC PUMP	110,849.	136,825.	169,303.	193,848.
NH ₃ RE-FLUX PUMP	52,190.	64,449.	79,701.	91,233.
OPTIMUM COST (\$)	14,383,650.	20,849,216.	29,164,560.	34,823,904.
COST/KW (NET) OUTPUT (\$/KW)	1438.36	1389.95	1458.23	1392.96

TABLE 2: QTEC Power System Comparisons (Aluminum Tubed Heat Exchanger)

EVAPORATOR	10 MW	15 MW	20 MW	25 MW
HT ABSORB (B U/HR)	1.51 E09	1.97 E09	2.80 E09	
SW FLOW (LB _m /HR)	2.53 E08	3.42 E08	3.89 E08	
NH ₃ FLOW (LB _m /HR)	2.86 E06	3.72 E06	5.29 E06	
OPER PRESS (LB _f /IN ²)	129.57	131.98	128.01	
OVL HT COEF (BTU/ HR·FT ² ·F)	646.7	643.2	625.5	
HT SURFACE (FT ²)	391,370	610,261	777,553	
TUBE OUTER DIA (IN)	1.221	1.046	0.982	
TUBE WALL THICK (IN)	0.065	0.065	0.065	
TUBE PROFILE - STAGGERED EQUILATERAL TRIANGLE				
PITCH RATIO	1.4	1.46	1.6	
TUBE LENGTH (FT)	47.68	42.42	41.63	
TUBE SHEET DIA (FT)	23.97	30.73	34.68	
TOT NR OF TUBES	25,669	52,512	72,662	

INFEASIBLE DESIGN

TABLE 2: OTEC Power System Comparisons (Continued)

CONDENSER	10 MW	15 MW	20 MW	25 MW
HT REJECT (BTU/HR)	1.47 E09	1.89 E09	2.71 E09	
SW FLOW (LB _m /HR)	2.44 E08	3.04 E08	4.38 E08	
NH ₃ FLOW (LB _m /HR)	2.86 E06	3.72 E06	5.30 E06	
OPER PRESS (LB _f /IN ²)	88.52	89.18	87.85	
OVL HT COEF (BTU/ HR·FT ² ·F)	454.57	453.54	446.48	
HT SURFACE (FT ²)	554,011	690,395	1,173,216	
TUBE OUTER DIA (IN)	1.176	1.092	1.001	
TUBE WALL THICK (IN)	0.065	0.065	0.065	
TUBE PROFILE - STAGGERED EQUILATERAL TRIANGLE				
PITCH RATIO	1.4	1.46	1.5	
TUBE LENGTH (FT)	64.04	57.46	57.24	
TUBE SHEET DIA (FT)	24.15	28.61	36.82	
TOT NR OF TUBES	28,091	42,035	78,198	

INFEASIBLE DESIGN

TABLE 2: OTEC Power System Comparisons (Continued)

PIPING SYSTEMS	10 MW	15 MW	20 MW	25 MW
SW HOT PIPE (300 FT LENGTH)				
INNER DIA (FT)	17.89	20.25	21.33	
SW VEL (FT/SEC)	4.38	4.63	4.74	
PRESS DROP (LB_f/IN^2)	0.295	0.326	0.341	
SW COLD PIPE (3000 FT LENGTH)				
INNER DIA (FT)	16.53	17.93	20.7	
SW VEL (FT/SEC)	4.93	5.23	5.64	
PRESS DROP (LB_f/IN^2)	0.478	0.504	0.523	
NH ₃ CIRC PIPE (150 FT LENGTH)				
INNER DIA (FT)	1.99	2.0	2.0	
PRESS DROP (LB_f/IN^2)	13.78	15.94	17.89	
NH ₃ RE-FLUX PIPE (50 FT LENGTH)				
INNER DIA (FT)	2.0	2.0	2.0	
PRESS DROP (LB_f/IN^2)	8.996	10.788	11.916	

INFEASIBLE DESIGN

TABLE 2: OTEC Power System Comparisons (Continued)

PUMP SYSTEMS	10 MW	15 MW	20 MW	25 MW
EVAP SW PUMP (EFFICIENCY 85 PCT)				
HEAD (FT)	10.42	10.27	10.06	
CAPACITY (GAL/MIN)	494,239	669,211	760,748	
COND SW PUMP (EFFICIENCY 85 PCT)				
HEAD (FT)	21.32	20.80	21.05	
CAPACITY (GAL/MIN)	474,918	592,656	851,978	
NH ₃ CIRC PUMP (EFFICIENCY 75 PCT)				
HEAD (FT)	203.5	218.32	216.63	
CAPACITY (GAL/MIN)	9144.3	11,895.6	16,911.6	
NH ₃ RE-FLUX PUMP (EFFICIENCY 75 PCT)				
HEAD (FT)	34.33	41.27	45.66	
CAPACITY (GAL/MIN)	2818.4	3669.9	5210.5	

INFEASIBLE DESIGN

TABLE 2: OTEC Power System Comparisons (Continued)

	10 MW	15 MW	20 MW	25 MW
EFFICIENCY OF OPERATION				
TURBINE-GENERATOR (TURB MECH 99.8 PCT, GEN MECH AND ELECT 96.6 PCT)				
TURB INTERNAL (PCT)	83.37	89.76	88.05	
OUTLET QUALITY (PCT)	97.06	96.73	96.93	
POWER REQUIREMENTS (MEGAWATTS)				
TURB EFFIC LOSSES	0.373	0.559	0.745	
EVAP SW PUMP	1.191	1.590	1.770	
COND SW PUMP	2.351	2.863	4.166	
NH ₃ CIRC PUMP	0.299	0.416	0.588	
NH ₃ RE-FLUX PUMP	0.015	0.024	0.037	
TURB-GEN GROSS	14.229	20.452	27.306	
PCT PARASITIC POWER	27.10	23.92	24.03	
THERMO CYCLE EFFIC (PCT)	2.34	2.70	2.53	

INFEASIBLE DESIGN

TABLE 2: OTEC POWER SYSTEM COMPARISONS (CONTINUED)

COMPONENT COSTS (\$)	10 MW	15 MW	20 MW	25 MW
EVAPORATOR	20,848,960.	34,297,296.	44,203,408.	
CONDENSER	24,633,360.	31,812,640.	55,404,448.	
GEN-TURBINE	1,496,339.	1,576,449.	1,664,688.	
GENERATOR	758,998.	932,173.	1,122,921.	
EVAP SW PUMP	509,021.	667,809.	750,878.	
COND SW PUMP	491,487.	598,335.	833,670.	
NH ₃ CIRC PUMP	114,361.	135,329.	169,505.	
NH ₃ RE-FLUX PUMP	53,845.	63,756.	79,790.	
OPTIMUM COST (\$)	48,852,480.	70,020,000.	104,149,488.	

INFEASIBLE DESIGN

COST/KW (NET) OUTPUT (\$/KW)

4885.25 4668.00 5207.47

TABLE 3: Heat Exchanger Comparisons (Titanium Tubed)

EVAPORATOR	10 MW	15 MW	20 MW	25 MW
HT ABSORB (BTU/HR)	1.44 E09	2.01 E09	2.80 E09	3.46 E09
SW FLOW (LB _m /HR)	2.27 E08	3.34 E08	4.14 E08	4.86 E08
SW TEMP IN (DEG F)	80.0	80.0	80.0	80.0
SW TEMP OUT (DEG F)	73.36	73.72	72.92	72.56
NH ₃ FLOW (LB _m /HR)	2.73 E06	3.78 E06	5.29 E06	6.53 E06
OPER PRESS (LB _f /IN ²)	129.0	130.1	127.72	127.1
SAT TEMP (DEG F)	70.11	70.59	69.54	69.27
OUTLET TEMP (DEG F)	70.06	70.51	69.47	69.19
OUTLET QUALITY (PCT)	92	92	92	92
NH ₃ PRESS DROP (LB _f /IN ²)	0.105	0.162	0.165	0.174
TUBE CHARACTERISTICS				
OUTER DIA (IN)	0.947	0.952	0.945	0.929
WALL THICK (IN)	0.025	0.025	0.025	0.025
LENGTH (FT)	43.66	42.18	42.27	42.56

TABLE 3: Heat Exchanger Comparisons (Continued)

EVAPORATOR	10 MW	15 MW	20 MW	25 MW
TUBE PROFILE - STAGGERED EQUILATERAL TRIANGLE				
PITCH RATIO	1.4	1.4	1.47	1.52
ENHANCEMENT - PLAIN TUBE				
SW VEL (FT/SEC)	6.3	6.03	5.80	5.64
T WALL (DEG F)	71.09	71.47	70.51	70.22
FILM TEMP (DEG F)	70.57	70.99	69.99	69.71
DELTA T BOILING (DEG F)	1.027	0.952	1.041	1.032
LMTD	6.00	5.76	6.31	6.34
EFFECTIVENESS	0.671	0.667	0.677	0.693
NTU	1.112	1.098	1.13	1.182
OVL HT COEF (BTU/ HR·FT ² ·F)	623.19	612.97	601.47	595.73
h (WATER)	1156.01	1115.97	1081.6	1059.15
h (FOULING)	3787.7	3788.5	3787.35	3784.37

TABLE 3: Heat Exchanger Comparisons (Continued)

	10 MW	15 MW	20 MW	25 MW
EVAPORATOR				
h (METAL)	4413.77	4404.7	4415.43	4429.66
h (AMMONIA)	4015.73	4088.4	4040.26	4090.74
SW PRESS DROP (LB _f /IN ²)	4.593	4.061	3.824	3.727
MOISTURE SEPARATOR				
OPER PRESS (LB _f /IN ²)	128.9	129.94	127.55	126.92
OUTLET TEMP (DEG F)	69.92	70.33	69.22	68.89
OUTLET QUALITY (PCT)	99.5	99.5	99.5	99.5
NH ₃ PRESS DROP (LB _f /IN ²)	0.311	0.416	0.578	0.681
CONDENSER				
HT REJECT (BTU/HR)	1.44 E09	2.01 E09	2.80 E09	3.46 E09
SW FLOW (LB _m /HR)	2.27 E08	3.34 E08	4.14 E08	4.86 E08

TABLE 3: Heat Exchanger Comparisons (Continued)

CONDENSER	10 MW	15 MW	20 MW	25 MW
SW TEMP IN (DEG F)	40.0	40.0	40.0	40.0
SW TEMP OUT (DEG F)	46.29	46.06	46.00	46.16
NH ₃ FLOW (LB _m /HR)	2.73 E06	3.79 E06	5.29 E06	6.53 E06
OPER PRESS (LB _f /IN ²)	88.16	88.15	87.46	87.49
SAT TEMP (DEG F)	49.36	49.36	49.95	48.97
OUTLET TEMP (DEG F)	49.3	49.24	49.84	48.85
NH ₃ PRESS DROP (LB _f /IN ²)	0.127	0.206	0.173	0.195
TUBE CHARACTERISTICS				
OUTER DIA (IN)	0.935	0.972	0.957	0.940
WALL THICK (IN)	0.025	0.025	0.025	0.025
LENGTH (FT)	58.57	57.42	58.32	59.09
TUBE PROFILE - STAGGERED EQUILATERAL TRIANGLE				
PITCH RATIO	1.4	1.4	1.48	1.51

TABLE 3: Heat Exchanger Comparisons (Continued)

CONDENSER	10 MW	15 MW	20 MW	25 MW
ENHANCEMENT - PLAIN TUBE				
SW VEL (FT/SEC)	6.12	6.02	5.72	5.60
T WALL (DEG F)	48.39	48.33	48.04	48.07
FILM TEMP (DEG F)	48.84	48.79	48.44	48.46
DELTA T COND (DEG F)	0.895	0.901	0.808	0.781
LMTD	5.56	5.68	5.29	5.17
EFFECTIVENESS	0.678	0.655	0.679	0.696
NTU	1.133	1.065	1.136	1.191
OVL HT COEF (BTU/ HR·FT ² ·F)	454.4	446.83	438.4	435.73
h (WATER)	719.6	704.4	678.0	669.3
h (FOULING)	3785.5	3792.0	3789.4	3786.4
h (METAL)	4424.2	4393.6	4405.6	4420.1
h (AMMONIA)	3118.9	3058.6	3171.5	3219.8
SW PRESS DROP (LB _f /IN ²)	6.31	5.64	5.30	5.28

TABLE 4: Heat Exchanger Comparisons (Aluminum Tubed)

EVAPORATOR	10 MW	15 MW	20 MW	25 MW
HT ABSORB (BTU/HR)	1.51 E09	1.97 E09	2.80 E09	
SW FLOW (LB _m /HR)	2.53 E08	3.42 E08	3.89 E08	
SW TEMP IN (DEG F)	80.0	80.0	80.0	
SW TEMP OUT (DEG F)	73.74	73.99	72.47	
NH ₃ FLOW (LB _m /HR)	2.86 E06	3.72 E06	5.29 E06	
OPER PRESS (LB _f /IN ²)	129.57	131.98	128.01	
SAT TEMP (DEG F)	70.35	71.4	69.67	
OUTLET TEMP (DEG F)	70.32	71.4	69.61	
OUTLET QUALITY (PCT)	92.0	92.0	92.0	
NH ₃ PRESS DROP (LB _f /IN ²)	0.070	0.087	0.136	
TUBE CHARACTERISTICS				
OUTER DIA (IN)	1.221	1.046	0.982	
WALL THICK (IN)	0.065	0.065	0.065	

INFEASIBLE DESIGN

TABLE 4: Heat Exchanger Comparisons (Continued)

EVAPORATOR	10 MW	15 MW	20 MW	25 MW
LENGTH (FT)	47.68	42.42	41.63	
TUBE PROFILE - STAGGERED EQUILATERAL TRIANGLE				
PITCH RATIO	1.4	1.46	1.50	
ENHANCEMENT - PLAIN TUBE				
SW VEL (FT/SEC)	6.6	6.2	5.89	
T WALL (DEG F)	71.49	72.25	70.63	
FILM TEMP (DEG F)	70.90	71.80	70.12	
DELTA T BOILING (DEG F)	1.163	0.885	1.02	
LMTD	6.0	5.03	5.8	
EFFECTIVENESS	0.649	0.699	0.729	
NTU	1.047	1.199	1.307	
OVL HT COEF (BTU/ HR·FT ² ·F)	646.7	643.2	625.5	
h (WATER)	1090.0	1052.5	1011.5	

INFEASIBLE DESIGN

TABLE 4: Heat Exchanger Comparisons (Continued)

	10 MW	15 MW	20 MW	25 MW
EVAPORATOR				
h (FOULING)	5574.5	3505.1	3470.5	
h (METAL)	15,444.8	13,512.9	13,252.2	
h (AMMONIA)	5640.3	4097.4	4058.5	
SW PRESS DROP (LB _f /IN ²)	4.32	4.22	4.11	
MOISTURE SEPARATOR				
OPER PRESS (LB _f /IN ²)	129.5	131.89	127.88	
OUTLET TEMP (DEG F)	70.22	71.23	69.38	
OUTLET QUALITY (PCL)	99.5	99.5	99.5	
NH ₃ PRESS DROP (LB _f /IN ²)	0.24	0.307	0.522	
CONDENSER				
HI REJECT (BTU/HR)	1.47 E09	1.89 E09	2.71 E09	

INFEASIBLE DESIGN

TABLE 4: Heat Exchanger Comparisons (Continued)

CONDENSER	10 MW	15 MW	20 MW	25 MW
SW FLOW (LB _m /HR)	2.44 E08	3.04 E08	4.38 E09	
SW TEMP IN (DEG F)	40.0	40.0	40.0	
SW TEMP OUT (DEG F)	46.30	46.53	46.49	
NH ₃ FLOW (LB _m /HR)	2.86 E06	3.72 E06	5.30 E06	
OPER PRESS (LB _f /IN ²)	88.52	89.18	87.83	
SAT TEMP (DEG F)	49.52	49.97	49.17	
OUTLET TEMP (DEG F)	49.52	49.90	49.08	
NH ₃ PRESS DROP (LB _f /IN ²)	0.088	0.111	0.148	
TUBE CHARACTERISTICS				
OUTER DIA (IN)	1.176	1.092	1.001	
WALL THICK (IN)	0.065	0.065	0.065	
LENGTH (FT)	64.04	57.46	57.24	
TUBE PROFILE - STAGGERED EQUILATERAL TRIANGLE				

INFEASIBLE DESIGN

TABLE 4: Heat Exchanger Comparisons (Continued)

	10 MW	15 MW	20 MW	25 MW
CONDENSER				
PITCH RATIO	1.4	1.46	1.5	
ENHANCEMENT - PLAIN TUBE				
SW VEL. (FT/SEC)	6.31	6.23	5.87	
T WALL (DEG F)	48.51	48.85	48.25	
FILM TEMP (DEG F)	49.02	49.38	48.67	
DELTA T COND (DEG F)	1.020	1.055	0.832	
LMTD	5.820	6.062	5.175	
EFFECTIVENESS	0.661	0.660	0.715	
NTU	1.082	1.078	1.254	
OVL HT COEF (BTU/ HR·FT ² ·F)	454.57	453.56	446.48	
h (WATER)	670.0	668.56	641.97	
h (FOULING)	3557.0	3523.7	3480.59	
h (METAL)	13,414.54	13,351.18	13,271.11	
h (AMMONIA)	2842.96	2853.65	3131.0	
SW PRESS DROP (LB _f /IN ²)	5.92	5.66	5.74	

INFEASIBLE DESIGN

APPENDIX A

SAMPLE INPUT DATA FOR OTEC ANALYSIS

EVAPORATOR - HORIZONTAL

TUBE O.D.	1.000(IN)	25.400(MM)
TUBE LENGTH	40.000(FT)	12.192(M)
SW TUBE VEL	6.000(FT/S)	1.829(M/S)
OPER PRESSURE	130.000(LBF/IN2)	0.896(MPA)
TUBE MATERIAL - TITANIUM		
THERMAL COND(K)	9.500(BTU/HR.FT.F)	16.502(W/M.C)
TUBE PROFILE - STAGGERED EQUI-LATERAL		
PITCH RATIO	1.50	
ENHANCEMENT - PLAIN TUBE		

CONDENSER - HORIZONTAL

TUBE O.D.	1.000(IN)	25.400(MM)
TUBE LENGTH	56.500(FT)	17.221(M)
SW TUBE VEL	6.000(FT/S)	1.829(M/S)
OPER PRESSURE	89.000(LBF/IN2)	0.614(MPA)
TUBE MATERIAL - TITANIUM		
THERMAL COND(K)	9.500(BTU/HR.FT.F)	16.502(W/M.C)
TUBE PROFILE - STAGGERED EQUI-LATERAL		
PITCH RATIO	1.50	
ENHANCEMENT - PLAIN TUBE		

SALT WATER HOT PIPE

PIPE I.D.	19.300(FT)	5.883(M)
PIPE LENGTH	300.000(FT)	91.440(M)
SW PIPE VEL	4.500(FT/S)	1.372(M/S)
SW INLET TEMP	80.000(DEG F)	26.667(DEG C)
SW SALINITY	35.0/000	

SALT WATER COLD PIPE

PIPE I.D.	19.600(FT)	5.974(M)
PIPE LENGTH	3000.000(FT)	914.400(M)
SW PIPE VEL	5.500(FT/S)	1.676(M/S)
SW INLET TEMP	40.000(DEG F)	4.444(DEG C)
SW SALINITY	35.0/000	

AMMONIA CIRC PIPE		
PIPE I.D.	2.000(FT)	0.610(M)
PIPE LENGTH	150.000(FT)	45.720(M)
AMMONIA RE-FLUX PIPE		
PIPE I.D.	2.000(FT)	0.610(M)
PIPE LENGTH	50.000(FT)	15.240(M)
PUMP AND GEN-TURB PERFORMANCE		
EVAP SW PUMP		
EFFICIENCY MECH	95.00(PCT)	MOTOR 98.00(PCT)
COND SW PUMP		
EFFICIENCY MECH	85.00(PCT)	MOTOR 98.00(PCT)
AMMONIA CIRC PUMP		
EFFICIENCY MECH	75.00(PCT)	MOTOR 98.00(PCT)
GEN-TURB EFFICIENCIES		
GEN MECH&ELECT	96.60(PCT)	
TURB MECH	99.80(PCT)	
POWER REQUIREMENTS		
NET POWER OUTPUT		15.000(Mw)

APPENDIX B

SAMPLE OTEC ANALYSIS OPTIMIZATION OUTPUT DATA

EVAPORATOR - HORIZONTAL

HT ABSORB	2005013760.0(BTU/HR)	537.601(MW)
SW FLOW	334081230.0(LBM/HR)	15153590+.0(KG/HR)
SW TEMP IN	80.000(DEG F)	26.667(DEG C)
SW TEMP OUT	73.724(DEG F)	23.130(DEG C)
NH3 FLOW	3788703.0(LBM/HR)	1718519.0(KG/HR)
OPER PRESSURE	130.097(LBF/IN2)	396.987(KPA)
EVAP SAT TEMP	70.535(DEG F)	21.436(DEG C)
OUTLET TEMP	70.514(DEG F)	21.397(DEG C)
OUTLET QUALITY	92.00(PCT)	
NH3 PRESS DROP	0.162(LBF/IN2)	1.115(KPA)
TUBE CHARACTERISTICS		
OUTER DIA	0.952(IN)	24.180(MM)
WALL THICK	0.025(IN)	0.639(MM)
LENGTH	42.132(FT)	12.857(M)
MATERIAL - TITANIUM		
TUBE PROFILE - STAGGERED EQUI-LATERAL		
PITCH RATIO	1.40	
ENHANCEMENT - PLAIN TUBE		
SW VELOCITY	6.026(FT/S)	1.337(M/S)
T WALL(SHELLSIDE)	71.466(DEG F)	21.926(DEG C)
FILM TEMP	70.990(DEG F)	21.661(DEG C)
DELTA T BOILING	0.952(DEG F)	0.529(DEG C)
L.M.T.D.	5.757(DEG F)	3.198(DEG C)
EVAP EFFECTIVENESS	0.667	
NR OF TRANSFER UNITS	1.093	
UVL HT COEF	612.97(BTU/HR.FT2.F)	3460.58(W/42.C)
H(WATER)	1115.97(BTU/HR.FT2.F)	6336.71(W/42.C)
H(FOULING)	3738.54(BTU/HR.FT2.F)	21512.07(W/42.C)
H(METAL)	4409.72(BTU/HR.FT2.F)	25039.23(W/42.C)
H(AMMONIA)	4088.44(BTU/HR.FT2.F)	23215.00(W/42.C)

HT SURFACE	572405.00(FT ²)	53178.12(M ²)
TUBE SHEET DIA	27.213(FT)	8.294(M)
TOT NR OF TUBES	5449.	
SW PRESS DROP	4.061(LBF/IN ²)	23.003(KPA)
MOISTURE SEPARATOR-INSIDE EVAP SHELL		
OPER PRESSURE	129.935(LBF/IN ²)	395.872(KPA)
OUTLET TEMP	70.333(DEG F)	21.296(DEG C)
OUTLET QUALITY	99.50(PCT)	
NH3 PRESS DROP	0.416(LBF/IN ²)	2.353(KPA)

CONDENSER - HORIZONTAL

HT REJECT	1935472896.0(BTU/HR)	567.221(MW)
SW FLOW	334871552.0(LBM/HR)	151894363.0(KG/HR)
SW TEMP IN	40.000(DEG F)	4.444(DEG C)
SW TEMP OUT	46.055(DEG F)	7.308(DEG C)
NH3 FLCW	3738708.0(LBM/HR)	1718519.0(KG/HR)
OPER PRESSURE	63.151(LBF/IN ²)	607.731(KPA)
COND SAT TEMP	49.351(DEG F)	9.645(DEG C)
OUTLET TEMP	49.238(DEG F)	9.577(DEG C)
NH3 PRESS DROP	0.206(LBF/IN ²)	1.423(KPA)

TUBE CHARACTERISTICS

OUTTER DIA	0.972(IN)	24.683(M)
WALL THICK	0.025(IN)	0.642(MM)
LENGTH	57.416(FT)	17.500(M)

MATERIAL - TITANIUM

TUBE PROFILE - STAGGERED EQUI-LATERAL

PITCH RATIO 1.40

ENHANCEMENT - PLAIN TUBE

SW VELOCITY	6.017(FT/S)	1.834(M/S)
T WALL(SHELLSIDE)	48.331(DEG F)	9.073(DEG C)
FILM TEMP	48.785(DEG F)	9.325(DEG C)
DELTA T COND	0.907(DEG F)	0.504(DEG C)
L.M.T.D.	5.683(DEG F)	3.157(DEG C)
COND EFFECTIVENESS	0.655	
NR OF TRANSFER UNITS	1.065	

CVL HT COEF	445.83(BTU/HR.FT2.F)	2537.13(W/M2.C)
H(WATER)	704.35(BTU/HR.FT2.F)	3999.47(W/M2.C)
H(FOULING)	3792.00(BTU/HR.FT2.F)	21531.75(W/M2.C)
H(METAL)	+593.63(BTU/HR.FT2.F)	24947.90(W/M2.C)
H(AMMONIA)	3053.55(BTU/HR.FT2.F)	17367.63(W/M2.C)
HT SURFACE	762190.25(F2)	70809.69(M2)
TUBE SHEET DIA	27.194(FT)	9.289(M)
TOT NR OF TUBES	52179.	
SW PRESS DROP	5.636(LBF/IN2)	38.861(KPA)

SALT WATER HOT PIPE

PIPE I.D.	20.077(FT)	6.120(M)
PIPE LENGTH	300.000(FT)	91.440(M)
SW PIPE VEL	4.537(FT/S)	1.401(M/S)
SW FLOW	334081280.0(LB4/HR)	151535904.0(KG/HR)
SW INLET TEMP	80.000(DEG F)	26.667(DEG C)
SW SALINITY	35.0/000	
SW PRESS DROP	0.322(LBF/IN2)	2.217(KPA)

SALT WATER COLD PIPE

PIPE I.D.	18.622(FT)	5.676(M)
PIPE LENGTH	3000.000(FT)	914.400(M)
SW PIPE VEL	5.334(FT/S)	1.625(M/S)
SW FLOW	334871552.0(LB4/HR)	151394368.0(KG/HR)
SW INLET TEMP	40.000(DEG F)	4.444(DEG C)
SW SALINITY	35.0/000	
SW PRESS DROP	0.508(LBF/IN2)	3.501(KPA)

AMMONIA CIRC PIPE

PIPE I.D.	2.001(FT)	0.610(M)
PIPE LENGTH	150.000(FT)	45.720(M)
NH3 FLOW	3788708.0(LB4/HR)	1718519.0(KG/HR)
NH3 PRESS DROP	15.033(LBF/IN2)	103.650(KPA)

AMMONIA RE-FLUX CIRC PIPE

PIPE I.D.	2.000(FT)	0.610(M)
PIPE LENGTH	50.000(FT)	15.240(M)
NH3 FLOW	1136612.0(LB4/HR)	515555.3(KG/HR)
NH3 PRESS DROP	9.874(LBF/IN2)	68.079(KPA)

PUMP AND GEN-TURB PERFORMANCE

EVAP SW PUMP

HEAD PRESS	9.898(FT)	3.017(M)
CAPACITY	555259.5(GAL/MIN)	2472587.0(LIT/MIN)
EFFICIENCY MECH	35.00(PCT)	MOTOR 98.00(PCT)

COND SW PUMP

HEAD PRESS	20.753(FT)	9.227(M)
CAPACITY	652119.2(GAL/MIN)	2468271.0(LIT/MIN)
EFFICIENCY MECH	35.00(PCT)	MOTOR 98.00(PCT)

AMMONIA CIRC PUMP

HEAD PRESS	212.327(FT)	64.717(M)
CAPACITY	12101.7(GAL/MIN)	45305.0(LIT/MIN)
EFFICIENCY MECH	75.00(PCT)	MOTOR 99.00(PCT)

AMMONIA RE-FLUX PUMP

HEAD PRESS	33.016(FT)	11.597(M)
CAPACITY	5752.4(GAL/MIN)	14127.1(LIT/MIN)
EFFICIENCY MECH	75.00(PCT)	MOTOR 98.00(PCT)

GEN-TURB EFFICIENCIES

GEN MECH&ELECT	96.60(PCT)
TURB MECH	99.80(PCT)
TURB INTERNAL	99.83(PCT)

TURB OUTLET QUALITY 96.77(PCT)

POWER REQUIREMENTS

TURB-GEN GROSS	27663.313(HP)	20.633(MW)
EFFICIENCY LOSSES		0.559(MW)
EVAP SW PUMP	1964.851(HP)	1.496(MW)
COND SW PUMP	4129.313(HP)	3.143(MW)
NH3 CIRC PUMP	541.714(HP)	0.412(MW)
NH3 RE-FLUX PUMP	29.097(HP)	0.022(MW)

NET POWER OUTPUT 15.000(MW)

PERCENT PARASITIC POWER 24.59(PCT)

THERMODYNAMIC CYCLE EFFICIENCY 2.65(PCT)

COST OF COMPONENTS

EVAPORATOR	3223672.00(DOLLARS)
CONDENSER	3567154.00(DOLLARS)
GEN-TURBINE	1578776.00(DOLLARS)
GENERATOR	937205.06(DOLLARS)
EVAP SW PUMP	653332.94(DOLLARS)
COND SW PUMP	552298.06(DOLLARS)
NH3 CIRC PUMP	136824.94(DOLLARS)
NH3 RE-FLUX PUMP	64448.34(DOLLARS)

OPTIMUM COST	20849216.00(DOLLARS)
COST PER NET KW OUTPUT	1389.95(DOLLARS)

APPENDIX C

SAMPLE COPES OPTIMIZATION AND SENSITIVITY ANALYSIS DATA

```

$BLOCK A (TITLE CARD)
OCEAN THERMAL ENERGY CONVERSION (OTEC) POWER SYSTEM
$BLOCK B (PROGRAM CONTROL PARAMETERS)
2,16,16
$BLOCK C (INTEGER OPT CONTROL PARAMETERS)
5,0,0,5
$BLOCK D (FLOATING PT OPT PRG PARAMETERS)
0.0
0.0
0.0
$BLOCK E (TOT NR DESIGN VAR, DESIGN OBJ IDENT AND SIGN)
16,27,-1.0
$BLOCK F (DESIGN VARIABLE BOUNDS, INIT VALUES & SCALE FACTOR)
1.0,1.0+20
1.0,1.0+20
1.0,1.0+20
1.0,1.0+20
1.0,1.0+20
85.0,1+3.0
85.0,1+8.0
0.5,2.5
0.5,2.5
10.0,1.0+20
10.0,1.0+20
2.0,10.0
2.0,10.0
2.0,10.0
2.0,10.0
1.4,3.0
1.4,3.0
$BLOCK G (DESIGN VARIABLE IDENT)
1,1,1.0
2,2,1.0
3,3,1.0
4,4,1.0
5,5,1.0

```

```

6,6,1.0      5      5      1.0
7,7,1.0      7      7      1.0
8,8,1.0      8      8      1.0
9,9,1.0      9      9      1.0
10,10,1.0    10     10     1.0
11,11,1.0    11     11     1.0
12,12,1.0    12     12     1.0
13,13,1.0    13     13     1.0
14,14,1.0    14     14     1.0
15,15,1.0    15     15     1.0
16,16,1.0    16     16     1.0

```

```

$BLOCK H (NR OF CONSTRAINED PARAMETERS)
5

```

```

$BLOCK I (CONSTRAINT IDENT AND BOUNDS)
17

```

```

1.,0.,0.,3.,0.0      0.0      3.      0.0
18,20      1.      0.0      3.      0.0
0.1,0.0,1.0+20,0.0    0.1      0.0      1.0+20     0.0
21,23      21      23
0.,0.0,1.0+20,0.0    0.      0.0      1.0+20     0.0
24
30.,0.0,90.,0.)      30.      0.0      90.      0.0
25,26      25      26
10.,0.0,1.0+20,0.0    10.      0.0      1.0+20     0.0

```

```

$BLOCK P (SENSITIVITY OBJECTIVES)
27,0

```

```

1,2,3,4,5,6,7,8,9,10,11,12,13,14,15,16,17,18,19,20,
      1      2      3      4      5
      9      10     11     12     13
      17     18     19     20     21
21,22,23,24,25,26,27
      6      7      8
      14     15     16
      22     23     24

```

```

$BLOCK Q (SENSITIVITY VARIABLE BOUNDS)
1,6

```

```

18.,10.,15.,18.,20.,25.      13.      10.      15.      18.      20.      25.
2,6
18.,10.,15.,18.,20.,25.      18.      10.      15.      18.      20.      25.
3,6

```

2., 0.5, 1. ³ , 2., 3., 4. ⁰	0.5	1.	2.	3.	4.
4, 0					
2., 0.5, 1. ⁴ , 2., 3., 4. ⁶	0.5	1.	2.	3.	4.
5, 6					
130., 128. ⁵ , 129., 130. ⁶ , 131., 132. ⁶	128., 129.	130.	131.	132.	
6, 6					
89., 87., 88. ⁶ , 89., 90. ⁶ , 91. ⁶	89., 87.	89.	90.	91.	
7, 0					
1., .5, .75, ⁷ 1., 1.25, 1. ⁶ 1.5	.5	.75	1.	1.25	1.5
8, 6					
1., .5, .75, ⁸ 1., 1.25, 1. ⁶ 1.5	.5	.75	1.	1.25	1.5
9, 6					
40., 30., 35. ⁹ , 40., 45. ⁶ , 50. ⁶	40., 30.	35.	40.	45.	50.
10, 6					
55., 45., 50. ¹⁰ , 55., 60. ⁶ , 65. ⁶	55., 45.	50.	55.	60.	65.
11, 6					
7., 5., 6., 7. ¹¹ , 8., 9. ⁶	7.	5.	6.	7.	8.
12, 0					
4., 2., 3., 4. ¹² , 5., 6. ⁶	4.	3.	4.	5.	6.
13, 6					
7., 5., 6., 7. ¹³ , 8., 9. ⁶	7.	6.	7.	8.	9.
14, 6					
4., 2., 3., 4. ¹⁴ , 5., 6. ⁶	4.	3.	4.	5.	6.
15, 6					
1.0, 1.4, 1. ¹⁵ 1.5, 1.0, 1.7, ⁵ 1.8	1.6	1.5	1.0	1.7	1.8
16, 6					
1.0, 1.4, 1. ¹⁶ 1.5, 1.6, 1.7, ⁶ 1.3	1.6	1.5	1.0	1.7	1.8
END					

THESIS PRESENTATION: MODEL ANALYSIS OF THE CLOSED-CYCLE
 OCEAN THERMAL ENERGY CONVERSION (OTEC) POWER SYSTEM
 BY LCDR RAYMOND C. SCHAUBEL, USN

NOMENCLATURE

AC(TDDC) - SUBROUTINE TO COST COND AL TUBING/FT (\$/FT)
 ACC(TDDC) - SUBROUTINE TO COST ENHANCED COND AL TUBE (\$/FT)
 AE - SUBROUTINE TO COST ENHANCED COND AL TUBE THICK(IN)
 AEC(TDDC) - SUBROUTINE TO SIZE ENHANCED COND TUBING(IN)
 AF - EVAP TUBE ENHANCED COND TUBE (\$/FT)
 ATNT - PROJECTED ANNUAL INFLATION RATE (DECIMAL)
 AP(TDDC) - TUBE BANK MINIMUM FLOW AREA (FT2)
 AP(TDDE) - SUBROUTINE TO SIZE COND AL TUBE WALL THICK(IN)
 BAND - VERT. TUBED COND INLET DISTRIBUTION BAND
 BTUC - 778.2 FT LBF/8TU
 C1 - CONDENSER TUBING MACHING COST (\$/FT)
 C2 - CONDENSER TUBE MACHING COST (\$)
 CAFF - CONDENSER TUBE FLOW AREA (FT2)
 CAO - CONDENSER SURFACE AREA OF CONDENSER TUBE PROFILE (IN2)
 CAREA - TOTAL SURFACE AREA BETWEEN TUBES-CENTER TO CENTER (IN)
 CBFCFC - BUSTLE FLANGES AND CHANNELS COST (\$)
 CBFCFE - EVAP FLANGES AND FLOW PLATES COST (\$)
 CCSWP - TOTAL OF COND. OR SW COLD PIPE PUMP (DOLLARS)
 COPBC - CONDENSER FABRICATION COST (\$)
 CELEV - CONDENSER NH3 DISTRIBUTION PLATE AND BAFFLES COST (\$)
 CELEVP - COST OF ELECT POWER GENERATION (\$)
 CESWP - TWO-PHASE EVAP SW PUMP (DOLLARS)
 CFFCT - CONDENSER SHELL SIDE FRICTION (LBF/IN2)
 CFFTC - TWO-PHASE EFFECT OF COND PIPE FRICTION (LBF/IN2)
 CFTC - CONDENSER FILM TEMPERATURE (DEG F)
 CGEN - CONDENSER ON OF TPT TO S.I. UNITS (DEG C)
 CGFC - COST OF AMMONIA GENERATOR (\$)
 CGH - COND MASS VELOCITY FOR MIN HEAD COST (\$)
 CHE - CONDENSER HEAT EXCHANGER HEADS COST (\$)
 CHSC - CONDENSER HEAT EXCH SHELL COST (\$)
 NPU04410
 NPU02500
 NPU00910
 NPU04010
 NPU03460
 NPU04030
 NPU04120
 NPU04070
 NPU04110
 NPU04080
 NPU05660
 NPU01500
 NPU04930
 NPU04090
 NPU04020
 NPU00850
 NPU03370
 NPU04130
 NPU04140
 NPU01730
 NPU01740
 NPU02100
 NPU01120
 NPU01080
 NPU02330
 NPU05420
 NPU02380
 NPU06510
 NPU02320
 NPU05410
 NPU00630
 NPU01830
 NPU06180
 NPU01720
 NPU01810
 NPU01470
 NPU02540
 NPU00620
 NPU01750
 NPU02340
 NPU05430
 NPU02300

C CHSE - EVAP HEAT EXCHANGER SHELL COST(\$)
 C CHT - VERT DIST BETWEEN TUBES-CENTER TO CENTER(IN)
 C CL - COND TUBE PROFILE CHANNEL LENGTH(FT)
 C CLMID - CONDENSER LOG MEAN TEMPERATURE DIFFERENCE(DEG F)
 C CLMIDC - CONVERSION OF CLMID TO S.I. UNITS(DEG C)
 C CMINC - CAPACITY RATE OF CONDENSER SW(BTU/HR.F)
 C CMINE - EVAP SW CAPACITY RATE(BTU/HR.F)
 C CMOM - TWO-PHASE EFFECT OF COND DROP MOMENTUM(LBF/IN2)
 C CMW - 746 MW/HP
 C CNH3P - COST OF AMMONIA CIRC PUMP(DOLLARS)
 C CNTJ - NUMBER OF CONDENSER RE-FLUX PUMP(\$)
 C CONG - COLD PIPE SALINITY CONCENTRATION
 C CONH - HOT PIPE SALINITY CONCENTRATION
 C CORR - CORRECTION FACTOR FOR REVISED NH3 HT COEF
 C CPKE - CONDENSER INLET RESISTANCE COEFFICIENT
 C CPLAT - CONDENSER INLET RESISTANCE COEFFICIENT
 C CPLONG - VERT DIST BETWEEN TUBES-CENTER TO CENTER(IN)
 C CPNH3E - HORIZ HEAT OF AMMONIA IN EVAP(BTU/LBM.F)
 C CPR - CONDENSER TUBE PROFILE PITCH RATIO(IN)
 C CPSWC - CONDENSER TUBE HEAT(SW(BTU/LBM.F))
 C CPSW(TBLKE) - EVAP SW SPECIFIC HEAT(BTU/LBM.F)
 C CPSW(TBLKE) - SUBROUTINE SW SPECIFIC HEAT(BTU/LBM.F)
 C CRKE - CONDENSER INLET RESISTANCE COEFFICIENT
 C CSF - FLUID-SURFACE COMBINATION VALUE
 C CTAREA - CONDENSER TUBE PROFILE AREA-CENTER TO CENTER(IN2)
 C CTIE - EVAP TUBE INSTALLATION COST(\$)
 C CTMC - CONDENSER TUBE MATERIAL COST(\$)
 C CTME - CONDENSER TUBE MATERIAL COST(\$)
 C CTR2C - THERMAL RESISTANCE FOR COND TUBE SW(HR.F/BTU)
 C CTR3C - THERMAL RESISTANCE FOR COND TUBE THICK(HR.F/BTU)
 C CTR5C - THERMAL RESISTANCE FOR AMMONIA(HR.F/BTU)
 C CTRIE - THERMAL RESIST EVAP(TUBE) SW(HR.F/BTU)
 C CTR3E - THERMAL RESIST EVAP(TUBE) SW FOULING(HR.F/BTU)
 C CTR5E - THERMAL RESIST EVAP(TUBE) WALL THICK(HR.F/BTU)
 C CTSLC - CONDENSER SHEET LABOR COSTS(\$)
 C CTSLE - CONDENSER SHEET LABOR(\$)
 C CTSME - CONDENSER SHEET MATERIAL COST(\$)
 C CTSMB - COST OF AMMONIA TURBINE(\$)
 C CTVL - CONDENSER TUBE WALL TEMPERATURE(DEG F)

NPU05400
 NPU01050
 NPU00840
 NPU01150
 NPU02530
 NPU00700
 NPU04670
 NPU01820
 NPU03400
 NPU06720
 NPU00270
 NPU01210
 NPU03380
 NPU03390
 NPU02060
 NPU06260
 NPU06250
 NPU01110
 NPU01100
 NPU05110
 NPU03660
 NPU00680
 NPU04650
 NPU00810
 NPU04660
 NPU06360
 NPU06350
 NPU05280
 NPU01090
 NPU02290
 NPU05390
 NPU02280
 NPU05380
 NPU01390
 NPU01410
 NPU01960
 NPU01430
 NPU04940
 NPU04950
 NPU04960
 NPU04970
 NPU02260
 NPU05360
 NPU02270
 NPU05370
 NPU00610
 NPU01450

C	CTW2	CONDENSER SHELLSIDE WALL TEMPERATURE (DEG F)	NP001460
C	CTW2C	CONVERSION OF CTW2 TO S.I. UNITS (DEG C)	NP002550
C	CTWC	CONDENSER TUBE WELDING COST (\$)	NP002370
C	CWINS	EVAP WATER INLET NOZZLES AND SUPPORTS COST (\$)	NP005450
C	CWINS2	EVAP WATER INLET NOZZLES & SUPPORTS COST (\$)	NP005440
C	DBLKTC	ABSOLUTE DIFFERENCE BETWEEN TBLKE & RTBLKE (DEG F)	NP002360
C	DCONDC	ABSOLUTE DIFFERENCE BETWEEN ASSUMED TBLK TEMP AND SUPPORTS COST (\$)	NP004900
C	DCOREE	DIFFERENCE BETWEEN REVERSE CONDENSER (LBF/IN2) AND SUPPORTS COST (\$)	NP001170
C	DDENCT	TOTAL PRESSURE LOSS TO S.I. UNITS (KPA)	NP006430
C	DDUCTH	CONDENSER TUBING FRICTION LOSSES (LBF/IN2)	NP002560
C	DELB	EVAPORATOR TUBING FRICTION LOSSES (LBF/IN2)	NP006080
C	DELC	EVAPORATOR TUBING FRICTION LOSSES (LBF/IN2)	NP006310
C	DELTA3	EVAPORATOR TUBING FRICTION LOSSES (LBF/IN2)	NP000990
C	DELTA4	EVAPORATOR TUBING FRICTION LOSSES (LBF/IN2)	NP006270
C	DELTA5	EVAPORATOR TUBING FRICTION LOSSES (LBF/IN2)	NP003110
C	DELTA6	EVAPORATOR TUBING FRICTION LOSSES (LBF/IN2)	NP004920
C	DELTA7	EVAPORATOR TUBING FRICTION LOSSES (LBF/IN2)	NP001190
C	DELTA8	EVAPORATOR TUBING FRICTION LOSSES (LBF/IN2)	NP002090
C	DELTA9	EVAPORATOR TUBING FRICTION LOSSES (LBF/IN2)	NP005300
C	DELTA10	EVAPORATOR TUBING FRICTION LOSSES (LBF/IN2)	NP006000
C	DELTA11	EVAPORATOR TUBING FRICTION LOSSES (LBF/IN2)	NP001880
C	DELTA12	EVAPORATOR TUBING FRICTION LOSSES (LBF/IN2)	NP001480
C	DELTA13	EVAPORATOR TUBING FRICTION LOSSES (LBF/IN2)	NP005020
C	DELTA14	EVAPORATOR TUBING FRICTION LOSSES (LBF/IN2)	NP002570
C	DELTA15	EVAPORATOR TUBING FRICTION LOSSES (LBF/IN2)	NP002580
C	DELTA16	EVAPORATOR TUBING FRICTION LOSSES (LBF/IN2)	NP005960
C	DELTA17	EVAPORATOR TUBING FRICTION LOSSES (LBF/IN2)	NP006090
C	DELTA18	EVAPORATOR TUBING FRICTION LOSSES (LBF/IN2)	NP002590
C	DELTA19	EVAPORATOR TUBING FRICTION LOSSES (LBF/IN2)	NP000830
C	DELTA20	EVAPORATOR TUBING FRICTION LOSSES (LBF/IN2)	NP000430
C	DELTA21	EVAPORATOR TUBING FRICTION LOSSES (LBF/IN2)	NP000980
C	DELTA22	EVAPORATOR TUBING FRICTION LOSSES (LBF/IN2)	NP002070
C	DELTA23	EVAPORATOR TUBING FRICTION LOSSES (LBF/IN2)	NP005290
C	DELTA24	EVAPORATOR TUBING FRICTION LOSSES (LBF/IN2)	NP003490
C	DELTA25	EVAPORATOR TUBING FRICTION LOSSES (LBF/IN2)	NP002600
C	DELTA26	EVAPORATOR TUBING FRICTION LOSSES (LBF/IN2)	NP003500
C	DELTA27	EVAPORATOR TUBING FRICTION LOSSES (LBF/IN2)	NP002610
C	DELTA28	EVAPORATOR TUBING FRICTION LOSSES (LBF/IN2)	NP003510
C	DELTA29	EVAPORATOR TUBING FRICTION LOSSES (LBF/IN2)	NP002620
C	DELTA30	EVAPORATOR TUBING FRICTION LOSSES (LBF/IN2)	NP003520
C	DELTA31	EVAPORATOR TUBING FRICTION LOSSES (LBF/IN2)	NP002630
C	DELTA32	EVAPORATOR TUBING FRICTION LOSSES (LBF/IN2)	NP006590
C	DELTA33	EVAPORATOR TUBING FRICTION LOSSES (LBF/IN2)	NP003870
C	DELTA34	EVAPORATOR TUBING FRICTION LOSSES (LBF/IN2)	NP000950
C	DELTA35	EVAPORATOR TUBING FRICTION LOSSES (LBF/IN2)	NP000130
C	DELTA36	EVAPORATOR TUBING FRICTION LOSSES (LBF/IN2)	NP006620
C	DELTA37	EVAPORATOR TUBING FRICTION LOSSES (LBF/IN2)	NP006300

C	DPIPC	CONVERSION OF DPIPC TO S.I. UNITS(KPA)	NPU02640
C	DPIPEH	SW COLD PIPE FRICTION LOSSES(LBF/IN2)	NPU06290
C	DPIPEH	SW HOT PIPE FRICTION LOSSES(LBF/IN2)	NPU03360
C	DPIPH	TOTAL SW HOT PIPE FRICTION LOSSES(LBF/IN2)	NPU04680
C	DPIPHC	CONVERSION OF DPIPH TO S.I. UNITS(KPA)	NPU02650
C	DPIPNC	AMMONIA PCIRC PIPE PRESSURE LOSSES(LBF/IN2)	NPU06630
C	DPIPNC	CONVERSION OF DPIPNC TO S.I. UNITS(KPA)	NPU02660
C	DPIPNR	RE-FLUX AMMONIA PIPE LOSSES(LBF/IN2)	NPU00140
C	DPMCC	CONVERSION OF DPMCC TO S.I. UNITS(M)	NPU02680
C	DPMCC	CONVERSION OF DPMCC TO S.I. UNITS(M)	NPU02690
C	DPMNC	MINOR INLET/OUTLET CONDENSER LOSSES(LBF/IN2)	NPU06370
C	DPMINE	MINOR INLET/OUTLET EVAPORATOR LOSSES(LBF/IN2)	NPU05620
C	DPMNC	CONVERSION OF DPMNC TO S.I. UNITS(M)	NPU02670
C	DPMPCC	COND. OR SW COLD PIPE PUMP PRESSURE HEAD(LBF/IN2)	NPU06450
C	DPMPCC	COND. OR SW HOT PIPE PUMP PRESSURE HEAD(LBF/IN2)	NPU06110
C	DPMPCC	COND. OR SW HOT PIPE PUMP PRESSURE HEAD(LBF/IN2)	NPU06120
C	DPMPCC	COND. OR SW HOT PIPE PUMP PRESSURE HEAD(LBF/IN2)	NPU06650
C	DPMPCC	COND. OR SW HOT PIPE PUMP PRESSURE HEAD(LBF/IN2)	NPU06660
C	DPMPNC	AMMONIA CIRC PUMP PRESSURE HEAD(LBF/IN2)	NPU00160
C	DPMPNC	AMMONIA CIRC PUMP PRESSURE HEAD(LBF/IN2)	NPU06580
C	DPNH3P	RE-FLUX AMMONIA PUMP HEAD(LBF/IN2)	NPU00110
C	DPNHRP	AMMONIA CIRCULATION PIPE FRICTION LOSSES(LBF/IN2)	NPU02700
C	DPNRC	CONVERSION OF DPNRC TO S.I. UNITS(KPA)	NPU02710
C	DPNRC	CONVERSION OF DPNRC TO S.I. UNITS(M)	NPU00170
C	DPNRC	RE-FLUX AMMONIA PUMP HEAD(FT)	NPU00170
C	DPNRC	RE-FLUX AMMONIA THERMO. PRESSURE HEAD(LBF/IN2)	NPU06640
C	DPNTHRF	PUMPED RE-FLUX AMMONIA PRESSURE DROP(LBF/IN2)	NPU00150
C	DSDEM	MOISTURE SEPARATOR PRESSURE DROP(LBF/IN2)	NPU05730
C	DSDEM	MOISTURE SEPARATOR PRESSURE DROP(LBF/IN2)	NPU02720
C	DSEVAP	CONVERSION OF SHELLSIDE PRESSURE DROP(LBF/IN2)	NPU05710
C	DSEVAP	CONVERSION OF SHELLSIDE PRESSURE DROP(LBF/IN2)	NPU02730
C	DSEVAP	CONVERSION OF SHELLSIDE PRESSURE DROP(LBF/IN2)	NPU02730
C	DSEVAP	CONVERSION OF SHELLSIDE PRESSURE DROP(LBF/IN2)	NPU02230
C	DSEVAP	CONVERSION OF SHELLSIDE PRESSURE DROP(LBF/IN2)	NPU05340
C	DSEVAP	CONVERSION OF SHELLSIDE PRESSURE DROP(LBF/IN2)	NPU04370
C	DSEVAP	CONVERSION OF SHELLSIDE PRESSURE DROP(LBF/IN2)	NPU04380
C	DSEVAP	CONVERSION OF SHELLSIDE PRESSURE DROP(LBF/IN2)	NPU05980
C	DSEVAP	CONVERSION OF SHELLSIDE PRESSURE DROP(LBF/IN2)	NPU01860
C	DSEVAP	CONVERSION OF SHELLSIDE PRESSURE DROP(LBF/IN2)	NPU02220
C	DSEVAP	CONVERSION OF SHELLSIDE PRESSURE DROP(LBF/IN2)	NPU05940
C	DSEVAP	CONVERSION OF SHELLSIDE PRESSURE DROP(LBF/IN2)	NPU04050
C	DSEVAP	CONVERSION OF SHELLSIDE PRESSURE DROP(LBF/IN2)	NPU04060
C	DSEVAP	CONVERSION OF SHELLSIDE PRESSURE DROP(LBF/IN2)	NPU01550
C	DSEVAP	CONVERSION OF SHELLSIDE PRESSURE DROP(LBF/IN2)	NPU04620
C	DSEVAP	CONVERSION OF SHELLSIDE PRESSURE DROP(LBF/IN2)	NPU04560
C	DSEVAP	CONVERSION OF SHELLSIDE PRESSURE DROP(LBF/IN2)	NPU03720
C	DSEVAP	CONVERSION OF SHELLSIDE PRESSURE DROP(LBF/IN2)	NPU03750

NPU006000
 NPU050000
 NPU004990
 NPU02760
 NPU06600
 NPU033780
 NPU00120
 NPU06400
 NPU06240
 NPU05650
 NPU02350
 NPU06560
 NPU02770
 NPU02780
 NPU06220
 NPU02790
 NPU04450
 NPU02800
 NPU05580
 NPU00050
 NPU00090
 NPU00820
 NPU03410
 NPU03430
 NPU03420
 NPU05670
 NPU05520
 NPU05540
 NPU05810
 NPU05550
 NPU05770
 NPU05800
 NPU05920
 NPU05880
 NPU05910
 NPU00400
 NPU05840
 NPU00440
 NPU05780
 NPU05890
 NPU05530
 NPU02170
 NPU02820
 NPU04820
 NPU002810
 NPU00410
 NPU05790
 NPU05900

ETURBP - CONVERSION OF ETURB(PCT)
 ETW1 - EVAP TUBESIDE WALL TEMPERATURE(DEG F)
 ETW2 - EVAP SHELLSIDE WALL TEMPERATURE(DEG F)
 ETW2C - CONVERSION OF ETW2 TO S.I. UNITS(DEG C)
 EZ1 - DATA OF AMMONIA PIPING CONFIG(FT)
 EZ2 - ELEVATION OF AMMONIA PIPING CONFIGURATION HEIGHT(FT)
 EZR - RE-FLOW AMMONIA PIPING CONDENSER TUBING
 FFCC - FRICTION FACTOR OF SW COLD PIPE
 FFCCP - FRICTION FACTOR OF EVAPORATOR PIPING
 FFHP - FRICTION FACTOR OF SW HOT PIPE
 FFN13P - FRICTION FACTOR OF PIPED AMMONIA
 FLN13C - CONVERSION OF FLONH3 TO S.I. UNITS(KG/HR)
 FLN13R - CONVERSION OF FLONHR TO S.I. UNITS(KG/HR)
 FLN13RC - COLD PIPE SW FLOW RATE(LBM/HR)
 FLOCPC - CONVERSION OF FLOCP TO S.I. UNITS(KG/HR)
 FLOHPC - HOT PIPE SW MASS FLOW RATE(LBM/HR)
 FLONH3 - AMMONIA MASS FLOW RATE(LBM/HR)
 FLONHR - RE-FLOW AMMONIA FLOW RATE(LBM/HR)
 FNH3RP - FRICTION FACTOR OF PIPED RE-FLOW AMMONIA
 FPF - FRICTION FACTOR FOR DOUBLE-FLOW GEN-TJRBINE
 G - 32.174 FT/SEC2
 GAL - 37.481 GAL/FT3
 GC - 32.174 FT LBM/LBF SEC2
 GF - NH3 MASS VEL THRU EVAP FREE-FLOW AREA(LBM/FT2 SEC)
 H1 - ENTHALPY AT STATE PT 1(BTU/LBM)
 H2 - ENTHALPY AT STATE PT 2(BTU/LBM)
 H3 - ENTHALPY OF AMMONIA AT STATE PT 3(BTU/LBM)
 H3A - ENTHALPY OF SAT LIQ AMMONIA AT STATE PT 3A(BTU/LBM)
 H3F - ENTHALPY OF SAT VAPOR AMMONIA AT STATE PT 3(BTU/LBM)
 H4 - ENTHALPY OF AMMONIA AT STATE PT 4(BTU/LBM)
 H4F - ENTHALPY OF SAT LIQ AMMONIA AT STATE PT 4(BTU/LBM)
 H4G - ENTHALPY OF SAT VAPOR AMMONIA AT STATE PT 4(BTU/LBM)
 H5 - ENTHALPY AT STATE PT 5(BTU/LBM)
 H5F - ENTHALPY OF LIQ AT STATE PT 5(BTU/LBM)
 H5G - ENTHALPY OF SAT LIQ AMMONIA(BTU/LBM)
 HF(P3) - SUBROUTINE FOR SAT LIQ AMMONIA(BTU/LBM)
 HF(P4) - SUBROUTINE FOR SAT LIQ AMMONIA(BTU/LBM)
 HF(PCOND) - SUBROUTINE FOR ENTHALPY(BTU/LBM)
 HFSWC - PSEUDO HT COEFF COND SW FOULING(BTU/HR FT2 F)
 HFSWC - CONVERSION OF HFSWC TO S.I. UNITS(W/M2 C)
 HFSWC - PSEUDO HT COEFF FOR EVAP SW FOULING(BTU/HR FT2 F)
 HFSWC - CONVERSION OF HFSWC TO S.I. UNITS(W/M2 C)
 HFSWEC - CONVERSION OF HFSWEC TO S.I. UNITS(W/M2 C)
 HGS - ENTHALPY OF VAPOR AT STATE AMMONIA(BTU/LBM)
 HG(P3) - SUBROUTINE FOR SAT VAPOR AMMONIA(BTU/LBM)
 HG(P4) - SUBROUTINE FOR SAT VAPOR AMMONIA(BTU/LBM)

NPU00420
 NPU005570
 NPU002190
 NPU002840
 NPU004840
 NPU002850
 NPU002040
 NPU005160
 NPU003440
 NPU002810
 NPU003080
 NPU002160
 NPU002860
 NPU004810
 NPU002870
 NPU005240
 NPU005250
 NPU001400
 NPU004770
 NPU001250
 NPU004420
 NPU001360
 NPU004740
 NPU002180
 NPU002880
 NPU004830
 NPU002910
 NPU002830
 NPU002490
 NPU001840
 NPU005760
 NPU002890
 NPU005740
 NPU006730
 NPU005830
 NPU000010
 NPU003530
 NPU002900
 NPU003540
 NPU002920
 NPU003450
 NPU005170
 NPU001350
 NPU004730
 NPU002420
 NPU003710
 NPU004360
 NPU006470

C C H G (PCOND) - SUBROUTINE FOR ENTHALPY OF A VAPOR (BTU/LBM)
 C C H G (PEVAP) - SUBROUTINE FOR ENTHALPY (BTU/LBM)
 C C H NH3C - SEUDO HT COEFF COND AMMONIA (BTU/HR.FT2.F)
 C C H NH3CC - CONVERSION OF HNH3C TO S.I. UNITS (W/M2.C)
 C C H NH3EC - SEUDO HT COEFF FOR EVAP AMMONIA (BTU/HR.FT2.F)
 C C H NH3ECR - CONVERSION OF HNH3E TO S.I. UNITS (W/M2.C)
 C C H NH3ER - REVISED AMMONIA HT COEFF COND. (BTU/HR.FT2.F)
 C C H PC - 550 FT.LBFF/SEC.HP
 C C H PKI - INLET DUCT TO SW HOT PIPE RESISTANCE COEFFICIENT
 C C H PKE - OUTLET SW HOT PIPE RESISTANCE COEFFICIENT
 C C H SWC - SEUDO HT COEFF COND SW (BTU/HR.FT2.F)
 C C H SWCC - CONVERSION OF HSWC TO S.I. UNITS (W/M2.C)
 C C H SWEC - SEUDO HT COEFF FOR EVAP SW (BTU/HR.FT2.F)
 C C H TDR - EVAP NH3 HT COEFF DEVELOPING REGION (BTU/HR.FT2.F)
 C C H TDFDR - EVAP NH3 HT COEFF FULLY DEVELOPED REG (BTU/HR.FT2.F)
 C C H TFSWC - HT COEFF FOR COND. SW FOULING COEF (BTU/HR.FT2.F)
 C C H TFSWE - EVAP SW FOULING COEF (BTU/HR.FT2.F)
 C C H TNH3C - INITIAL SHELLSIDE HT COEFFICIENT (BTU/HR.FT2.F)
 C C H TNH3E - EVAP SHELLSIDE HT COEFFICIENT (BTU/HR.FT2.F)
 C C H TSWC - HT COEFFICIENT FOR CONDENSER SW (BTU/HR.FT2.F)
 C C H TSWE - EVAP TUBESIDE HT COEFFICIENT (BTU/HR.FT2.F)
 C C H HWC - SEUDO HT COEFF COND WALL THICK. (BTU/HR.FT2.F)
 C C H HWC - CONVERSION OF HWC TO S.I. UNITS (W/M2.C)
 C C H HMEC - SEUDO HT COEFF FOR EVAP WALL THICK (BTU/HR.FT2.F)
 C C H HMEC - CONVERSION OF HME TO S.I. UNITS (W/M2.C)
 C C H MATL - TUBING MATERIAL SELECTION
 C C H OBJ - OBJECTIVE FUNCTION TO MINIMIZE COST
 C C H P1 - PRESSURE OF SAT AMMONIA AT STATE PT 1 (LBF/IN2)
 C C H P3 - PRESSURE OF AMMONIA AT STATE PT 3 (LBF/IN2)
 C C H P3C - CONVERSION OF P3 TO S.I. UNITS (KPA)
 C C H P4 - PRESSURE OF AMMONIA AT STATE PT 4 (LBF/IN2)
 C C H PARAL - PARASITIC PUMP REQUIREMENTS (MW)
 C C H PAVGD - AVG PRESSURE ACROSS MOISTURE SEPARATOR (LBF/IN2)
 C C H PAVGE - AVERAGE EVAPORATOR PRESSURE (LBF/IN2)
 C C H PCONDC - OPERATION PRESSURE OF THE CONDENSER (LBF/IN2)
 C C H PEVAP - OPERATING PRESSURE OF PCOND TO S.I. UNITS (KPA)
 C C H PEVAPC - OPERATING PRESSURE OF THE EVAPORATOR (LBF/IN2)
 C C H PIE - 3.141592654
 C C H PNH3E - PRANDTL NUMBER FOR EVAP SHELLSIDE FLOW
 C C H PNSWC - PRANDTL NUMBER FOR CONDENSER SW
 C C H PNSWE - PRANDTL NUMBER FOR EVAP TUBESIDE FLOW
 C C H PPP - PERCENT OF PARASITIC POWER (PCT)
 C C H PROF - TUBE PROFILE SELECTION
 C C H PRSYST - SYSTEM PRESS RATIO
 C C H PWRCP - POWER COND. OR CSW COLD PIPE PUMP (HP)

NPU02020
 NPU05150
 NPU05230
 NPU06550
 NPU00080
 NPU06390
 NPU05720
 NPU02310
 NPU01950
 NPU05490
 NPU05590
 NPU00030
 NPU01030
 NPU01670
 NPU05680
 NPU06190
 NPU04430
 NPU04890
 NPU01040
 NPU00520
 NPU00480
 NPU00490
 NPU00550
 NPU00560
 NPU04910
 NPU01180
 NPU02080
 NPU05330
 NPU05990
 NPU01870
 NPU05950
 NPU00530
 NPU00500
 NPU01640
 NPU00540
 NPU00510
 NPU01920
 NPU04550
 NPU01660
 NPU04580
 NPU04590
 NPU01510
 NPU04240
 NPU03020
 NPU01850
 NPU04280

RNH3CV -- PSEUDO REYNOLDS NO. FOR VERT. CONDENSER
 RNH3EH -- PSEUDO REYNOLDS NR FOR THIN FILM EVAPORATION
 RNH3EV -- PSEUDO REYNOLDS NR FOR CONVECTIVE EVAPORATION
 RNH3P -- REYNOLDS NUMBER OF PIPE AMMONIA FLOW
 RNH3RP -- REYNOLDS NUMBER OF RE-FLUX AMMONIA PIPE FLOW
 RNSWC P -- REYNOLDS NUMBER OF CONDENSER TUBESIDE FLOW
 RNSWE P -- REYNOLDS NUMBER OF EVAPORATOR TUBESIDE FLOW
 RNSWHP -- REYNOLDS NUMBER OF HOT PIPE SW FLOW
 RNH3C -- DENSITY OF AMMONIA (LBM/FT3)
 RNH3E -- EVAP SHELLSIDE AMMONIA DENSITY (LBM/FT3)
 RNH3P -- RE-FLUX AMMONIA DENSITY (LBM/FT3)
 RNH3R -- NH3 DENSITY AT MOISTURE SEPARATOR INLET (LBM/FT3)
 RNH3S -- CONDENSER SHELLSIDE VAPOR DENSITY (LBM/FT3)
 RNH3T -- EVAPORATOR AMMONIA VAPOR DENSITY (LBM/FT3)
 ROSHCP -- DENSITY OF COLD PIPE SW (LBM/FT3)
 ROSWHP -- HOT PIPE SW DENSITY (LBM/FT3)
 RTBLK C -- REVISED COND TBLK TEMPERATURE (DEG F)
 RTBLKE -- REVISED EVAP TBLK TEMPERATURE (DEG F)
 RTNCT -- REVISED NUMBER OF CONDENSER TUBES
 S4 -- ENTROPY AT STATE PT 4 (BTU/LBM.R)
 S4F -- ENTROPY OF LIQ AT STATE PT 4 (BTU/LBM.R)
 S4G -- ENTROPY OF VAPOR AT STATE PT 4 (BTU/LBM.R)
 S5F -- ENTROPY OF A LIQ AT STATE PT 5 (BTU/LBM.R)
 S5G -- ENTROPY OF A VAPOR AT STATE PT 5 (BTU/LBM.R)
 SCALBC -- ABSOLUTE CONDENSER HT COEFF
 SCALC -- ABSOLUTE COAMMONIA HT COEFF
 SCALH -- ABSOLUTE VALUE OF TR3 (DEG F)
 SCALT1 -- ABSOLUTE VALUE OF TIR (DEG F)
 SCALV -- ABSOLUTE VALUE FOR VNH3 (FT/SEC)
 SF(T1) -- SUBROUTINE FOR ENTROPY OF A LIQ (BTU/LBM.R)
 SF(T4) -- SUBROUTINE FOR ENTROPY OF A LIQ (BTU/LBM.R)
 SF(T5) -- SUBROUTINE FOR ENTROPY OF A SAT LIQ NH3 (BTU/LBM.R)
 SG(T1) -- SUBROUTINE FOR ENTROPY OF A VAPOR (BTU/LBM.R)
 SG(T4) -- SUBROUTINE FOR ENTROPY OF A VAPOR (BTU/LBM.R)
 SG(T5) -- SUBROUTINE FOR ENTROPY OF A SAT VAP NH3 (BTU/LBM.R)
 SNC -- VERTICAL HEIGHT BETWEEN TUBES
 SPEC -- VERTICAL DISTANCE BETWEEN CONDENSER TUBES (IN)
 SWFC -- SALT WATER FOULING RATE AT STATE PT 1 (DEG F)
 T1 -- SALT LIQ AMMONIA TEMPERATURE AT STATE PT 1 (DEG F)
 T1C -- CONVERSION OF T1 TO S.I. UNITS (DEG C)
 T1R -- REVISED TEMPERATURE OF AMMONIA AT STATE PT 1 (DEG F)
 T3 -- AMMONIA VAPOR TEMPERATURE AT STATE PT 3 (DEG F)

T3A - SAT VAPOR AMMONIA TEMP AT STATE PT 3A(DEG F)
 T3AC - CONVERSION OF T3A TO S.I. UNITS(DEG C)
 T3C - REVERSED TEMPERATURE AT STATE PT 3(DEG F)
 T3C - REVERSED TEMPERATURE AT STATE PT 3(DEG F)
 T4 - TEMPERATURE OF AMMONIA AT STATE PT 4(DEG F)
 T4C - CONVERSION OF T4 TO S.I. UNITS(DEG C)
 T5 - TEMPERATURE OF AMMONIA AT STATE PT 5(DEG F)
 T5C - CONVERSION OF T5 TO S.I. UNITS(DEG C)
 TAVG - AVERAGE EVAPORATOR TEMPERATURE(DEG F)
 TBLKCR - CONDENSER SW BULK TEMPERATURE(DEG F)
 TBLKE - EVAPORATOR SW BULK TEMPERATURE(DEG F)
 TBLKER - CONVERSION OF TBLKE(DEG F) TO S.I. UNITS(DEG C)
 TCE - THERMODYNAMIC CYCLE EFFICIENCY(PCT)
 TICIC - CONDENSER SW INLET TEMPERATURE(DEG F)
 TICIC - CONVERSION OF TICIC TO S.I. UNITS(DEG C)
 TICOC - CONDENSER SW OF OUTLET TEMPERATURE(DEG F)
 TICOC - CONVERSION OF TICOC TO S.I. UNITS(DEG C)
 TIC(TDOE) - SUBROUTINE TO COST EVAP TI TUBING\$/FT(\$/FT)
 TIC(TDOE) - SUBROUTINE TO COST EVAP TI TUBING O/FT(\$/FT)
 TIC(TDOE) - SUBROUTINE TO COST COND TI TUBING\$/FT(\$/FT)
 TIC(TDOE) - SUBROUTINE TO COST COND TI TUBING O/FT(\$/FT)
 TDIC - CONDENSER TUBE INNER DIAMETER(IN)
 TDIC - CONVERSION OF TDIC(FT) TO S.I. UNITS(MM)
 TDIEC - EVAPORATOR TUBE INNER DIAMETER(IN)
 TDIEC - CONVERSION OF TDIEC(FT) TO S.I. UNITS(MM)
 TDOCC - CONDENSER TUBE OUTER DIAMETER(IN)
 TDOCC - CONVERSION OF TDOCC(FT) TO S.I. UNITS(MM)
 TDOEC - EVAPORATOR TUBE OUTER DIAMETER(IN)
 TDOEC - CONVERSION OF TDOEC(FT) TO S.I. UNITS(MM)
 TENS - SURFACE TENSION OF TDOE(FT)
 TE(TDOE) - SUBROUTINE TO SIZE ENHANCED EVAP TI TUBING(IN)
 TE(TDOE) - SUBROUTINE TO SIZE ENHANCED EVAP TI TUBING(IN)
 THTAC - TOTAL CONDENSER HT SURFACE AREA(FT2)
 THTAC - CONVERSION OF THTAC TO S.I. UNITS(M2)
 THTAEC - TOTAL EVAP HEAT TRANSFER AREA(FT2)
 THTAEC - CONVERSION OF THTAEC TO S.I. UNITS(M2)
 THTAER - REVERSED EVAP HEAT TRANSFER AREA(FT2)
 THTAER - CONVERSION OF THTAER TO S.I. UNITS(M2)
 THIEC - EVAPORATOR INLET SW TEMPERATURE(DEG F)
 THIEC - CONVERSION OF THIEC TO S.I. UNITS(DEG C)
 THOEC - EVAP SW OUTLET TEMP(DEG F)
 THOEC - CONVERSION OF THOEC TO S.I. UNITS(DEG C)
 TKNH3C - COND AMMONIA THERMAL CONDUCTIVITY(BTU/HR.FT.F)
 TKNH3(CFT) - SUBROUTINE FOR NH3 THERMAL CONDUCTIVITY
 TKNH3E - THERMAL COND AMMONIA IN EVAP(BTU/HR.FT.F)
 TKNH3(LEFT) - THERMAL COND AMMONIA IN COND(BTU/HR.FT.F)
 TKSWC - CONDENSER SW THERMAL CONDUCTIVITY(BTU/HR.FT.F)

NPU004270
 NPU003030
 NPU003040
 NPU005970
 NPU005820
 NPU003050
 NPU001530
 NPU000020
 NPU006320
 NPU006330
 NPU004460
 NPU004690
 NPU002450
 NPU000710
 NPU003060
 NPU000720
 NPU003070
 NPU004210
 NPU004160
 NPU004230
 NPU004290
 NPU001290
 NPU004310
 NPU004330
 NPU003560
 NPU004340
 NPU003090
 NPU003570
 NPU004350
 NPU003100
 NPU004180
 NPU005270
 NPU004220
 NPU004170
 NPU002200
 NPU003140
 NPU004530
 NPU003150
 NPU005310
 NPU003580
 NPU003120
 NPU004880
 NPU003130
 NPU001980
 NPU001990
 NPU006030
 NPU005470
 NPU001320

NPU05190
 NPU00380
 NPU00360
 NPU00370
 NPU02430
 NPU05080
 NPU05070
 NPU01560
 NPU05750
 NPU05860
 NPU05850
 NPU05870
 NPU00450
 NPU00570
 NPU00580

C WEA - AMMONIA FLOW RATE PER UNIT AXIAL LENGTH(LBM/HR. FT)
 C WELC - ELECTRICAL LOADING(MW)
 C WELP - NET ELECTRICAL OUTPUT AS A F(EFFICIENCY)(MW)
 C WELT - NET ELECTRIC LOSSES IN EFFICIENCY(MW)
 C WNET - NET WORK IN THERMODYNAMIC CIRC PUMP WORK(BTU/LBM)
 C WPSNH3 - THERMODYNAMIC AMMONIA CIRC PUMP WORK(BTU/LBM)
 C X3A - ISENTROPIC AMMONIA AT STATE PT 3(DECIMAL)
 C X3P - QUALITY OF AMMONIA AT STATE PT 3(DECIMAL)
 C X4P - QUALITY OF AMMONIA AT STATE PT 4(DECIMAL)
 C X5P - QUALITY OF AMMONIA AT STATE PT 5(DECIMAL)
 C X5S - CONVERSION OF X5(PCT)
 C X5SP - CONVERSION OF X5S(PCT)

C	TYPEE=3.	HORIZONTAL EVAPORATOR	BOILING CORRELATION	49
C	TYPEC=1.	HORIZONTAL CONDENSER		50
C	TYPEC=2.	VERTICAL CONDENSER		51
C	TYPEC=1.			52
C	TYPEE=1.			53
C	ENHANCEMENT SELECTION			54
C	EHFE=1.	PLAIN TUBE EVAPORATOR		55
C	EHFC=1.	PLAIN TUBE CONDENSER		56
C	EHFE=2.	LINDE-PROMOTER EVAPORATOR (NOT CODED)		57
C	EHFC=2.	LINDE-PROMOTER CONDENSER (NOT CODED)		58
C	EHFC=1.			59
C	EHFE=1.			60
C	TUBE FIN EFFICIENCY			61
C	EFFIE=1.0			62
C	EFFOE=1.0			63
C	EFFOC=1.0			64
C	EFFIC=1.0			65
C	TUBE PROFILE SELECTION			66
C	PROF=1.	STAGGERED EQUI-LATERAL		67
C	PROF=2.	IN-LINE EQUI-SIDED		68
C	PROF=1.			69
C	SYSTEM PIPE GEOMETRY AND MATERIAL			70
C	ECC=150.E-06			71
C	ECP=500.E-06			72
C	ECE=150.E-06			73
C	ERP=500.E-06			74
C	ELBOW=30.			75
C	ENH3P=500.E-06			76
C	TLC=3000.			77
C	TLHP=300.			78
C	TLNH3P=150.			79
C	TLNHRP=50.			80
C	TUBING MATERIAL SELECTION			81
C	TMATL=1.	ALUMINIUM		82
C	TMATL=2.	TITANIUM		83
C	TMATL=1.			84
C	TKW=77.			85
C				86
C				87
C				88
C				89
C				90
C				91
C				92
C				93
C				94
C				95
C				96

145
 146
 147
 148
 149
 150
 151
 152
 153
 154
 155
 156
 157
 158
 159
 160
 161
 162
 163
 164
 165
 166
 167
 168
 169
 170
 171
 172
 173
 174
 175
 176
 177
 178
 179
 180
 181
 182
 183
 184
 185
 186
 187
 188
 189
 190
 191
 192

```

TLNRPC=.3048*TLNHRP
TLCPC=.3048*TLCP
VSWCC=.3048*VSWC
VSMWC=.3048*VSMW
VSMWPC=.3048*VSMWCP
VSMWHP=.3048*VSMWHP

C SUMMARY OF INPUT DATA
C
10 WRITE (6,1150)
   IF (TYPE.EQ.2.) GO TO 10
   WRITE (6,1160)
   CONTINUE
20 WRITE (6,1170)
   CONTINUE
   WRITE (6,1180) TDOE, TDOECC
   WRITE (6,1190) TLE, TLEC
   WRITE (6,1200) VSMW, VSMWC
   WRITE (6,1210) PEVAP, PEVAPC
   IF (TMA.TL.EQ.2.) GO TO 30
   WRITE (6,1220) TKW, TKWC
   GO TO 40
30 CONTINUE
40 WRITE (6,1230) TKM, TKMC
   CONTINUE
   IF (PROF.EQ.2.) GO TO 50
   WRITE (6,1240)
   GO TO 60
50 CONTINUE
60 WRITE (6,1250)
   CONTINUE
   WRITE (6,1260) EPR
   IF (EHFE.EQ.2.) GO TO 70
   WRITE (6,1270)
   GO TO 80
70 CONTINUE
80 WRITE (6,1280)
   CONTINUE
   IF (TYPEC.EQ.2.) GO TO 90
   WRITE (6,1290)
   GO TO 100
90 CONTINUE
100 WRITE (6,1300)
   CONTINUE
   WRITE (6,1310) TDOCC, TDOCCC
   WRITE (6,1320) TLEC, TLECC
   WRITE (6,1330) VSMWC, VSMWCC
  
```

193
 A 194
 A 195
 A 196
 A 197
 A 198
 A 199
 A 200
 A 201
 A 202
 A 203
 A 204
 A 205
 A 206
 A 207
 A 208
 A 209
 A 210
 A 211
 A 212
 A 213
 A 214
 A 215
 A 216
 A 217
 A 218
 A 219
 A 220
 A 221
 A 222
 A 223
 A 224
 A 225
 A 226
 A 227
 A 228
 A 229
 A 230
 A 231
 A 232
 A 233
 A 234
 A 235
 A 236
 A 237
 A 238
 A 240

WRITE (6,1340) PCOND,PCONDC
 IF (TMATL.EQ.2.) GO TO 110
 WRITE (6,1350) TKW,TKWC
 GO TO 120
 CONTINUE
 WRITE (6,1360) TKW,TKWC
 CONTINUE
 IF (PROF.EQ.2.) GO TO 130
 WRITE (6,1370)
 GO TO 140
 CONTINUE
 WRITE (6,1380)
 CONTINUE
 WRITE (6,1390) EPR
 IF (EHFC.EQ.2.) GO TO 150
 WRITE (6,1400)
 GO TO 160
 CONTINUE
 WRITE (6,1410)
 CONTINUE
 WRITE (6,1420)
 WRITE (6,1430) DIHP,DIHPC
 WRITE (6,1440) TLHP,TLHPC
 WRITE (6,1450) VSWHP,VSWHPC
 WRITE (6,1460) THIE,THIEC
 WRITE (6,1470) CONH
 WRITE (6,1480)
 WRITE (6,1490) DICP,DICPC
 WRITE (6,1500) TLCP,TLPCPC
 WRITE (6,1510) VSWCP,VSWCPC
 WRITE (6,1520) TCIC,TCICC
 WRITE (6,1530) CONC
 WRITE (6,1540)
 WRITE (6,1550) DINH3,DINH3C
 WRITE (6,1560) TLNH3P,TLNHPC
 WRITE (6,1570)
 WRITE (6,1590) DINH3R,DINHRC
 WRITE (6,1600) TLNH3RP,TLNHRPC
 WRITE (6,1610)
 WRITE (6,1620) EPE,EME
 WRITE (6,1630)
 WRITE (6,1640) EPC,EMC
 WRITE (6,1650) EPNH3,EMNH3
 WRITE (6,1660)
 WRITE (6,1670) EEP
 WRITE (6,1680) ETRP
 WRITE (6,1690)

241
 A A 242
 A A 243
 A A 244
 A A 245
 A A 246
 A A 247
 A A 248
 A A 249
 A A 250
 A A 251
 A A 252
 A A 253
 A A 254
 A A 255
 A A 256
 A A 257
 A A 258
 A A 259
 A A 260
 A A 261
 A A 262
 A A 263
 A A 264
 A A 265
 A A 266
 A A 267
 A A 268
 A A 269
 A A 270
 A A 271
 A A 272
 A A 273
 A A 274
 A A 275
 A A 276
 A A 277
 A A 278
 A A 279
 A A 280
 A A 281
 A A 282
 A A 283
 A A 284
 A A 285
 A A 286
 A A 287
 A A 288

```

170 WRITE (6,1700) ELECT
C WRITE (6,1710) ELECT
C RETURN
C CONTINUE
C **** EXECUTION OF INPUT DATA ****
C TUBE WALL THICKNESS(INCH) AND TUBE COST PER FT($/FT)
C ALUMINUM TUBING
C IF (TMAIL.GT.1.5) GO TO 210
C IF (EHFE.GT.1.5) GO TO 180
C TTE=AP(TDOE)
C E1=AC(TDOE)
C E2=0.0
C GO TO 190
C CONTINUE
C TTE=AE(TDOE)
C E1=AEC(TDOE)
C E2=0.0
C CONTINUE
C IF (EHFC.GT.1.5) GO TO 200
C TTC=AP(TDOC)
C C1=AC(TDOC)
C C2=0.0
C GO TO 250
C CONTINUE
C TTC=AE(TDOC)
C C1=ACC(TDOC)
C C2=0.0
C GO TO 250
C TITANIUM TUBING
C CONTINUE
C IF (EHFE.EQ.2.) GO TO 220
C TTE=TP(TDOE)
C E1=TC(TDOE)
C E2=1.21
C GO TO 230
C CONTINUE
C TTE=TE(TDOE)
C E1=TEC(TDOE)
C E2=1.21
C CONTINUE
C IF (EHFC.EQ.2.) GO TO 240
C TTC=TP(TDOC)
C C1=TC(TDOC)

```



```

C C INITIALLY ASSUME AN EVAP TUBE LENGTH(FT)
C C ASSUME A HT COEF FOR EVAP SHELLSIDE
C C HTNH3E=1000.
C C HOT PIPE SW MASS FLOW RATE(LBM/HR)
C C ROSWHP=RHOSW*(THIE)
C C FLOHP=3600.*ROSWHP*PIE*DIHP**2*VSWHP/4.
C C EVAP SW DENSITY(INITIAALLY ASSUME TBULK=THIE)
C C TBLKE=THIE
C C CONTINUE
C C RHOSWE=RHOSW*(TBLKE)
C C TKSWE=TKSW*(TBLKE)
C C TOTAL NUMBER OF EVAP TUBES
C C TNET=4.*FLOHP/(3600.*RHOSWE*PIE*TDIEC**2*VSWE)
C C TUBE SHEET DIAMETER(FT)
C C TUBE PROFILE - STAGGERED
C C IF (PROF.EQ.2.) GO TO 270
C C EHT=EPR*TD0E*0.5
C C EBASE=EPR*TD0E*0.866
C C ETAREA=EHT*EBASE*2.
C C SN=2.*EHT
C C SPE=2.*EBASE-TDOE
C C SPEC=SPE/12.
C C GO TO 280
C C CONTINUE
C C TUBE PROFILE - IN-LINE
C C EPLONG=EPR*TD0E
C C SN=EPLONG
C C EPLAT=EPR*TD0E
C C ETAREA=EPLONG*EPLAT
C C SPE=EPR*TD0E-TDOE
C C SPEC=SPE/12.
C C CONTINUE
C C EAREA=ETAREA*TNET
C C TSDE=((4.*EAREA/PIE)**0.5)/12.
C C TOTAL HT AREA OF EVAP(FT2 OR M2)

```

```

337
338
339
340
341
342
343
344
345
346
347
348
349
350
351
352
353
354
355
356
357
358
359
360
361
362
363
364
365
366
367
368
369
370
371
372
373
374
375
376
377
378
379
380
381
382
383
384

```

```

C      THTAE=TNET*PIE*TDIEC*TLI
C      CMIN FOR EVAP(BTU/HR.F OR W/C)
C      CPSWE=CPSW(TBLKE)
C      CMINE=FLOHP*CPSWE
C      OVERALL HT COEF(BTU/HR.FT2.F OR W/M2.C)
C      TBLKER=TBLKE*459.69
C      REYNOLDS NUMBER FOR EVAP TUBESIDE
C      VISSWE=VISSW(TBLKE)
C      RNSWE=3600.*RHOSWE*VSWE*TDIEC/VISSWE
C      PRANDTL NUMBER FOR EVAP TUBESIDE
C      PNSWE=CPSWE*VISSWE/TKSWE
C      HT COEF FOR EVAP TUBESIDE
C      IF (RNSWE.GT.2300.) GO TO 290
C      LAMINAR FLOW USING SIEDER-TATE CORRELATION
C      HTSWE=1.86*TKSWE*(RNSWE*PNSWE)**.3333*(TDIEC/TLE)**.3333/TDIEC
C      GO TO 300
C      CONTINUE
C      TURBULENT FLOW USING DITUS-BOELTER CORRELATION
C      (INITIALLY ASSUME TBLKE=THIE)
C      HTSWE=.023*TKSWE*RNSWE**.8*PNSWE**.4/TDIEC
C      CONTINUE
C      THERMAL RESISTANCE FOR SW(HR.FT2.F/BTU)
C      TRIE=TDIEC/(EFFIE*HTSWE*TDIEC)
C      THERMAL RESISTANCE FOR SW FOULING(HR.FT2.F/BTU)
C      HTFSWE=1./SWFC
C      TR2E=TDIEC/(EFFIE*HTFSWE*TDIEC)
C      THERMAL RESISTANCE FOR WALL THICKNESS(HR.FT2.F/BTU)

```

```

A 385
A 386
A 387
A 388
A 389
A 390
A 391
A 392
A 393
A 394
A 395
A 396
A 397
A 398
A 399
A 400
A 401
A 402
A 403
A 404
A 405
A 406
A 407
A 408
A 409
A 410
A 411
A 412
A 413
A 414
A 415
A 416
A 417
A 418
A 419
A 420
A 421
A 422
A 423
A 424
A 425
A 426
A 427
A 428
A 429
A 430
A 431
A 432

```

```

C C TR3E=TD0EC*ALOG(TD0E/TD1E)/(2.*TKW)
C C THERMAL RESISTANCE FOR NH3 FOULING(HR.FT2.F/8TU)
C C CONSIDERED NEGLIGIBLE
C C
C C THERMAL RESISTANCE FOR NH3
C C
C C EFFOE=1.
C C TR5E=1./((EFFOE*HTNH3E)
C C
C C PSEUDO HT COEF FOR SW(8TU/HR.FT2.; OR W/M2.C)
C C HSWE=1./TR1E
C C
C C PSEUDO HT COEF FOR SW FOULING(BTU/HR.FT2.F OR W/M2.C)
C C HFSWE=1./TR2E
C C
C C PSEUDO HT COEF FOR WALL THICK(BTU/HR.FT2.F OR W/M2.C)
C C HWE=1./TR3E
C C
C C PSEUDO HT COEF FOR AMMONIA(BTU/HR.FT2.F OR W/M2.C)
C C HNH3E=1./TR5E
C C
C C OVERALL HT COEF CALCULATION-OUTER
C C SURFACE(BTU/HR.FT2.F OR W/M2.C)
C C
C C UE=1./((TR1E+TR2E+TR3E+TR5E)
C C
C C NUMBER OF TRANSFER UNITS FOR EVAP(NTU)
C C
C C ENTU=UE*THTAE/CMINE
C C
C C EVAP EFFECTIVENESS(EPSILON)
C C
C C EPSE=1.-EXP(-ENTU)
C C
C C EVAP SW OUTLET TEMP(F OR C)
C C
C C THOE=THIE-(THIE-T3A)*(1.-EXP(-ENTU))
C C
C C REVISED SW AVG BULK TEMP(F)
C C RT8LKE=(THOE+THIE)/2.
C C

```

```

A 433
A 434
A 435
A 436
A 437
A 438
A 439
A 440
A 441
A 442
A 443
A 444
A 445
A 446
A 447
A 448
A 449
A 450
A 451
A 452
A 453
A 454
A 455
A 456
A 457
A 458
A 459
A 460
A 461
A 462
A 463
A 464
A 465
A 466
A 467
A 468
A 469
A 470
A 471
A 472
A 473
A 474
A 475
A 476
A 477
A 478
A 479
A 480

```

```

C TEST FOR A SAT TBULK TEMPERATURE
C
DBLKT=ABS(TBLKE-RTBLKE)
SCALB=ABS(TBLKE)
IF (SCALB.LT.0.1) SCALB=0.1
DELB=OBLKT/SCALB
IF (DELB.LT.0.001) GO TO 310
TBLKE=RTBLKE
GO TO 260
CONTINUE
TBLKE=RTBLKE
310
C
C FILM TEMP FOR PROPERTY EVALUATION
C INITIALLY ASSUME T3(IDEAL)=T3(ACTUAL)
C
C THERMAL RESISTANCES FOR SINGLE TUBE CONDUCTANCE(UA)
C (BTU/HR.F)
AO=PIE*IDDEC*ILE
C
C THERMAL RESISTANCE SW(HR.F/BTU)
CTR1E=TR1E/AO
C
C THERMAL RESISTANCE SW FOULING(HR.F/BTU)
CTR2E=TR2E/AO
C
C THERMAL RESISTANCE WALL THICKNESS(HR.F/BTU)
CTR3E=TR3E/AO
C
C THERMAL RESISTANCE FOR NH3 FOULING(HR.F/BTU)
NEGLIGIBLE
C
C THERMAL RESISTANCE NH3(HR.F/BTU)
CTR5E=TR5E/AO
C
C HEAT TRANSFERED PER TUBE(8TU/HR)
QET=(TBLKE-T3)/(CTR1E+CTR2E+CTR3E+CTR5E)
C
C SHELLSIDE WALL TEMPERATURE(F)
ETW2=TBLKE-QET*(CTR1E+CTR2E+CTR3E)
C

```

```

481
A A 482
A A 483
A A 484
A A 485
A A 486
A A 487
A A 488
A A 489
A A 490
A A 491
A A 492
A A 493
A A 494
A A 495
A A 496
A A 497
A A 498
A A 499
A A 500
A A 501
A A 502
A A 503
A A 504
A A 505
A A 506
A A 507
A A 508
A A 509
A A 510
A A 511
A A 512
A A 513
A A 514
A A 515
A A 516
A A 517
A A 518
A A 519
A A 520
A A 521
A A 522
A A 523
A A 524
A A 525
A A 526
A A 527
A A 528

```

A 529
 A 530
 A 531
 A 532
 A 533
 A 534
 A 535
 A 536
 A 537
 A 538
 A 539
 A 540
 A 541
 A 542
 A 543
 A 544
 A 545
 A 546
 A 547
 A 548
 A 549
 A 550
 A 551
 A 552
 A 553
 A 554
 A 555
 A 556
 A 557
 A 558
 A 559
 A 560
 A 561
 A 562
 A 563
 A 564
 A 565
 A 566
 A 567
 A 568
 A 569
 A 570
 A 571
 A 572
 A 573
 A 574
 A 575
 A 576

C C TUBESIDE WALL TEMPERATURE(F)
 C C ETW1=TBLKE-QET*(CTR1E+CTR2E)
 C C EVAP FILM TEMP CALCULATION(F)
 C C EFT=(ETW2+T3)/2.
 C C DELTA T TEMPERATURE(F)
 C C DELTAE=ETW2-T3
 C C AMOUNT OF HEAT ADDITION(BTU/HR OR W)
 C C QE=CMINE*(THIE-THOE)
 C C LOG MEAN TEMPERATURE DIFFERENCE OF EVAP(F OR C)
 C C INITIALLY ASSUME T3(IDEAL)=T3(ACTUAL)
 C C ELMTD=(1.-EXP(-ENTU))*CMINE*(THIE-T3)/(UE*THTAE)
 C C ISENTROPIC NH3 PUMP WORK(BTU/LBM)
 C C INITIALLY ASSUME P1(IDEAL)=P1(ACTUAL)
 C C VF1=1./RFNH3(T1)
 C C WPSNH3=VF1*(PEVAP-P1)*144./BTUC
 C C THERMODYNAMIC NH3 PUMP WORK(BTU/LBM)
 C C EPNH3C=EPNH3/100.
 C C WPNH3=WPSNH3/EPNH3C
 C C WORKING FLUID PROPERTIES
 C C CPNH3E=CPNH3(EFT)
 C C VSNH3E=VSNH3(EFT)
 C C TKNH3E=TKNH3(EFT)
 C C RONH3E=RFNH3(EFT)
 C C ENTHALPY AT STATE PT 2(BTU/LBM)
 C C H2=H1+WPNH3
 C C ENTHALPY AT STATE PT 3A(BTU/LBM)
 C C H3A=HF(PEVAP)
 C C INITIALIZE NH3 MASS FLOW RATE(LBM/HR)

```

C      H3=HG(PEVAP)
      FLONH3=QE/(H3-H2)
      CONTINUE
320
C      PRESS DROP EVAP SHELLSIDE(LBF/IN2)
C      ASSUME VISCOSITY(TWALL)=VISCOSITY(TBULK)
C      MAX VELOCITY THRU MIN-FLOW AREA F(TUBE PROFILE)
C      RONH3P=RFNH3(T1)
      VINH3E=4.*FLONH3/(3600.*RONH3P*PIE*DINH3**2)
      VMAXE=VINH3E*(SN/(SN-TDOE))
C      REYNOLDS NO. FOR MAX SHELLSIDE FLOW
      REMAX=3600.*RONH3E*VMAXE*TDOE/(12.*VSNH3E)
C      EMPIRICAL FRICTION FACTOR USING CORRELATION BY JAKOB
      IF (PROF.EQ.2.) GO TO 330
      EFF=(0.25+0.118/((SN-TDOE)/TDOE)**1.08)*REMAX**(-.16)
      GO TO 340
      CONTINUE
      EFF=(0.44+(0.08*SN/TDOE)/((SN-TDOE)/TDOE)**(0.43+1.13*TDOE/SN))*RE
      MAX**(-.15)
      CONTINUE
330
C      MASS VELOCITY FOR MIN FREE-FLOW AREA(LBM/FT2.SEC)
      EAF=TSOE*TLE
      E*F=EAF*(SN-TDOE)/SN
      EGF=FLONH3/(3600.*EAF)
C      CALCULATION OF PRESS DROP EVAP SHELLSIDE(LBF/IN2)
      USING THE HOMOGENEOUS TWO-PHASE MODEL
      X3A=1.0
      EDE=(EPR*TDOE-TDOE)/12.
      VLIQE=1./RGNH3(T3A)
      VAPE=1./RGNH3(PEVAP)
      VAVGE=VLIQE*(1.+X3A*(VAPE-VLIQE)/VLIQE)
      EFRICT=(EFF*EGF**2*VAVGE)/(144.*GC)
      EMOM=(EGF**2*VAVGE)/(144.*GC)
      EELEV=(EGF*TSOE)/(144.*GC)
      DSEVAP=EFRICT+EMOM+EELEV
C      ENTHALPY AT STATE PT 3(BTU/LBM)

```

```

577
A 578
A 579
A 580
A 581
A 582
A 583
A 584
A 585
A 586
A 587
A 588
A 589
A 590
A 591
A 592
A 593
A 594
A 595
A 596
A 597
A 598
A 599
A 600
A 601
A 602
A 603
A 604
A 605
A 606
A 607
A 608
A 609
A 610
A 611
A 612
A 613
A 614
A 615
A 616
A 617
A 618
A 619
A 620
A 621
A 622
A 623
A 624

```

```

C ASSUME QUALITY EVAPORATOR OUTLET X3P
C
X3=X3P/100.
P3=PEVAP-DSEVAP
H3F=HF(P3)
H3G=HG(P3)
H3=H3F+X3*(H3G-H3F)
C
C PRESSURE DROP ACROSS THE MOISTURE SEPARATOR(LBF/IN2)
C
RONH3S=RGNH3(P3)
ESPACE=0.1*TSDE*TL
VNH3S=FLONH3/(3600.*RONH3S*ESPACE)
VHEAD=RONH3S*VNH3S**2/(2.*GC*144.)
DSDEM=20.*VHEAD
C
C MOISTURE SEPARATOR DISCHARGE DRAIN ENTHALPY(BTU/LBM)
C
P4=P3-DSDEM
T4=TSAT(P4)
PAVGD=(P3+P4)/2.
HDE=HF(PAVGD)
C
C ENTHALPY AT STATE PT 4(BTU/LBM)
C
C ASSUME QUALITY OF MOISTURE SEPARATOR OUTLET X4P
X4=X4P/100.
H4F=HF(P4)
H4G=HG(P4)
H4=H4F+X4*(H4G-H4F)
C
C REVISED AMMONIA FLOW RATE(LBM/HR)
C
FLONH3=QE/((X4/X3)*H3-H2-(X4/X3-1.)*HDE)
C
C REVISED AMMONIA SHELLSIDE VELOCITY(FT/SEC)
C
VNH3ER=4.*FLONH3/(3600.*RONH3P*PIE*DINH3**2)
C
C TEST FOR SAT VNH3E(FT/SEC)
C
DVNH3E=ABS(VNH3ER-VNH3E)
SCALV=ABS(VNH3ER)
IF (SCALV.LT.0.1) SCALV=0.1
DELV=DVNH3E/SCALV
IF (DELV.LT.0.001) GO TO 350
VNH3E=VNH3ER
GO TO 320

```

```

A 625
A 626
A 627
A 628
A 629
A 630
A 631
A 632
A 633
A 634
A 635
A 636
A 637
A 638
A 639
A 640
A 641
A 642
A 643
A 644
A 645
A 646
A 647
A 648
A 649
A 650
A 651
A 652
A 653
A 654
A 655
A 656
A 657
A 658
A 659
A 660
A 661
A 662
A 663
A 664
A 665
A 666
A 667
A 668
A 669
A 670
A 671
A 672

```

```

350 CONTINUE
    VNH3E=VNH3ER
C REVISD TEMP AT STATE PT 3(DEG F)
C
C T3R=TSAT(P3)
C TEST FOR SAT T3(IDEG F)
C
    DTEMP3=ABS(T3R-T3)
    SCALT=ABS(T3R)
    IF (SCALT.LT.0.1) SCALT=0.1
    DELT3=DTEMP3/SCALT
    IF (DELT3.LT.0.001) GO TO 360
    T3=T3R
    GO TO 260
360 CONTINUE
    T3=T3R
C PRANDTL NUMBER
C
    PNH3E=CPNH3E*VSNH3E/TKNH3E
C EVAPORATOR TYPE IDENTIFICATION
C TYPEE=1:HORIZONTAL OWENS CORRELATION
C TYPEE=2:HORIZONTAL NON-BOILING CORRELATION
C TYPEE=3:HORIZONTAL BOILING CORRELATION
C
    IF (TYPEE.GT.1.) GO TO 380
C HORIZONTAL NON-BOILING USING OWENS CORRELATION
C
    TRANSITION REYNOLDS NUMBER
    TRNE1=1680.*(CPNH3E*VSNH3E/TKNH3E)**(-1.5)
C
    REYNOLDS NUMBER(PSEUDO)
    WE=FLOH3/TNET
    RNH3EH=4.*WE/(ILE*VSNH3E)
    IF (RNH3EH.GT.TRNE1) GO TO 370
C LAMINAR FLOW USING OWENS CORRELATION
C
    HNH3ER=2.*2*(SPEC/TDOEC)**.1*(VSNH3E**2/(3600.**2)*G*RNH3E**2*TKNH3
    LE**3)***(-.3333)*RNH3EH**(-.3333)
    GO TO 420
C CONTINUE
370

```

```

A 673
A 674
A 675
A 676
A 677
A 678
A 679
A 680
A 681
A 682
A 683
A 684
A 685
A 686
A 687
A 688
A 689
A 690
A 691
A 692
A 693
A 694
A 695
A 696
A 697
A 698
A 699
A 700
A 701
A 702
A 703
A 704
A 705
A 706
A 707
A 708
A 709
A 710
A 711
A 712
A 713
A 714
A 715
A 716
A 717
A 718
A 719
A 720

```



```

C C C TURBULENT FLOW USING OWENS CORRELATION
C C C HNH3ER=.185*(SPEC/IDDEC)**.1*(VSNH3E**2/(3600.**2*G*RONH3E**2*TKNH
C C C 13E**3)***(-.3333)*PNH3E**.5
C C C GO TO 420
C C C CONTINUE
C 380
C C IDENTIFY PARAMETERS FOR TYPEE=2 OR 3
C C FLOW RATE AVERAGED PER TUBE
C C WE=FLONH3/TNET
C C FLOW RATE PER UNIT AXIAL LENGTH OF TUBE
C C WEA=WE/(PIE*IDDEC/2.)
C C TUBE LENGTH FOR DEVELOPING FLOW(FT)
C C TLD=WEA**(.4/.3.1)/(4.*PIE*TKNH3E/CPNH3E)*(3.*VSNH3E/(3600.**2*RONH3
C C C IE**2*G)***.3333
C C TUBE LENGTH FOR FULLY DEVELOPED FLOW(FT)
C C TLFD=TNET**.5*PIE*IDDEC/2.
C C IF (TYPEE.GT.2.) GO TO 400
C C HORIZONTAL NON-BOILING LORENZ AND YUNG CORRELATIONS
C C TRANSITION REYNOLDS NUMBER FOR CORRELATIONS
C C TRNE2=5800.*(CPNH3E*VSNH3E/TKNH3E)**(-1.06)
C C REYNOLDS NUMBER(PSEUDO-VERTICAL)
C C RNH3EV=4.*WE/(PIE*IDDEC*VSNH3E)
C C IF (RNH3EV.GT.TRNE2) GO TO 390
C C LAMINAR FLOW USING LORENZ AND YUNG CORRELATIONS
C C CONVECTION IN DEVELOPING REGION
C C HTDR=3.*CPNH3E*WEA/TLFD
C C CONVECTION IN FULLY DEVELOPED REGION
C C HTFDR=.821*(VSNH3E**2/(3600.**2*RONH3E**2*TKNH3E**3*G)***(-.3333))*

```

```

A 721
A 722
A 723
A 724
A 725
A 726
A 727
A 728
A 729
A 730
A 731
A 732
A 733
A 734
A 735
A 736
A 737
A 738
A 739
A 740
A 741
A 742
A 743
A 744
A 745
A 746
A 747
A 748
A 749
A 750
A 751
A 752
A 753
A 754
A 755
A 756
A 757
A 758
A 759
A 760
A 761
A 762
A 763
A 764
A 765
A 766
A 767
A 768

```

```

C C IRNH3EV**(-.22)*(1.-TLD/TLFD)
C C LAMINAR FLOW CALCULATIONS
C C HNH3ER=HTDR+HTFDR
390 C C GO TO 420
C C CONTINUE
C C TURBULENT FLOW USING LORENZ AND YUNG CORRELATIONS
C C CONVECTION IN DEVELOPING REGION
C C HTDR=3.*CPNH3E*WEA/TLFD
C C CONVECTION IN FULLY DEVELOPED REGION
C C HIFDK=3.8E-03*(VSNH3E**2/(3600.**2*RONH3E**2*TKNH3E**3*G)**(-.333
13)*RNH3EV**.4*PNH3E**.65
C C TURBULENT FLOW CALCULATION
C C HNH3ER=HTDR+HTFDR
400 C C GO TO 420
C C CONTINUE
C C HORIZONTAL BOILING USING LORENZ AND YUNG CORRELATIONS
C C TRANSITION REYNOLDS NUMBER FOR CORRELATIONS
C C TRNE3=5800.*(CPNH3E*VSNH3E/TKNH3E)**(-1.06)
C C REYNOLDS NUMBER(PSEUDO-VERTICAL)
C C RNH3EV=4.*WE/(PIE*TDACC*VSNH3E)
C C IF (RNH3EV.GT.TRNE3) GO TO 410
C C LAMINAR FLOW USING LORENZ AND YUNG CORRELATIONS
C C CONVECTION IN DEVELOPING REGION
C C HTDR=3.*CPNH3E*WEA/TLFD
C C CONVECTION IN FULLY DEVELOPED REGION
C C HIFDR=.821*(VSNH3E**2/(3600.**2*RONH3E**2*TKNH3E**3*G)**(-.3333)*
C C IRNH3EV**(-.22)*(1.-TLD/TLFD)
C C BOILING USING LORENZ AND YUNG CORRELATION

```

```

A 769
A 770
A 771
A 772
A 773
A 774
A 775
A 776
A 777
A 778
A 779
A 780
A 781
A 782
A 783
A 784
A 785
A 786
A 787
A 788
A 789
A 790
A 791
A 792
A 793
A 794
A 795
A 796
A 797
A 798
A 799
A 800
A 801
A 802
A 803
A 804
A 805
A 806
A 807
A 808
A 809
A 810
A 811
A 812
A 813
A 814
A 815
A 816

```

```

      HFNH3E=HF(P3)
      HGNH3E=HG(P3)
      TENS=1.6038998E-03
      CSF=.0154
      HTB=VSNH3E*(HGNH3E-HFNH3E)/(CSF**3*(TENS/RONH3E)**.5)*(CPNH3E/(HG
      1NH3E-HFNH3E)*PNH3E)**3*DELTAE**2
      LAMINAR FLOW CORRELATION
      HNH3ER=HTB+HTDR+HTFDR
      GO TO 420
      CONTINUE
      TURBULENT FLOW USING LORENZ AND YUNG CORRELATIONS
      CONVECTION IN DEVELOPING REGION
      HTDR=3.*CPNH3E*WEA/TLFD
      CONVECTION IN FULLY DEVELOPED REGION
      HTFDR=3.8E-03*(VSNH3E**2/(3600.**2*RONH3E**2*TKNH3E**3*G)***(-.333
      13)*RNH3E**4*PNH3E**65
      BOILING USING LORENZ AND YUNG CORRELATION
      HGNH3E=HG(P3)
      HFNH3E=HF(P3)
      TENS=1.6038998E-03
      CSF=.0154
      HTB=VSNH3E*(HGNH3E-HFNH3E)/(CSF**3*(TENS/RONH3E)**.5)*(CPNH3E/(HG
      1NH3E-HFNH3E)*PNH3E)**3*DELTAE**2
      TURBULENT FLOW CALCULATIONS
      HNH3ER=HTB+HTDR+HTFDR
      CONTINUE
      420
      C TEST FOR SAT HTNH3E
      C
      DHTNH3=ABS(HNH3ER-HTNH3E)
      SCALH=ABS(HNH3ER)
      IF (SCALH.LT.0.1) SCALH=0.1
      DELH=DHTNH3/SCALH
      IF (DELH.LT.0.001) GO TO 430
      HTNH3E=HNH3ER
      GO TO 260
      CONTINUE
      430

```

HTNH3E=HNNH3ER
 C REVISED EVAP HEAT TRANSFER AREA(FT2) A 865
 C THIAER=ENTU*CMINE/UE A 866
 C REVISED EVAP TUBE LENGTH(FT) A 867
 C TLER=THTAER/(PIE*TD0EC*TNET) A 868
 C TEST FOR SAT TUBE LENGTH A 869
 C COST CF EVAPORATOR UNIT(\$)
 C IF (TSDE.GT.35.) GO TO 480 A 870
 C EVAPORATOR TUBE SHEET DIAMETER(10-35)FT A 871
 C DRILLING TIME/TUBE SHELL THICK(MIN/IN) A 872
 C DTE=0.66*(TD0E-.5) A 873
 C THICKNESS OF TUBE SHEET(IN) A 874
 C TTSE=0.56*TSDE**0.68 A 875
 C TUBE SHEET LABOR COST(\$)
 C CTSLE=156695.*(TNET/9630.)*(DTE/0.66)*(TTSE/4.) A 876
 C TUBE SHEET MATERIAL COST(\$)
 C CTSME=189.486*TSDE**2.3
 C IF (TMATL.EQ.1.) GO TO 440 A 877
 C TUBE MATERIAL COST(\$)
 C CTME=(E1*ILE+E2)*TNET*(TD0E/1.5) A 878
 C TUBE INSTALLATION COST(\$)
 C CTIE=34.*TNET*TD0E**0.7
 C GO TO 450
 C CONTINUE
 C TUBF MATERIAL COST(\$)
 C CTIME=(E1*ILE+E2)*TNET*(TD0E/1.5)*(1.+(1.+AINT/100.))**10+(1.+AINT/1
 C 100.)**20 A 879
 A 880
 A 881
 A 882
 A 883
 A 884
 A 885
 A 886
 A 887
 A 888
 A 889
 A 890
 A 891
 A 892
 A 893
 A 894
 A 895
 A 896
 A 897
 A 898
 A 899
 A 900
 A 901
 A 902
 A 903
 A 904
 A 905
 A 906
 A 907
 A 908
 A 909
 A 910
 A 911
 A 912

AD-A098 567

NAVAL POSTGRADUATE SCHOOL MONTEREY CA
OPTIMIZATION OF A LOW DELTA T RANKINE POWER SYSTEM.(U)
DEC 80 R C SCHAUBEL

F/G 20/13

UNCLASSIFIED

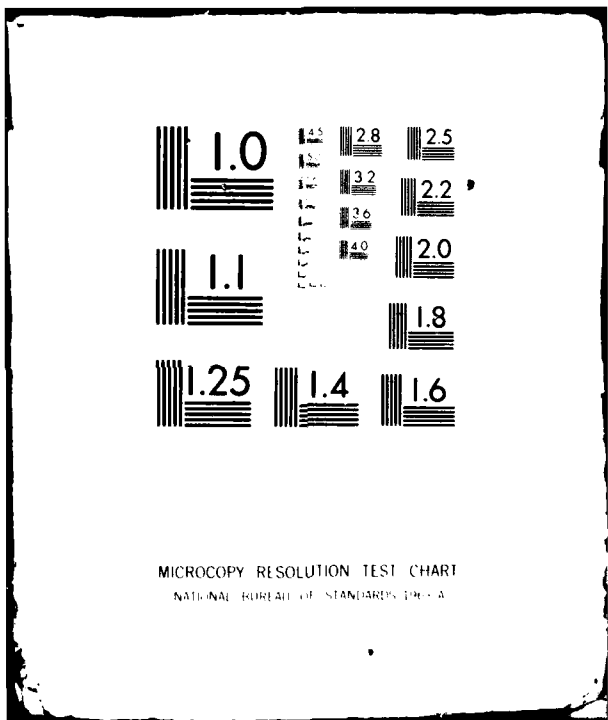
NL

3-3

AD-A098 567



END
DATE
FILMED
5 81
DTIC



MICROCOPY RESOLUTION TEST CHART
NATIONAL BUREAU OF STANDARDS 1963-A

961
 A A 962
 A A 963
 A A 964
 A A 965
 A A 966
 A A 967
 A A 968
 A A 969
 A A 970
 A A 971
 A A 972
 A A 973
 A A 974
 A A 975
 A A 976
 A A 977
 A A 978
 A A 979
 A A 980
 A A 981
 A A 982
 A A 983
 A A 984
 A A 985
 A A 986
 A A 987
 A A 988
 A A 989
 A A 990
 A A 991
 A A 992
 A A 993
 A A 994
 A A 995
 A A 996
 A A 997
 A A 998
 A A 999
 A A1000
 A A1001
 A A1002
 A A1003
 A A1004
 A A1005
 A A1006
 A A1007
 A A1008

TTSE=0.56*TSDE**0.68
 C C
 TUBE SHEET MATERIAL AND LABOR COSTS(\$)
 C C
 IF (TMAIL.EQ.1.) GO TO 490
 CTSLE=55.189*TNET**0.791*TSDE**0.68*DTE
 CTSME=29.566*TSDE**2.014*TTSE
 GO TO 500
 490 CONTINUE
 CTSLE=73.81*TNET**0.791*TSDE**0.68*DTE
 CTSME=354.3*TSDE**1.61*TTSE
 500 CONTINUE
 C C
 IF (TMAIL.EQ.1.) GO TO 510
 C C
 TUBE MATERIAL COST(\$)
 C C
 CTME=(E1*TLE+E2)*TNET*(TDOE/1.5)
 C C
 TUBE INSTALLATION COST(\$)
 C C
 CTIE=36.542*TNET*TDOE**0.7
 GO TO 520
 510 CONTINUE
 C C
 TUBE MATERIAL COST(\$)
 C C
 CTME=(E1*TLE+C2)*TNET*(TDOE/1.5)*(1.+(1.+AINT/100.))**10+(1.+AINT/1
 100.)*20
 C C
 TUBE INSTALLATION COST(\$)
 C C
 CTIE=36.542*TNET*TDOE**0.7*(1.+(1.+AINT/100.))**10+(1.+AINT/100.)*20
 120) CONTINUE
 520
 C C
 HEAT EXCH SHELL COST(\$)
 C C
 CHSE=12.544*(TLE+6.)*TSDE**2.06
 C C
 NH3 DIST PLATE AND BAFFLES COST(\$)
 C C
 CDPBE=158.099*TSDE**1.82+72.419*TNET**0.873*DTE
 C C
 BUSTLE, FLANGE, CHANNELS AND FLOW PLATE COSTS(\$)
 C C
 CBFCFE=472.977*TSDE**2.12
 C C
 HEAT EXCH HEAD COST(\$)
 C C

A1009
 A1010
 A1011
 A1012
 A1013
 A1014
 A1015
 A1016
 A1017
 A1018
 A1019
 A1020
 A1021
 A1022
 A1023
 A1024
 A1025
 A1026
 A1027
 A1028
 A1029
 A1030
 A1031
 A1032
 A1033
 A1034
 A1035
 A1036
 A1037
 A1038
 A1039
 A1040
 A1041
 A1042
 A1043
 A1044
 A1045
 A1046
 A1047
 A1048
 A1049
 A1050
 A1051
 A1052
 A1053
 A1054
 A1055
 A1056

```

C      CHE=1725.31*TSDE**1.45
C      WATER INLET,NOZZLES AND SUPPORTS COST($ )
C      CWINSE=7445.297*TSDE**1.1
C      TUBE WELDING COSTS($ )
C      CTWE=0.0
C      IF (THATL.EQ.1.) GO TO 540
C      IF (TNET.GT.3600) GO TO 530
C      CTWE=14.73*TNET**1.03*(TDOE/1.5)**0.7
C      GO TO 540
C      CONTINUE
530    CTWE=0.8797*TNET**1.3*(TDOE/1.5)**0.7
540    CEVAP=(CTSLE+CTSME+CTME+CTIE+CHSE+CDPBE+CBFCFE+CHE+CHINSE+CTWE)
550    CONTINUE
C      *****
C      *
C      * PARASITIC LOSS SECTION *
C      *
C      *****
C      EVAPORATOR SALT WATER PUMP OR HOT PIPE PUMP
C      DELTA P EVAP SW PUMP
C      ROSWHP=RHOSW*(THIE)
C      THIER=THIE+459.69
C      VISWHP=VISSW*(THIE)
C      DELTA P SW HOT PIPE USING DARCEY-WEISBACH CORRELATION
C      (LBF/IN2)
C      REYNOLDS NUMBER FOR HOT PIPE FLOW
C      RNSWHP=3600.*ROSWHP*VSMWP*DIHP/VISWHP
C      FRICTION FACTOR FOR LAMINAR FLOW
C      IF (RNSWHP.GT.2300.) GO TO 560
C      FFHP=64./RNSWHP
C      GO TO 570
  
```

A1057
 A1058
 A1059
 A1060
 A1061
 A1062
 A1063
 A1064
 A1065
 A1066
 A1067
 A1068
 A1069
 A1070
 A1071
 A1072
 A1073
 A1074
 A1075
 A1076
 A1077
 A1078
 A1079
 A1080
 A1081
 A1082
 A1083
 A1084
 A1085
 A1086
 A1087
 A1088
 A1089
 A1090
 A1091
 A1092
 A1093
 A1094
 A1095
 A1096
 A1097
 A1098
 A1099
 A1100
 A1101
 A1102
 A1103
 A1104

560 CONTINUE
 C FRICITION FACTOR TURBULENT FLOW USING STREETER CORR
 C
 C
 570 FFHP=1.325/(ALOG(EHP/(3.7*DIHP))+5.74/RNSWHP**.9))**2
 C CONTINUE
 C
 C INTAKE DUCT LOSSES(ASSUME K=1.5 FOR INLET SCREEN AND
 C ENTERS PLENUM PRIOR TO EVAP WHERE AREA IS ABRUPTLY
 C CHANGED TO 2 TIMES THE PIPE DIAMETER(LBF/IN2)
 C
 C HPKI=1.5
 C HPKE=(1.-(DIHP/(2.*DIHP))**.2)**2
 C DDUCTH=(HPKI+HPKE)*ROSWHP*VSWHP**2/(2.*GC*144.)
 C
 C PIPE FRICTION LOSSES(LBF/IN2)
 C
 C RKHP=FFHP*TLHP/DIHP
 C DPIPEH=RKHP*ROSWHP*VSWHP**2/(2.*GC*144.)
 C
 C OUTLET DUCT LOSSES(ASSUME NO OUTLET PIPING)
 C
 C
 C DELTA P PIPE LOSS CALCULATION(LBF/IN2)
 C
 C DPIPEH=DDUCTH+DPIPEH
 C
 C DELTA P EVAPORATOR(ASSUME NO OUTLET PIPING) USING DARCEY-
 C WEISBACH CORRELATION(LBF/IN2)
 C
 C
 C MINOR ENTRY/EXIT LOSSES(ASSUME KI=.05 WELL ROUNDED
 C TUBE ENTRANCE AND KE=1. EXPANSION TO AN INFINITE
 C RESEVOIR)(LBF/IN2)
 C
 C RKI=.05
 C RKE=1.
 C DPMINE=(RKI+RKE)*RHOSWE*VSWE**2/(2.*GC*144.)
 C
 C DELTA P EVAPORATOR CORE(LBF/IN2)
 C
 C REYNOLDS NUMBER FOR EVAP(DETERMINED IN EVAP SECTION)
 C
 C FRICTION FACTOR LAMINAR FLOW
 C
 C IF (RNSWE.GT.2300.) GO TO 580
 C FFE=64./RNSWE
 C GO TO 590
 C CONTINUE
 580

A1105
 A1106
 A1107
 A1108
 A1109
 A1110
 A1111
 A1112
 A1113
 A1114
 A1115
 A1116
 A1117
 A1118
 A1119
 A1120
 A1121
 A1122
 A1123
 A1124
 A1125
 A1126
 A1127
 A1128
 A1129
 A1130
 A1131
 A1132
 A1133
 A1134
 A1135
 A1136
 A1137
 A1138
 A1139
 A1140
 A1141
 A1142
 A1143
 A1144
 A1145
 A1146
 A1147
 A1148
 A1149
 A1150
 A1151
 A1152

C C FRICTION FACTOR TURBULENT FLOW USING STREETER CORR
 C C FFE=1.325/(ALOG(ECE/(3.7*TDIEC)+5.74/RNSWE**.9))**.2
 C 590 CONTINUE
 C C DELTA P EVAP CORE CALCULATED(LBF/IN2)
 C C RKHE=FFE*ILE/TDIEC
 C C DCOREE=RKHE*RHOSWE*VSWE**2/(2.*GC*144.)
 C C DELTA P EVAPORATOR CALCULATED(LBF/IN2)
 C C DEVAP=DPMINE+DCOREE
 C C DELTA P EVAP SW PUMP CALCULATION(LBF/IN2 OR FT)
 C C DPMPE=DDUCTH+DP IPEH+DPMINE+DCOREE
 C C DPMPEC=144.*DP IPE*GC/(ROSHHP*G)
 C C POWER EVAP SW PUMP (HP)
 C C EPEC=EPE/100.
 C C PWREP=FLOHP*DPMPEC*G/(EPEC*HPC*3600.*GC)
 C C POWER EVAP SW PUMP MOTOR(MW)
 C C EMEC=EME/100.
 C C PWREPH=PWREP*CMW/EMEC
 C C DISCHARGE RATE EVAP SW PUMP (FT3/SEC OR GAL/MIN)
 C C QEPMP=PIE*DIHP**2*VSWHP/4.
 C C QEPHPC=QEPMP*60.*GAL
 C C COST OF EVAP SW PUMP (\$)
 C C CESWP=(QEPMPC/1000.)*.75+50.)*1.21E+03
 C C CONDENSER SALT WATER PUMP OR COLD PIPE PUMP
 C C DELTA P CONDENSER SW PUMP (ASSUME TSW(IN)=TSW(OUT),V1=V2)
 C C ROSWCP=RHOSW(TCIC)
 C C TCICR=TCIC+459.69
 C C VISWCP=VISSW(TCIC)
 C C FLOCP=3600.*ROSWCP*PIE*DICP**2*VSWMCP/4.
 C C DELTA P SW COLD PIPE (ASSUME V1=V2,TSW(IN)=TSW(OUT) USING

```

C DARCEY-WEISBACH CORRELATION(LBF/IN2)
C
C REYNOLDS NUMBER FOR COLD PIPE FLOW
C
C RNSWCP=3600.*ROSWCP*VSWCP*DICP/VISWCP
C
C FRICTION FACTOR LAMINAR FLOW
C
C IF (RNSWCP.GT.2300.) GO TO 600
C FFCP=64./RNSWCP
C GO TO 610
C CONTINUE
C
C FRICTION FACTOR TURBULENT FLOW USING STREETER CORR
C
C FFCP=1.325/(ALOG(ECP/(3.7*DICP))+5.74/RNSWCP**.9)**2
C CONTINUE
C
C 600
C
C MINOR ENTRY/EXIT LOSSES(ASSUME KI=.05 WELL ROUNDED
C PIPE ENTRANCE AND ENTERS PLENUM PRIOR TO CONDENSER
C WHERE AREA IS ABRUPTLY CHANGED TO 2 TIMES PIPE
C DIAMETER)(LBF/IN2)
C
C CPKI=.05
C CPKE=(1.-(DICP/(2.*DICP))**.2)**2
C DDUCTC=(CPKI+CPKE)*ROSWCP*VSWCP**2/(2.*GC*144.)
C
C PIPE FRICTION LOSSES(LBF/IN2)
C
C RKCP=FFCP*(TLCF/DICP+EL80W)
C DPIPEC=RKCP*ROSWCP*VSWCP**2/(2.*GC*144.)
C
C DELTA P PIPE LOSS CALCULATION(LBF/IN2)
C
C DPIPCC=DDUCTC+DPIPEC
C
C DELTA P DUE TO SM DENSITY(LBF/IN2)
C
C RDEPTH=RHOSMD(TLCP)
C RAVG=(RDEPTH+64.184)/2.
C DHEAD=(RDEPTH-64.184)/RDEPTH)*TLCF/2.
C DDENC=G*RAVG*DHEAD/(144.*GC)
C
C DELTA P CONDENSER(ASSUME NO OUTLET PIPING) USING
C DARCEY-WEISBACH CORRELATION(LBF/IN2)
C
C INITIALLY ASSUME TBLK=TSW(IN)
C TBLKC=TCIC

```

```

A1153
A1154
A1155
A1156
A1157
A1158
A1159
A1160
A1161
A1162
A1163
A1164
A1165
A1166
A1167
A1168
A1169
A1170
A1171
A1172
A1173
A1174
A1175
A1176
A1177
A1178
A1179
A1180
A1181
A1182
A1183
A1184
A1185
A1186
A1187
A1188
A1189
A1190
A1191
A1192
A1193
A1194
A1195
A1196
A1197
A1198
A1199
A1200

```

AI201
AI202
AI203
AI204
AI205
AI206
AI207
AI208
AI209
AI210
AI211
AI212
AI213
AI214
AI215
AI216
AI217
AI218
AI219
AI220
AI221
AI222
AI223
AI224
AI225
AI226
AI227
AI228
AI229
AI230
AI231
AI232
AI233
AI234
AI235
AI236
AI237
AI238
AI239
AI240
AI241
AI242
AI243
AI244
AI245
AI246
AI247
AI248

```

620 CONTINUE
      TBLKCR=TBLK*459.69
      RHOSWC=RHOSW(TBLK)
      C
      C
      C
      C
      MINOR ENTRY/EXIT LOSSES(ASSUME KI=.05 WELL ROUNDED
      TUBE ENTRANCE AND KE=1. EXPANSION TO AN INFINITE
      RESEVOIR(LBF/IN2)
      C
      RKE=.05
      RKE=1
      DPHINC=(RKE+RKE)*RHOSWC*VSWC**2/(2.*GC*144.)
      C
      C
      C
      C
      DELTA P CONDENSER CORE(LBF/IN2)
      C
      C
      C
      C
      REYNOLDS NUMBER FOR COND TUBESIDE
      C
      VISSWC=VISSW(TBLK)
      RNSWC=3600.*RHOSWC*VSWC*TDICC/VISSWC
      C
      C
      FRICTION FACTOR LAMINAR FLOW
      C
      IF (RNSWC.GT.2300.) GO TO 630
      FFC=64./RNSWC
      GO TO 640
      C
      C
      CONTINUE
      FFC=1.325/(ALOG(ECC/(3.7*TDICC))+5.74/RNSWC**2)**2
      C
      C
      DELTA P COND CORE CALCULATION(LBF/IN2)
      C
      RKHC=FFC*TLC/TDICC
      DCOREC=RKHC*RHOSWC*VSWC**2/(2.*GC*144.)
      C
      C
      DELTA P CONDENSER DUE TO CORE ELEVATION(LBF/IN2)
      C
      C
      IF (TYPEC.GT.1.) GO TO 650
      DPELEC=0.
      GO TO 660
      C
      C
      CONTINUE
      C
      C
      VERTICAL TUBED CONDENSER SW INLET ENTERS AT THE TOP
      OF THE HEAT EXCHANGER
      C
      C
      DPELEC=0.
      C
      C
      CONTINUE
      C
      C
      DELTA P CONDENSER CALCULATION(LBF/IN2)
      C
      C
  
```

A1249
 A1250
 A1251
 A1252
 A1253
 A1254
 A1255
 A1256
 A1257
 A1258
 A1259
 A1260
 A1261
 A1262
 A1263
 A1264
 A1265
 A1266
 A1267
 A1268
 A1269
 A1270
 A1271
 A1272
 A1273
 A1274
 A1275
 A1276
 A1277
 A1278
 A1279
 A1280
 A1281
 A1282
 A1283
 A1284
 A1285
 A1286
 A1287
 A1288
 A1289
 A1290
 A1291
 A1292
 A1293
 A1294
 A1295
 A1296

C DCOND=DPMINC+DCOREC+DPELEC
 C DELTA P COND SW PUMP CALCULATION(LBF/IN2 OR FT)
 C DPMPC=DDUCTC+DDENC+DPMINC+DCOREC+DPIPEC
 C DPMPC=144.*DPMPC*GC/(ROSWC*P*G)
 C POWER COND SW PUMP(HP)
 C EPCC=EPC/100.
 C PWRCP=FLOCP*DPMPCC*G/(EPCC*HPC*3600.*GC)
 C POWER COND SW PUMP MOTOR(MW)
 C EMCC=EMC/100.
 C PWRCPM=PWRCP*CMW/EMCC
 C DISCHARGE RATE OF COND SW PUMP(FT3/SEC OR GAL/MIN)
 C QCPMP=PIE*DICP**2*VSMCP/4.
 C QCPHPC=QCPMP*60.*GAL
 C COST OF COND SW PUMP(\$)
 C CCSWP=((QCPMP/1000.)*0.75+50.)*1.21E+03
 C AMMONIA CIRCULATION PUMP
 C DELTA P NH3 CIRC PUMP
 C VSNH3P=VSNH3(T1)
 C RONH3P=RFNH3(T1)
 C DELTA P NH3 PUMP(ASSUME V1=V2)USING DARCEY-WEISBACH
 C CORRELATION(LBF/IN2)
 C NH3 PIPE FLOW VELOCITY(FT/SEC)
 C VNH3P=4.*FLONH3/(3600.*RONH3P*PIE*DINH3**2)
 C REYNOLDS NUMBER FOR NH3 PIPE FLOW
 C RNH3P=3600.*RONH3P*VNH3P*DINH3/VSNH3
 C FRICTION FACTOR LAHINAR FLOW
 C IF (RNH3P.GT.2300.) GO TO 670
 C FFNH3P=64./RNH3P

A1297
 A1298
 A1299
 A1300
 A1301
 A1302
 A1303
 A1304
 A1305
 A1306
 A1307
 A1308
 A1309
 A1310
 A1311
 A1312
 A1313
 A1314
 A1315
 A1316
 A1317
 A1318
 A1319
 A1320
 A1321
 A1322
 A1323
 A1324
 A1325
 A1326
 A1327
 A1328
 A1329
 A1330
 A1331
 A1332
 A1333
 A1334
 A1335
 A1336
 A1337
 A1338
 A1339
 A1340
 A1341
 A1342
 A1343
 A1344

GO TO 680
 C CONTINUE
 C
 C FRICTION FACTOR TURBULENT FLOW USING STREETER CORR
 C
 C FFNH3P=1.325/(ALOG(ENH3P/(3.7*DINH3)+5.74/RNH3P**.9))**2
 C CONTINUE
 C 680
 C
 C PIPE FRICTION LOSSES(LBF/IN2)
 C
 C RKNH3P=FFNH3P*(TLNH3P/DINH3+4.*ELBOW)
 C DPNH3=RKNH3P*RONH3P*VNH3P**2/(2.*GC*144.)
 C
 C DELTA P CORE EVAPORATOR
 C
 C DPCORE=DSEVAP+DSDEM
 C
 C DELTA P DUE TO PIPING ELEVATION(LBF/IN2)
 C
 C EZ1=0.
 C EZ2=TSDE+25
 C DPELEV=RONH3P*G*(EZ2-EZ1)/(GC*144.)
 C
 C DELTA P PIPE LOSS CALCULATION(LBF/IN2)
 C DPIPND=DPNH3+DPELEV
 C
 C DELTA P THERMODYNAMICALLY(LBF/IN2)
 C DPOTHER=PEVAP-PCOND
 C
 C DELTA P NH3 CIRC PUMP(LBF/IN2 OR FT)
 C DPMN=DPNH3+DPCORE+DPELEV+DPOTHER
 C DPMNC=144.*DPMN*GC/(RONH3P*G)
 C
 C POWER NH3 CIRC PUMP(HP)
 C
 C EPNH3C=EPNH3/100.
 C PWRNP=FLONH3*DPMNC*G/(EPNH3C*HPC*3600.*GC)
 C
 C POWER NH3 CIRC PUMP MOTOR(MW)
 C
 C EMNH3C=EMNH3/100.
 C PWRNPM=PWRNP*CMW/EMNH3C
 C
 C DISCHARGE RATE NH3 CIRC PUMP(FT3/SEC OR GAL/MIN)
 C
 C

A1345
 A1346
 A1347
 A1348
 A1349
 A1350
 A1351
 A1352
 A1353
 A1354
 A1355
 A1356
 A1357
 A1358
 A1359
 A1360
 A1361
 A1362
 A1363
 A1364
 A1365
 A1366
 A1367
 A1368
 A1369
 A1370
 A1371
 A1372
 A1373
 A1374
 A1375
 A1376
 A1377
 A1378
 A1379
 A1380
 A1381
 A1382
 A1383
 A1384
 A1385
 A1386
 A1387
 A1388
 A1389
 A1390
 A1391
 A1392

QNPMP=PIE*0 INH3**2*VNH3P/4.
 QNPMPC=QNPMP*60.*GAL
 C COST OF NH3 CIRC PUMP(\$)
 C
 VF1=1./RFNH3(T1)
 CNH3P=(FLONH3*VF1/80100.)**0.64*1.21E+05
 C EVAPORATOR RE-FLUX PUMP
 C ASSUME RE-FLUX MASS FLOW RATE=0.3 X FLONH3
 C
 C DELTA P NH3 RE-FLUX PIPING(ASSUME V1=V2)
 C USING DARCEY-WEISBACH CORRELATION(LBF/IN2)
 C PAVGE=(PEVAP+P3)/2.
 C TAVGE=T SAT(TAVGE)
 C RONH3R=RFNH3(TAVGE)
 C VSNHRP=VSNH3(TAVGE)
 C
 C NH3 FLOW VELOCITY(FT/SEC)
 C
 FLONHR=0.3*FLDNH3
 VNHRP=4.*FLONHR/(3600.*RONH3*PIE*DINH3**2)
 C
 REYNOLDS NO FOR NH3 RE-FLUX PIPE FLOW
 C
 RNHRP=3600.*RONH3*VNHRP*DINH3/VSNHRP
 C
 C FRICTION FACTOR LAMINAR FLOW
 C
 IF (RNHRP.GT.2300.) GO TO 690
 FNHRP=64./RNHRP
 GO TO 700
 CONTINUE
 C
 C FRICTION FACTOR TURBULENT FLOW USING STREETER CORR
 C
 FNHRP=L.325/(ALOG(ENH3P/(3.7*DINH3)+5.74/RNHRP**0.9))**2
 CONTINUE
 C
 C PIPE FRICTION LOSSES(LBF/IN2)
 C
 RKNHRP=FNHRP*(TLNHRP/DINH3+4.*ELBOW)
 DPNHRP=RKNHRP*RONH3*VNHRP**2/(2.*GC*144.)
 C
 C DELTA P DUE TO PIPING ELEVATION(LBF/IN2)
 C
 EZR=TSDE+10
 DPELER=RONH3R*G*(EZR-EZ1)/(GC*144.)

A1393
 A1394
 A1395
 A1396
 A1397
 A1398
 A1399
 A1400
 A1401
 A1402
 A1403
 A1404
 A1405
 A1406
 A1407
 A1408
 A1409
 A1410
 A1411
 A1412
 A1413
 A1414
 A1415
 A1416
 A1417
 A1418
 A1419
 A1420
 A1421
 A1422
 A1423
 A1424
 A1425
 A1426
 A1427
 A1428
 A1429
 A1430
 A1431
 A1432
 A1433
 A1434
 A1435
 A1436
 A1437
 A1438
 A1439
 A1440

C DELTA P PIPE LOSSES(LBF/IN2)
 C DPIPNR=DPNHRP+DPELER
 C
 C DELTA P NH3 RE-FLUX THERMODYNAMICALLY(LBF/IN2)
 C USING A SINGLE PHASE PRESSURE MODEL
 C
 C RONHEV=RGNH3(PEVAP)
 C DPTHRF=2.*EFF*EGF**2*TNET**0.5/(144.*RONHEV*GC)
 C
 C DELTA P NH3 RE-FLUX PUMP(LBF/IN OR FT)
 C
 C DPMNRR=DPNHRP+DPELER+DPTHRF
 C DPPNRC=144.*DPMNRR*GC/(RONH3R*G)
 C
 C POWER NH3 RE-FLUX PUMP(HP)
 C
 C EPNHRC=EPNHR/100.
 C PWRRP=FLONHR*DPNRC*G/(EPNHRC*HPC*3600.*GC)
 C
 C POWER NH3 RE-FLUX PUMP MOTOR(MW)
 C
 C EMNHRC=EMNHR/100.
 C PWRRM=PWRRP*C MW/EMNHR
 C
 C DISCHARGE RATE NH3 RE-FLUX PUMP(FT3/SEC OR GAL/MIN)
 C
 C QRPMP=PIE*DINH3R**2*VNH3RP/4.
 C QRPMP C=QRPMP*60.*GAL
 C
 C COST OF NH3 RE-FLUX PUMP(\$)
 C
 C VFR=1./RFNH3(TAVGE)
 C CNH3RP=(FLONHR*VFR/80100.)*0.64*1.21E+05
 C
 C PARASITIC PUMP LOSSES(MW)
 C
 C PARAL=PWREPM+PWRCPM+PWRNPM+PWRRM
 C
 C *****
 C *
 C * TURBINE AND ELECTRICAL POWER SECTION *
 C *
 C *
 C *****

C	GROSS ELECTRICAL LOAD(MW)	A1441
C	NET ELECTRICAL OUTPUT DESIRED(ELECT- PROVIDED IN INITIAL PARAMETERS)(MW)	A1442
C	ELECTRICAL LOADING AS EFFECTED BY EFFICIENCY(MW)	A1443
C	EEP=ECP/100.	A1444
C	ETRPC=EIRP/100.	A1445
C	WELECT=ELECT/(EEP*ETRPC)	A1446
C	WELOSS=WELECT-ELECT	A1447
C	GROSS ELECT LOADING INCL PARASITIC LOSSES(MW)	A1448
C	WELECG=WELECT+PARAL	A1449
C	POWER GENERATOR-TURBINE(HP)	A1450
C	PWRTR=1341.*WELECG	A1451
C	TURBINE EFFICIENCY REQUIREMENT(PCT)	A1452
C	ENTHALPY AT STATE PT 5(BTU/LBM)	A1453
C	H5=H4-(3412.2E+03*WELECG/FLOH3)	A1454
C	CONSTRAINT FOR SAT STATE PT 5	A1455
C	H5G=HG(PCOND)	A1456
C	DH5=H5G-H5	A1457
C	QUALITY OF NH3 AT STATE PT5(PCT)	A1458
C	H5F=HF(PCOND)	A1459
C	X5=(H5-H5F)/(H5G-H5F)	A1460
C	X5P=X5*100.	A1461
C	QUALITY OF NH3 EXHAUST AT STATE PT 5S(PCT)	A1462
C	S4F=SF(T4)	A1463
C	S4G=SG(T4)	A1464
C	S4=X4F+X4*(S4G-S4F)	A1465
C	S5F=SF(T5)	A1466
C	S5G=SG(T5)	A1467
C	X5S=(S4-S5F)/(S5G-S5F)	A1468
C	X5SP=X5S*100.	A1469
C		A1470
C		A1471
C		A1472
C		A1473
C		A1474
C		A1475
C		A1476
C		A1477
C		A1478
C		A1479
C		A1480
C		A1481
C		A1482
C		A1483
C		A1484
C		A1485
C		A1486
C		A1487
C		A1488

A1489
 A1490
 A1491
 A1492
 A1493
 A1494
 A1495
 A1496
 A1497
 A1498
 A1499
 A1500
 A1501
 A1502
 A1503
 A1504
 A1505
 A1506
 A1507
 A1508
 A1509
 A1510
 A1511
 A1512
 A1513
 A1514
 A1515
 A1516
 A1517
 A1518
 A1519
 A1520
 A1521
 A1522
 A1523
 A1524
 A1525
 A1526
 A1527
 A1528
 A1529
 A1530
 A1531
 A1532
 A1533
 A1534
 A1535
 A1536

C C CONSTRAINT FOR A SAT QUALITY AT STATE PT 55
 C C DX5=X5-X5S
 C C ENTHALPY AT STATE PT 55
 C C H5S=H5F+X5S*(H5G-H5F)
 C C TURBINE EFFICIENCY CALCULATION(PCT)
 C C ETURB=(H4-H5)/(H4-H5S)
 C C ETURBP=ETURB*100.
 C C COST OF NH3 TURBINE- GENERATOR(\$)
 C C FPF=1.447
 C C DF=2.0
 C C CTURB=(0.375+(WELECG*1000.)/(136000*DF))*FPF*2.42E+06
 C C CGEN=(WELECG*.023+.3)*1.21E+06
 C C CELECT=CGEN+CTURB
 C C *****
 C C *
 C C * CONDENSER SECTION *
 C C *
 C C *
 C C *****
 C C AMOUNT OF HEAT REJECTION(BTU/HR OR MW)
 C C QC=FLONH3*(H5-H1)
 C C CMIN FOR CONDENSER(BTU/HR.F)
 C C CPSWC=CPSW(TBLKC)
 C C CMINC=FLOCP*CPSWC
 C C COND SW OUTLET TEMP(F OR C)
 C C TCOC=TCIC+QC/CMINC
 C C TOTAL NUMBER OF CONDENSER TUBES
 C C RHOSWC=RHOSW(TBLKC)
 C C TNCT=4.*FLOCP/(3600.*RHOSWC*PIE*TDICC**2*VSWC)
 C C

A1537
 A1538
 A1539
 A1540
 A1541
 A1542
 A1543
 A1544
 A1545
 A1546
 A1547
 A1548
 A1549
 A1550
 A1551
 A1552
 A1553
 A1554
 A1555
 A1556
 A1557
 A1558
 A1559
 A1560
 A1561
 A1562
 A1563
 A1564
 A1565
 A1566
 A1567
 A1568
 A1569
 A1570
 A1571
 A1572
 A1573
 A1574
 A1575
 A1576
 A1577
 A1578
 A1579
 A1580
 A1581
 A1582
 A1583
 A1584

C TUBE SHEET DIAMETER(FT)
 C
 C TUBE PROFILE - STAGGERED
 C
 IF (PROF.EQ.2.) GO TO 710
 CHT=CPR*TDCC*0.5
 CBASE=CPR*TDCC*0.866
 CTAREA=CHT*CBASE*2.
 SNC=2.*CHT
 GO TO 720
 C CONTINUE
 C
 C 710
 C TUBE PROFILE - IN-LINE
 C
 CPLONG=CPR*TDCC
 CPLAT=CPR*TDCC
 CTAREA=CPLONG*CPLAT
 C CONTINUE
 CAREA=CTAREA*TNCT
 TSDC=((4.*CAREA/PIE)*0.5)/12.
 C
 C LOG MEAN TEMP DIFFERENCE OF CONDENSER(F OR C)
 C
 CLMTD=((T1-TCOC)-(T1-TCIC))/ALDG((T1-TCOC)/(T1-TCIC))
 C
 C COND SW AVG BULK TEMP(F)
 C
 RTBLKC=(TCOC+TCIC)/2.
 C
 C TEST FOR SAT TBLKC
 C
 DBLKTC=ABS(TBLKC-RTBLKC)
 SCALBC=ABS(TBLKC)
 IF (SCALBC.LT.0.1) SCALBC=0.1
 DELBC=DBLKTC/SCALBC
 IF (DELBC.LT.0.001) GO TO 730
 TBLKC=RTBLKC
 GO TO 620
 C CONTINUE
 TBLKC=RTBLKC
 TBLKCR=TBLKC*459.69
 C
 C 730
 C CONDENSER CONDUCTANCE(BTU/HR.F)
 C
 UAC=QC/CLMTD
 C
 C NUMBER OF TRANSFER UNITS FOR COND(NTU)
 C

C CNTU=UAC/CMINC
 C COND EFFECTIVENESS(EPSILON)
 C EPSC=1.-EXP(-CNTU)
 C INITIALLY ASSUME A TLC
 C OVERALL HEAT TRANSFER COEFFICIENT(BTU/HR.FT2.F OR W/M2)
 C INITIALLY ASSUME HTNH3
 C HTNH3C=1000.
 C CONTINUE
 C REYNOLDS NUMBER FOR COND TUBESIDE
 C (PROPERTIES EVAL AT TBULK)
 C VISSWC=VISSW(TBLKCI)
 C RHOSHR=RHOSW(TBLKCI)
 C RNSWC=3600.*RHOSHR*VSWC*TDICC/VISSWC
 C PRANDTL NUMBER FOR COND TUBESIDE
 C CPSWC=CPSW(TBLKCI)
 C TKSWC=TKSW(TBLKCI)
 C PNSWC=CPSWC*VISSWC/TKSWC
 C HEAT TRANSFER COEF FOR COND SW TUBESIDE
 C (BTU/HR.FT2.F OF W/M2)
 C IF (RNSWC.GT.2300.) GO TO 750
 C LAMINAR FLOW USING SEIDER-TATE CORRELATION(ASSUME
 C VISCOSITY(TBULK)=VISCOSITY(TWALL))
 C HTSWC=1.86*TKSWC*((RNSWC*PNSWC)**.3333)*(TDICC/TLC)**.3333/TDICC
 C GO TO 760
 C CONTINUE
 C TURBULENT FLOW USING DITTUS-BOELTER CORRELATION
 C HTSWC=.023*TKSWC*RNSWC**.8*PNSWC**.3/TDICC
 C CONTINUE
 C 750
 C FILM TEMP FOR PROPERTY EVALUATION
 C THERMAL RESISTANCES FOR SINGLE TUBE CONDUCTANCE
 C UA - OUTSIDE(BTU/HR.F)

AI585
 AI586
 AI587
 AI588
 AI589
 AI590
 AI591
 AI592
 AI593
 AI594
 AI595
 AI596
 AI597
 AI598
 AI599
 AI600
 AI601
 AI602
 AI603
 AI604
 AI605
 AI606
 AI607
 AI608
 AI609
 AI610
 AI611
 AI612
 AI613
 AI614
 AI615
 AI616
 AI617
 AI618
 AI619
 AI620
 AI621
 AI622
 AI623
 AI624
 AI625
 AI626
 AI627
 AI628
 AI629
 AI630
 AI631
 AI632

A1633
 A1634
 A1635
 A1636
 A1637
 A1638
 A1639
 A1640
 A1641
 A1642
 A1643
 A1644
 A1645
 A1646
 A1647
 A1648
 A1649
 A1650
 A1651
 A1652
 A1653
 A1654
 A1655
 A1656
 A1657
 A1658
 A1659
 A1660
 A1661
 A1662
 A1663
 A1664
 A1665
 A1666
 A1667
 A1668
 A1669
 A1670
 A1671
 A1672
 A1673
 A1674
 A1675
 A1676
 A1677
 A1678
 A1679
 A1680

C C THERMAL RESISTANCE SW(HR.F/BTU)
 C C CTR1C=1/(EFFIC*HTSWC*PIE*TDICC*TLC)
 C C THERMAL RESISTANCE FOR SW FOULING(HR.F/BTU)
 C C H1FSWC=1./SWFC
 C C CTR2C=1./((EFFIC*HTFSWC*PIE*TDICC*TLC)
 C C THERMAL RESISTANCE FOR WALL THICKNESS(HR.F/BTU)
 C C CTR3C=ALOG(TDOCC/TDICC)/(2.*PIE*TKW*TLC)
 C C THERMAL RESISTANCE FOR NH3 FOULING(HR.F/BTU)
 C C (CONSIDERED NEGLIGIBLE)
 C C THERMAL RESISTANCE FOR NH3(HR.F/BTU)
 C C CTR5C=1./((FFOC*HTNH3C*PIE*TD0CC*TLC)
 C C HEAT TRANSFERED PER TUBE(BTU/HR)
 C C QCT=(T1-TBLKC)/(CTR1C+CTR2C+CTR3C+CTR5C)
 C C TUBE SIDE WALL TEMP(F)
 C C CTW1=TBLKC+QCT*(CTR1C+CTR2C)
 C C SHELLSIDE WALL TEMP(F)
 C C CTW2=TBLKC+QCT*(CTR1C+CTR2C+CTR3C)
 C C COND FILM TEMP CALCULATION(F)
 C C CFT=(CTW2+T1)/2.
 C C CONDENSER DELTA T TEMP(F)
 C C DELTAC=T1-CTW2
 C C CONO SHELLSIDE HEAT TRANSFER COEF(BTU/HR.FT2.F OR W/M2)
 C VSNH3C=VSNH3(CFT)
 C RONH3C=RFNH3(CFT)
 C TKNH3C=TKNH3(CFT)
 C

```

C C REYNOLDS NUMBER(PSEUDO-HORIZ COND)
WC=FLONH3/TNCT
RNH3CH=2.*WC/(TLC*VSNH3C)
C C REYNOLDS NUMBER(PSEUDO-VERT COND) REF:MCADANS
RNH3CV=4.*WC/(PIE*TDCC*VSNH3C)
C C CONDENSER TYPE IDENTIFICATION
C C TYPEC=1 HORIZONTAL CONDENSER
C C TYPEC=2 VERTICAL CONDENSER
C C IF (TYPEC.GT.1.) GO TO 780
C C HORIZONTAL TYPE CONDENSER
C C IF (RNH3CH.GT.2100.) GO TO 770
C C LAMINAR FLOW USING NUSSELT CORRELATION
HMH3CR=.95*{(3600.**2*TKNH3C**3*RONH3C**2*G*TLC)/(VSNH3C*WC)**.33
133
GO TO 800
CONTINUE
C C TURBULENT FLOW USING NUSSELT CORR MOD BY MCADAMS
HMH3CR=1.045*{(3600.**2*TKNH3C**3*RONH3C**2*G*TLC)/(VSNH3C*WC)**.
1333
GO TO 800
CONTINUE
C C VERTICAL TYPE CONDENSER
C C IF (RNH3CV.GT.1800.) GO TO 790
C C LAMINAR FLOW USING NUSSELT CORR MOD BY MCADAMS
CORRF=1.28
HMH3CR=CORRF*1.47*(VSNH3C**2/(3600.**2*TKNH3C**3*RONH3C**2*G)**(-
1.3333)*RNH3CV**(-.3333)
GO TO 800
CONTINUE
C C TURBULENT FLOW USING KIRKBRIDE CORRELATION
HMH3CR=.0077*(VSNH3C**2/(3600.**2*TKNH3C**3*RONH3C**2*G)**(-.3333

```

```

A1681
A1682
A1683
A1684
A1685
A1686
A1687
A1688
A1689
A1690
A1691
A1692
A1693
A1694
A1695
A1696
A1697
A1698
A1699
A1700
A1701
A1702
A1703
A1704
A1705
A1706
A1707
A1708
A1709
A1710
A1711
A1712
A1713
A1714
A1715
A1716
A1717
A1718
A1719
A1720
A1721
A1722
A1723
A1724
A1725
A1726
A1727
A1728

```

A1729
 A1730
 A1731
 A1732
 A1733
 A1734
 A1735
 A1736
 A1737
 A1738
 A1739
 A1740
 A1741
 A1742
 A1743
 A1744
 A1745
 A1746
 A1747
 A1748
 A1749
 A1750
 A1751
 A1752
 A1753
 A1754
 A1755
 A1756
 A1757
 A1758
 A1759
 A1760
 A1761
 A1762
 A1763
 A1764
 A1765
 A1766
 A1767
 A1768
 A1769
 A1770
 A1771
 A1772
 A1773
 A1774
 A1775
 A1776

```

1)*HMH3CV**0.4
C CONTINUE
C TEST FOR SAT HTNH3C
DHNH3C=ABS(HNH3CR-HTNH3C)
SCALC=ABS(HNH3CRI)
IF (SCALC.LT.0.1) SCALC=0.1
DEL C=DHNH3C/SCALC
IF (DEL C.LT.0.001) GO TO 810
HTNH3C=HNH3CR
GO TO 740
CONTINUE
HTNH3C=HNH3CR
C PRESSURE DROP ACROSS CONDENSER SHELLSIDE(LBF/IN2)USING
C TWO-PHASE MODEL(HOMOGENEOUS)
C MAX VELOCITY THRU MINIMUM- FLOW AREA F(TUBE PROFILE)
RONH3T=RGMH3(PCOND)
VMH3C=4.*FLONH3/(3600.*RONH3T*PIE*TSDC**2)
VMAXC=VNH3C*(SNC/(SNC-TDOC))
C REYNOLDS NUMBER FOR MAXIMUM SHELLSIDE FLOW
REMAXC=3600.*RONH3C*VMAXC*TDOC/(12.*VSNH3C)
C EMPIRICAL FRICTION FACTOR USING CORRELATION BY JAKOB
IF (PROF.EQ.2) GO TO 820
CFF=(0.25+0.118)/(SNC-TDOC)/(SNC-TDOC)**1.08*REMAXC**(-.16)
GO TO 830
CONTINUE
CFF=(0.44+10.08*SNC/TDOC)/((SNC-TDOC)/(TDOC)**(0.43+1.13*TDOC/SNC))
1*REMAXC**(-.15)
CONTINUE
C MASS VELOCITY FOR MINIMUM FREE-FLOW AREA(LBM/FT2.SEC)
IF (TYPEC.GT.1.) GO TO 840
CAF=TSDC*TL C
CL=TSDC
GO TO 850
CONTINUE
BAND=TL C
CAF=PIE*TSDC*BAND
CL=TL C
CONTINUE
850
  
```


AI777
 AI778
 AI779
 AI780
 AI781
 AI782
 AI783
 AI784
 AI785
 AI786
 AI787
 AI788
 AI789
 AI790
 AI791
 AI792
 AI793
 AI794
 AI795
 AI796
 AI797
 AI798
 AI799
 AI800
 AI801
 AI802
 AI803
 AI804
 AI805
 AI806
 AI807
 AI808
 AI809
 AI810
 AI811
 AI812
 AI813
 AI814
 AI815
 AI816
 AI817
 AI818
 AI819
 AI820
 AI821
 AI822
 AI823
 AI824

```

    CAFF=CAF*((SNC-TDOCC)/SNC)
    CGF=FLONH3/(3600.*CAFF)
  C  CALCULATION OF CONDENSER SHELLSIDE PRESSURE DROP(LBF/IN2)
  C  USING THE HOMOGENEOUS TWO-PHASE MODEL
  C
    EDC=(CPR*TDOCC-TDOCC)/12.
    VLIQC=1./RGNH3(T5)
    VAPC=1./RGNH3(PCOND)
    VAVGC=VLIQC*11.+X5*(VAPC-VLIQC)/VLIQC)
    CFRICT=(CGF*CGF**2*VAVGC*CL)/(144.*EDC*2.*GC)
    CMOM=(CGF**2*VAVGC)/(144.*GC)
    CELEV=(CGF*CL)/(144.*GC)
    DSCOND=CFRICT+CMOM+CELEV
  C  PROPERTIES AT STATE PT 1
  C
    P1=PCOND-DSCOND
    H1=HF(P1)
    TIR=TSAT(P1)
  C  TEST FOR SAT T1(DEG F)
  C
    OTEMP4=ABS(TIR-T1)
    SCAL T1=ABS(TIR)
    YF (SCAL T1-LT.0.1) SCAL T1=0.1
    DEL T4=DTEMP4/SCAL T1
    IF (DEL T4-LT.0.001) GO TO 860
    T1=TIR
    GO TO 260
  C  CONTINUE
  C  T1=TIR
  C
  C  THERMAL RESISTANCES FOR OVERALL HEAT TRANSFER COEF - U
  C  OUTSIDE(HR.FT2.F/BTU)
  C
    OUTSIDE TUBE SURFACE AREA(FT2)
    CAD=PIE*TDOCC*TLC
  C  THERMAL RESISTANCE FOR SW(HR.FT2.F/BTU)
  C
    TRIC=CAO*CTRIC
  C  THERMAL RESISTANCE FOR SW FOULING(HR.FT2.F/BTU)
  C
    TR2C=CAO*CTR2C
  C
  
```

860

C C THERMAL RESISTANCE FOR WALL THICKNESS(HR.FT2.F/BTU)
 C TR3C=CAO*CTR3C
 C C THERMAL RESISTANCE FOR NH3 FOULING(HR.FT2.F/BTU)
 C C (CONSIDERED NEGLIGIBLE)
 C C THERMAL RESISTANCE FOR NH3(HR.FT2.F/BTU)
 C C TR5C=CAO*CTR5C
 C C OVERALL HEAT TRANSFER COEF U - OUTSIDE(BTU/HR.FT2.F
 C C OR W/M2)
 C UC=1./((TR1C+TR2C+TR3C+TR5C)
 C C PSEUDO HT COEF FOR SW(BTU/HR.FT1.F OR W/M2.C)
 C HSMC=1./TR1C
 C C PSEUDO HT COEF FOR SW FOULING(BTU/HR.FT2.F OR W/M2.C)
 C HFSWC=1./TR2C
 C C PSEUDO HT COEF FOR WALL THICK(BTU/HR.FT2.F OF W/M2.C)
 C HMC=1./TR3C
 C C PSEUDO HT COEF FOR NH3(BTU/HR.FT2.F OR W/M2.C)
 C HNH3C=1./TR5C
 C C TOTAL CONDENSER HEAT TRANSFER AREA(FT2 OR M2)
 C C THTAC=CN*CM*INC/UC
 C C REVISED CONDENSER TUBE LENGTH(FT)
 C C TLCCR=THTAC/(PIE*TD*CC*TNCT)
 C C CONSTRAINT FOR A SAT TUBE LENGTH
 C C DTLC=TLC-TLCCR
 C C COST OF CONDENSER UNIT(\$)
 C C IF (TSDC.GT.35.) GO TO 910
 C

AI825
 AI826
 AI827
 AI828
 AI829
 AI830
 AI831
 AI832
 AI833
 AI834
 AI835
 AI836
 AI837
 AI838
 AI839
 AI840
 AI841
 AI842
 AI843
 AI844
 AI845
 AI846
 AI847
 AI848
 AI849
 AI850
 AI851
 AI852
 AI853
 AI854
 AI855
 AI856
 AI857
 AI858
 AI859
 AI860
 AI861
 AI862
 AI863
 AI864
 AI865
 AI866
 AI867
 AI868
 AI869
 AI870
 AI871
 AI872

CC	CONDENSER TUBE SHEET DIAMETER(10-35)FT	AI873
CC	DRILLING TIME/TUBE SHELL THICK(MIN/IN)	AI874
CC	DTC=0.66*(TDOC-.5)	AI875
CC	THICKNESS OF TUBE SHEET(IN)	AI876
CC	TTSC=0.56*TSDC**0.68	AI877
CC	TUBE SHEET LABOR COSTS(\$)	AI878
CC	CTSLC=156695.*(TNCT/9630.)*(DTC/0.66)*(TTSC/4.0)	AI879
CC	TUBE SHEET MATERIAL COST(\$)	AI880
CC	CTSMC=189.486*TSDC**2.3	AI881
CC	IF (TMAFL.EQ.1.) GO TO 870	AI882
CC	TUBE MATERIAL COST(\$)	AI883
CC	CTMC=(C1*TLC+C2)*TNCT*(TDOC/1.5)	AI884
CC	TUBE INSTALLATION COST(\$)	AI885
CC	CTIC=34.*TNCT*TDOC**0.7	AI886
CC	GO TO 880	AI887
CC	CONTINUE	AI888
CC	TUBE MATERIAL COST(\$)	AI889
CC	CTMC=(C1*TLC+C2)*TNCT*(TDOC/1.5)*(1.+(1.+AINT/100.))**10+(1.+AINT/100.))**20)	AI890
CC	TUBE INSTALLATION COST(\$)	AI891
CC	CTIC=34.*TNCT*TDOC**0.7	AI892
CC	GO TO 880	AI893
CC	CONTINUE	AI894
CC	TUBE MATERIAL COST(\$)	AI895
CC	CTMC=(C1*TLC+C2)*TNCT*(TDOC/1.5)*(1.+(1.+AINT/100.))**10+(1.+AINT/100.))**20)	AI896
CC	TUBE INSTALLATION COST(\$)	AI897
CC	CTIC=34.*TNCT*TDOC**0.7	AI898
CC	GO TO 880	AI899
CC	CONTINUE	AI900
CC	TUBE MATERIAL COST(\$)	AI901
CC	CTMC=(C1*TLC+C2)*TNCT*(TDOC/1.5)*(1.+(1.+AINT/100.))**10+(1.+AINT/100.))**20)	AI902
CC	TUBE INSTALLATION COST(\$)	AI903
CC	CTIC=34.*TNCT*TDOC**0.7*(1.+(1.+AINT/100.))**10+(1.+AINT/100.))**20)	AI904
CC	CONTINUE	AI905
CC	TUBE MATERIAL COST(\$)	AI906
CC	CTMC=(C1*TLC+C2)*TNCT*(TDOC/1.5)*(1.+(1.+AINT/100.))**10+(1.+AINT/100.))**20)	AI907
CC	TUBE INSTALLATION COST(\$)	AI908
CC	CTIC=34.*TNCT*TDOC**0.7*(1.+(1.+AINT/100.))**10+(1.+AINT/100.))**20)	AI909
CC	CONTINUE	AI910
CC	HEAT EXCH SHELL COST(\$)	AI911
CC	CHSC=177265.*(TLC+6.)/31.*(TSDC/18.1)**2	AI912
CC	NH3 DIST PLATE AND BAFFLES COST(\$)	AI913
CC	CDPBC=1.539E-02*DTC*TNCT*TSDC**2	AI914
CC	BUSTLE, FLANGES, CHANNELS AND FLOW PLATES COST(\$)	AI915
CC		AI916
CC		AI917
CC		AI918
CC		AI919
CC		AI920

AI922
 AI923
 AI924
 AI925
 AI926
 AI927
 AI928
 AI929
 AI930
 AI931
 AI932
 AI933
 AI934
 AI935
 AI936
 AI937
 AI938
 AI939
 AI940
 AI941
 AI942
 AI943
 AI944
 AI945
 AI946
 AI947
 AI948
 AI949
 AI950
 AI951
 AI952
 AI953
 AI954
 AI955
 AI956
 AI957
 AI958
 AI959
 AI960
 AI961
 AI962
 AI963
 AI964
 AI965
 AI966
 AI967
 AI968

C CBFCFC=1185.286*TSDC**2
 C HEAT EXCH HEAD COST(\$)
 C CHC=53240.*(TSDC/18.)**3
 C WATER INLETS,NOZZLES AND SUPPORTS COST(\$)
 C CHINSC=10106.475*TSDC
 C TUBE WELDING COST(\$)
 C CTWC=0.0
 C IF (TMATL.EQ.1.) GO TO 900
 C IF (TNCT.GT.36000.) GO TO 890
 C CTWC=14.73*TNCT**1.03*(TDOC/1.5)**0.7
 C GO TO 900
 C CONTINUE
 C CTWC=0.8797*TNCT**1.3*(TDOC/1.5)**0.7
 C CONTINUE
 C CCOND=((CTSLC+CTSMC+CTMC+CTIC+CHSC+CDPBC+CBFCFC+CHC+CWINSC+CTWC)
 C GO TO 980
 C CONTINUE
 890
 900 C CONDENSER TUBE SHEET DIAMETER(35-50)FT
 910 C DRILLING TIME/TUBE SHELL THICKNESS(MIN/IN)
 C DTC=0.66*(TDOC-0.5)
 C THICKNESS OF TUBE SHEET(IN)
 C TTSC=0.56*TSDC**0.68
 C TUBE SHEET MATERIAL AND LABOR COST(\$)
 C IF (TMATL.EQ.1.) GO TO 920
 C CTSLC=55.189*TNCT**0.791*TSDC**0.68*DTC
 C CTSMC=29.566*TSDC**2.014*TTSC
 C GO TO 930
 C CONTINUE
 C CTSLC=73.81*TNCT**0.791*TSDC**0.68*DTC
 C CTSMC=354.3*TSDC**1.61*TTSC
 C CONTINUE
 C IF (TMATL.EQ.1.) GO TO 940
 920 C TUBE MATERIAL COST(\$)
 930 C
 C

A1969
 A1970
 A1971
 A1972
 A1973
 A1974
 A1975
 A1976
 A1977
 A1978
 A1979
 A1980
 A1981
 A1982
 A1983
 A1984
 A1985
 A1986
 A1987
 A1988
 A1989
 A1990
 A1991
 A1992
 A1993
 A1994
 A1995
 A1996
 A1997
 A1998
 A1999
 A2000
 A2001
 A2002
 A2003
 A2004
 A2005
 A2006
 A2007
 A2008
 A2009
 A2010
 A2011
 A2012
 A2013
 A2014
 A2015
 A2016

C CTMC=(C1*TLC+C2)*TNCT*(TDOC/1.5)
 C TUBE INSTALLATION COST(\$)
 C
 940 C TIC=36.542*TNCT*TDOC**0.7
 C GO TO 950
 C CONTINUE
 C TUBE MATERIAL COST(\$)
 C
 C CTMC=(C1*TLC+C2)*TNCT*(TDOC/1.5)*(1.+(1.+AINT/100.))**10+(1.+AINT/1
 C 100.))**20)
 C TUBE INSTALLATION COST(\$)
 C
 950 C TIC=36.542*TNCT*TDOC**0.7*(1.+(1.+AINT/100.))**10+(1.+AINT/100.))**
 C 120)
 C CONTINUE
 C HEAT EXCH SHELL COST(\$)
 C
 C CHSC=12.544*(TLC+6.)*TSDC**2.06
 C NH3 DIST PLATE AND BAFFLES COST(\$)
 C
 C CDPBC=9.8252*TNCT**0.978*DTC
 C BUSTLE, FLANGES, CHANNELS AND FLOW PLATES COST(\$)
 C
 C CBFCFC=383.824*TSDC**2.184
 C HEAT EXCH HEAD COST(\$)
 C
 C CHC=938.62*TSDC**1.43
 C WATER INLET, NOZZLES AND SUPPORTERS COST(\$)
 C
 C CHINSC=7453.6*TSDC**1.056
 C TUBE WELDING COST(\$)
 C
 C CTWC=0.0
 C IF (TMATL.EQ.1.) GO TO 970
 C IF (TNCT.GT.36000.) GO TO 960
 C CTWC=14.73*TNCT**1.03*(TDOC/1.5)**0.7
 C GO TO 970
 C CONTINUE
 960

A21113
 A21114
 A21115
 A21116
 A21117
 A21118
 A21119
 A21120
 A21121
 A21122
 A21123
 A21124
 A21125
 A21126
 A21127
 A21128
 A21129
 A21130
 A21131
 A21132
 A21133
 A21134
 A21135
 A21136
 A21137
 A21138
 A21139
 A21140
 A21141
 A21142
 A21143
 A21144
 A21145
 A21146
 A21147
 A21148
 A21149
 A21150
 A21151
 A21152
 A21153
 A21154
 A21155
 A21156
 A21157
 A21158
 A21159
 A21160

IDOCCC=25.4*IDOC
 TDOECC=25.4*IDOE
 THIEC=5.*(THIE-32.1)/9.
 THOEC=5.*(THOE-32.1)/9.
 THTACC=9.2903E-02*THTAC
 THAE=9.2903E-02*THTAE
 TKWC=1.7370*TKW
 ILCC=.3048*ILC
 ILCPC=.3048*ILCP
 ILECC=.3048*ILE
 ILLHPC=.3048*ILLHP
 ILLNHPC=.3048*ILLNH3P
 ILSDC=0.3048*ISDC
 TSDECC=0.3048*TSDE
 TTCC=25.4*TT
 TTTEC=25.4*TTTE
 UCC=5.6782*UC
 VSMCC=.3048*VSMC
 VSMWEC=.3048*VSMWE
 VSMWPC=.3048*VSMWCP
 VSMWHP=.3048*VSMWHP

C SUMMARY OF INPUT/OUTPUT DATA

WRITE (6,1720)
 IF (TYPE.EQ.2.) GO TO 990
 WRITE (6,1730)
 GO TO 1000
 CONTINUE
 WRITE (6,1740)
 CONTINUE
 WRITE (6,1750)
 WRITE (6,1760)
 WRITE (6,1770)
 WRITE (6,1780)
 WRITE (6,1790)
 WRITE (6,1800)
 WRITE (6,1810)
 WRITE (6,1820)
 WRITE (6,1830)
 WRITE (6,1840)
 WRITE (6,1850)
 WRITE (6,1860)
 WRITE (6,1870)
 WRITE (6,1880)
 IF (TMA.TL.EQ.2.) GO TO 1010
 WRITE (6,1890)
 QEC
 FLOHP, FLOHPC
 FLOHE, FLOHEC
 THOE, THOEC
 FLONH3, FLONH3C
 PEVAP, PEVAPC
 T3A, T3AC
 T3B, T3BC
 X3P
 DSEVAP, DSEVPC
 TDOE, TDOECC
 TTEC, TTECC
 TLER, TLERC

A2161
A2162
A2163
A2164
A2165
A2166
A2167
A2168
A2169
A2170
A2171
A2172
A2173
A2174
A2175
A2176
A2177
A2178
A2179
A2180
A2181
A2182
A2183
A2184
A2185
A2186
A2187
A2188
A2189
A2190
A2191
A2192
A2193
A2194
A2195
A2196
A2197
A2198
A2199
A2200
A2201
A2202
A2203
A2204
A2205
A2206
A2207
A2208

```

1010 GO TO 1020
      CONTINUE
      WRITE (6,1900)
1020 CONTINUE
      IF (PROF.EQ.2.) GO TO 1030
      WRITE (6,1910)
      GO TO 1040
1030 CONTINUE
      WRITE (6,1920)
1040 CONTINUE
      WRITE (6,1930) EPR
      IF (HFE.EQ.2.) GO TO 1050
      WRITE (6,1940)
      GO TO 1060
1050 CONTINUE
      WRITE (6,1950)
1060 CONTINUE
      WRITE (6,1960) VSWE, VSWEC
      WRITE (6,1970) ETW2, ETW2C
      WRITE (6,1980) EFT, EFTC
      WRITE (6,1990) DELTAE, DELTEC
      WRITE (6,2000) ELMTD, ELMTDC
      WRITE (6,2010) ELPSE
      WRITE (6,2020) ENTU
      WRITE (6,2030) UE, UEC
      WRITE (6,2040) HSWE, HSWEC
      WRITE (6,2050) HFSWE, HFSWEC
      WRITE (6,2060) HWE, HWEC
      WRITE (6,2070) HNH3E, HNH3EC
      WRITE (6,2080) THTAE, THTAEC
      WRITE (6,2090) TSDE, TSDEC
      WRITE (6,2100) TNET
      WRITE (6,2110) DEVAP, DEVAPC
      WRITE (6,2120) P3, P3C
      WRITE (6,2130) T4, T4C
      WRITE (6,2140) X4P
      WRITE (6,2150) DSDEM, DSDEMC
      IF (TYPEC.EQ.2.) GO TO 1070
      WRITE (6,2170)
      GO TO 1080
1070 CONTINUE
      WRITE (6,2180) QC, QCC
1080 CONTINUE
      WRITE (6,2190) FLOCPC, FLOCPC
      WRITE (6,2200) IT7C, IT7CC
      WRITE (6,2210) TCOC, TCOC
      WRITE (6,2220)

```

A22109
 A22110
 A22111
 A22112
 A22113
 A22114
 A22115
 A22116
 A22117
 A22118
 A22119
 A22120
 A22121
 A22122
 A22123
 A22124
 A22125
 A22126
 A22127
 A22128
 A22129
 A22130
 A22131
 A22132
 A22133
 A22134
 A22135
 A22136
 A22137
 A22138
 A22139
 A22140
 A22141
 A22142
 A22143
 A22144
 A22145
 A22146
 A22147
 A22148
 A22149
 A22150
 A22151
 A22152
 A22153
 A22154
 A22155
 A22156

WRITE (6, 2230) FLONH3, FLNH3C
 WRITE (6, 2240) PCOND, PCOND
 WRITE (6, 2250) T5, T5C
 WRITE (6, 2260) T1, T1C
 WRITE (6, 2270) DSCOND, DSCOND
 WRITE (6, 2280) TDOC, TDOCCC
 WRITE (6, 2290) TTC, TTCC
 WRITE (6, 2300) TCR, TCR
 IF (TMA TL EQ 2.) GO TO 1090
 WRITE (6, 2320)
 GO TO 1100
 CONTINUE
 WRITE (6, 2330)
 CONTINUE
 IF (PROF EQ 2.) GO TO 1110
 WRITE (6, 2340)
 GO TO 1120
 CONTINUE
 WRITE (6, 2350)
 CONTINUE
 WRITE (6, 2360) CPR
 IF (EHFC EQ 2.) GO TO 1130
 WRITE (6, 2370)
 GO TO 1140
 CONTINUE
 WRITE (6, 2380)
 CONTINUE
 WRITE (6, 2390) VSWC, VSWCC
 WRITE (6, 2400) CTW2, CTW2C
 WRITE (6, 2410) CFT, CFTC
 WRITE (6, 2420) DELTAC, DELTCC
 WRITE (6, 2430) CLMTD, CLMTDC
 WRITE (6, 2440) EPSC
 WRITE (6, 2450) CNUTU
 WRITE (6, 2460) UC, UCC
 WRITE (6, 2470) HSWC, HSWCC
 WRITE (6, 2480) HFSWC, HFSWCC
 WRITE (6, 2490) HWC, HWC
 WRITE (6, 2500) HNH3C, HNH3CC
 WRITE (6, 2510) THTAC, THTACC
 WRITE (6, 2520) TSDC, TSDCC
 WRITE (6, 2530) TNC
 WRITE (6, 2540) DCOND, DCOND
 WRITE (6, 2550) DIMP, DIMPC
 WRITE (6, 2560) TLHP, TLHPC
 WRITE (6, 2570) VSMHP, VSMHPC
 WRITE (6, 2580)

1150	WRITE	(6,3070)	PWRCP, PWRCPM	A2305
1160	WRITE	(6,3080)	PWRNP, PWRNPM	A2306
1170	WRITE	(6,3090)	PWRRP, PWRRM	A2307
1180	WRITE	(6,3100)	ELECT	A2308
1190	WRITE	(6,3110)	PPPP	A2309
1200	WRITE	(6,3120)	TCE	A2310
1210	WRITE	(6,3130)		A2311
	WRITE	(6,3140)	CEVAP	A2312
	WRITE	(6,3150)	CCOND	A2313
	WRITE	(6,3160)	CTURB	A2314
	WRITE	(6,3170)	CGEN	A2315
	WRITE	(6,3180)	CCSWP	A2316
	WRITE	(6,3190)	CNH3P	A2317
	WRITE	(6,3200)	CNH3RP	A2318
	WRITE	(6,3210)		A2319
	WRITE	(6,3220)		A2320
	WRITE	(6,3230)	OBJ	A2321
	WRITE	(6,3240)	CPKW	A2322
	WRITE	(6,3250)		A2323
	RETURN			A2324
1220	FORMAT	(1H,19X,21H) INITIAL DESIGN VALUES)		A2325
1230	FORMAT	(1H,2X,21H) HEVAPORATOR - HORIZONTAL)		A2326
1240	FORMAT	(1H,2X,21H) HEVAPORATOR - VERTICAL)		A2327
1250	FORMAT	(1H,4X,9H) TUBE O.D., 7X, F8.3, 4H(IN), 12X, F8.3, 4H(MM)		A2328
1260	FORMAT	(1H,4X,9H) TUBE LENGTH, 5X, F8.3, 6H(FT/S), 10X, F8.3, 5H(M/S)		A2329
1270	FORMAT	(1H,4X,11H) TUBE VEL, 5X, F8.3, 6H(FT/S), 10X, F8.3, 5H(M/S)		A2330
1280	FORMAT	(1H,4X,13H) OPER PRESSURE, 3X, F8.3, 9H(LBF/IN ²), 7X, F8.3, 5H(MPA)		A2331
1290	FORMAT	(1H,4X,24H) TUBE MATERIAL - ALUMINUM, //, 6X, 15HTHERMAL COND(K)		A2332
1300	FORMAT	(1H,4X,24H) TUBE MATERIAL - ALUMINUM, //, 6X, 15HTHERMAL COND(K)		A2333
1310	FORMAT	(1H,4X,24H) TUBE MATERIAL - TITANIUM, //, 6X, 15HTHERMAL COND(K)		A2334
1320	FORMAT	(1H,4X,37H) TUBE PROFILE - STAGGERED EQUI-LATERAL)		A2335
1330	FORMAT	(1H,4X,33H) TUBE PROFILE - IN-LINE EQUI-SIDED)		A2336
1340	FORMAT	(1H,4X,6X,11H) PITCH RATIO, 6X, F5.2)		A2337
1350	FORMAT	(1H,4X,24H) TUBE MATERIAL - ALUMINUM, //, 6X, 15HTHERMAL COND(K)		A2338
1360	FORMAT	(1H,4X,24H) TUBE MATERIAL - TITANIUM, //, 6X, 15HTHERMAL COND(K)		A2339
	FORMAT	(1H,4X,24H) TUBE MATERIAL - ALUMINUM, //, 6X, 15HTHERMAL COND(K)		A2340
	FORMAT	(1H,4X,24H) TUBE MATERIAL - TITANIUM, //, 6X, 15HTHERMAL COND(K)		A2341
	FORMAT	(1H,4X,24H) TUBE MATERIAL - ALUMINUM, //, 6X, 15HTHERMAL COND(K)		A2342
	FORMAT	(1H,4X,24H) TUBE MATERIAL - TITANIUM, //, 6X, 15HTHERMAL COND(K)		A2343
	FORMAT	(1H,4X,24H) TUBE MATERIAL - ALUMINUM, //, 6X, 15HTHERMAL COND(K)		A2344
	FORMAT	(1H,4X,24H) TUBE MATERIAL - TITANIUM, //, 6X, 15HTHERMAL COND(K)		A2345
	FORMAT	(1H,4X,24H) TUBE MATERIAL - ALUMINUM, //, 6X, 15HTHERMAL COND(K)		A2346
	FORMAT	(1H,4X,24H) TUBE MATERIAL - TITANIUM, //, 6X, 15HTHERMAL COND(K)		A2347
	FORMAT	(1H,4X,24H) TUBE MATERIAL - ALUMINUM, //, 6X, 15HTHERMAL COND(K)		A2348
	FORMAT	(1H,4X,24H) TUBE MATERIAL - TITANIUM, //, 6X, 15HTHERMAL COND(K)		A2349
	FORMAT	(1H,4X,24H) TUBE MATERIAL - ALUMINUM, //, 6X, 15HTHERMAL COND(K)		A2350
	FORMAT	(1H,4X,24H) TUBE MATERIAL - TITANIUM, //, 6X, 15HTHERMAL COND(K)		A2351
	FORMAT	(1H,4X,24H) TUBE MATERIAL - ALUMINUM, //, 6X, 15HTHERMAL COND(K)		A2352

1370	13H(8TU/HR.FT.FI)3X,F8.3,7H(W/M.CI)	A2353
1380	FORMAT ((IHO,4X,33HTUBE PROFILE - STAGGERED EQUI-LATERAL)	A2354
1390	FORMAT ((IHO,4X,33HTUBE PROFILE - IN-LINE EQUI-SIDED)	A2355
1400	FORMAT ((IHO,6X,11HPITCH RATIO,6X,F5.2)	A2356
1410	FORMAT ((IHO,4X,24HENHANCEMENT - PLAIN TUBE)	A2357
1420	FORMAT ((IHO,4X,19HSALT WATER HOT PIPE)	A2358
1430	FORMAT ((IHO,4X,9HPIPE I.D.,7X,F8.3,4H(FT),12X,F8.3,3H(M))	A2359
1440	FORMAT ((IHO,4X,11HPIPE LENGTH,5X,F8.3,4H(FT/S),10X,F8.3,5H(M/S))	A2360
1450	FORMAT ((IHO,4X,11HPIPE LENGTH,5X,F8.3,4H(FT/S),10X,F8.3,5H(M/S))	A2361
1460	FORMAT ((IHO,4X,13HSM INLET TEMP,3X,F8.3,7H(DEG F),9X,F8.3,7H(DEG C	A2362
	1))	A2363
1470	FORMAT ((IHO,4X,12HSM SALINITY,7X,F5.0,1X,5H0/000)	A2364
1480	FORMAT ((IHO,2X,20HSALT WATER COLD PIPE)	A2365
1490	FORMAT ((IHO,4X,9HPIPE I.D.,7X,F8.3,4H(FT),12X,F8.3,3H(M))	A2366
1500	FORMAT ((IHO,4X,11HPIPE LENGTH,5X,F8.3,4H(FT),12X,F8.3,3H(M))	A2367
1510	FORMAT ((IHO,4X,11HPIPE LENGTH,5X,F8.3,4H(FT/S),10X,F8.3,5H(M/S))	A2368
1520	FORMAT ((IHO,4X,13HSM INLET TEMP,3X,F8.3,7H(DEG F),9X,F8.3,7H(DEG C	A2369
	1))	A2370
1530	FORMAT ((IHO,4X,12HSM SALINITY,7X,F5.0,1X,5H0/000)	A2371
1540	FORMAT ((IHO,2X,17HAMMONIA CIRC PIPE)	A2372
1550	FORMAT ((IHO,4X,9HPIPE I.D.,7X,F8.3,4H(FT),12X,F8.3,3H(M))	A2373
1560	FORMAT ((IHO,4X,11HPIPE LENGTH,5X,F8.3,4H(FT),12X,F8.3,3H(M))	A2374
1570	FORMAT ((IHO,2X,20HAMMONIA RE-FLUX PIPE)	A2375
1580	FORMAT ((IHO,4X,9HPIPE I.D.,7X,F8.3,4H(FT),12X,F8.3,3H(M))	A2376
1590	FORMAT ((IHO,4X,11HPIPE LENGTH,5X,F8.3,4H(FT),12X,F8.3,3H(M))	A2377
1600	FORMAT ((IHO,2X,29HPUMP AND GEN - TURB PERFORMANCE)	A2378
1610	FORMAT ((IHO,4X,12HEVAP SW PUMP)	A2379
1620	FORMAT ((IHO,6X,10HEFFICIENCY,1X,4HMECH,2X,F5.2,5H(PCT),7X,5HMOTOR,	A2380
	1X,F5.2,5H(PCT))	A2381
1630	FORMAT ((IHO,4X,12HCOND SW PUMP)	A2382
1640	FORMAT ((IHO,6X,10HEFFICIENCY,1X,4HMECH,2X,F5.2,5H(PCT),7X,5HMOTOR,	A2383
	1X,F5.2,5H(PCT))	A2384
1650	FORMAT ((IHO,4X,17HAMMONIA CIRC PUMP)	A2385
1660	FORMAT ((IHO,6X,10HEFFICIENCY,1X,4HMECH,2X,F5.2,5H(PCT),7X,5HMOTOR,	A2386
	1X,F5.2,5H(PCT))	A2387
1670	FORMAT ((IHO,21MGEN-TURB EFFICIENCIES)	A2388
1680	FORMAT ((IHO,6X,14HGEN MECH,8X,F5.2,5H(PCT))	A2389
1690	FORMAT ((IHO,6X,9HTURB MECH,8X,F5.2,5H(PCT))	A2390
1700	FORMAT ((IHO,2X,18HPower REQUIREMENT)	A2391
1710	FORMAT ((IHO,4X,16HPNET POWER OUTPUT,10X,F8.3,4H(MW))	A2392
1720	FORMAT ((IHO,19HOPTIMIZATION VALUES)	A2393
1730	FORMAT ((IHO,2X,23HEVAPORATOR - HORIZONTAL)	A2394
1740	FORMAT ((IHO,2X,21HEVAPORATOR - VERTICAL)	A2395
1750	FORMAT ((IHO,4X,9HHT ABSORB,1X,F14.1,8H(8TU/HR),7X,F8.3,4H(MW))	A2396
1760	FORMAT ((IHO,4X,7HSM FLOW,3X,F14.1,8H(8TU/HR),1X,F14.1,7H(KG/HR))	A2397
1770	FORMAT ((IHO,6X,10HSM TEMP IN,4X,F8.3,7H(DEG F),8X,F8.3,7H(DEG C))	A2398
1780	FORMAT ((IHO,6X,11HSM TEMP OUT,3X,F8.3,7H(DEG F),8X,F8.3,7H(DEG C))	A2399
		A2400

1790	FORMAT	(1H0,4X,8HMH3 FLOW,2X,F14,1,8H(LBM/HR)),1X,F14,1,7H(KG/HR))	A2401
1800	FORMAT	(1H0,4X,13HOPER PRESSURE,3X,F8,3,9H(LBF/IN2)),6X,F8,3,5H(KPA	A2402
	1))		A2403
1810	FORMAT	(1H0,6X,13HEVAP SAT TEMP,1X,F8,3,7H(DEG F)),8X,F8,3,7H(DEG C	A2404
	1))		A2405
1820	FORMAT	(1H0,6X,11HOUTLET TEMP,3X,F8,3,7H(DEG F)),8X,F8,3,7H(DEG C))	A2406
1830	FORMAT	(1H0,6X,14HOUTLET QUALITY,4X,F5,2,5H(PCT)),	A2407
1840	FORMAT	(1H0,4X,14HMH3 PRESS DROP,2X,F8,3,9H(LBF/IN2)),6X,F8,3,5H(KP	A2408
	1A))		A2409
1850	FORMAT	(1H0,4X,20HTUBE CHARACTERISTICS)	A2410
1860	FORMAT	(1H0,6X,10HOUTTER DIA,4X,F8,3,4H(IN)),11X,F8,3,4H(MM))	A2411
1870	FORMAT	(1H0,6X,10HWALL THICK,4X,F8,3,4H(IN)),11X,F8,3,4H(MM))	A2412
1880	FORMAT	(1H0,6X,6HLENGTH,8X,F8,3,4H(F)),11X,F8,3,3H(M))	A2413
1890	FORMAT	(1H0,6X,19HMATERIAL - ALUMINIUM)	A2414
1900	FORMAT	(1H0,6X,19HMATERIAL - TITANIUM)	A2415
1910	FORMAT	(1H0,6X,37HTUBE PROFILE - STAGGERED EQUI-LATERAL)	A2416
1920	FORMAT	(1H0,6X,33HTUBE PROFILE - IN-LINE EQUI-SIDED)	A2417
1930	FORMAT	(1H0,8X,11HPITCH RATIO,4X,F5,2)	A2418
1940	FORMAT	(1H0,6X,24HENHANCEMENT - PLAIN TUBE)	A2419
1950	FORMAT	(1H0,6X,28HENHANCEMENT - LINDE-PROMOTER)	A2420
1960	FORMAT	(1H0,6X,11HSW VELOCITY,3X,F8,3,6H(FT/S)),9X,F8,3,5H(M/S))	A2421
1970	FORMAT	(1H0,4X,17HT WALL(SHELLSIDE)),F,3,7H(DEG F)),8X,F8,3,7H(DEG	A2422
	1C))		A2423
1980	FORMAT	(1H0,4X,9HFILM TEMP,7X,F8,3,7H(DEG F)),8X,F8,3,7H(DEG C))	A2424
1990	FORMAT	(1H0,4X,15HDELTA T BOILING,1X,F8,3,7H(DEG F)),8X,F8,3,7H(DEG	A2425
	1C))		A2426
2000	FORMAT	(1H0,4X,8HL.M.T.D.,8X,F8,3,7H(DEG F)),8X,F8,3,7H(DEG C))	A2427
2010	FORMAT	(1H0,4X,18HEVAP EFFECTIVENESS,7X,F8,3)	A2428
2020	FORMAT	(1H0,4X,20HNR OF TRANSFER UNITS,5X,F8,3)	A2429
2030	FORMAT	(1H0,4X,11HOVL HT COEF,5X,F8,2,14H(BTU/HR.FT2.F)),1X,F8,2,8H	A2430
	1(W/M2.C))		A2431
2040	FORMAT	(1H0,6X,8HH(WATER)),6X,F8,2,14H(BTU/HR.FT2.F)),1X,F8,2,8H(W/M	A2432
	12.C))		A2433
2050	FORMAT	(1H0,6X,10HH(FOULING)),4X,F8,2,14H(BTU/HR.FT2.F)),1X,F8,2,8H(A2434
	1W/M2.C))		A2435
2060	FORMAT	(1H0,6X,8HH(METAL)),6X,F8,2,14H(BTU/HR.FT2.F)),F9,2,8H(W/M2.C	A2436
	1))		A2437
2070	FORMAT	(1H0,6X,10HH(AMMONIA)),4X,F8,2,14H(BTU/HR.FT2.F)),1X,F8,2,8H(A2438
	1W/M2.C))		A2439
2080	FORMAT	(1H0,4X,10HHT SURFACE,2X,F12,2,5H(FT2)),6X,F12,2,4H(M2))	A2440
2090	FORMAT	(1H0,4X,14HTUBE SHEET DIA,2X,F8,3,4H(F)),11X,F8,3,3H(M))	A2441
2100	FORMAT	(1H0,6X,15HTOT NR OF TUBES,7X,F12,0)	A2442
2110	FORMAT	(1H0,4X,13HSW PRESS DROP,3X,F8,3,9H(LBF/IN2)),6X,F8,3,5H(KPA	A2443
	1))		A2444
2120	FORMAT	(1H0,2X,36HMOISTURE SEPARATOR-INSIDE EVAP SHELL)	A2445
2130	FORMAT	(1H0,4X,13HOPER PRESSURE,3X,F8,3,9H(LBF/IN2)),6X,F8,3,5H(KPA	A2446
	1))		A2447
2140	FORMAT	(1H0,6X,11HOUTLET TEMP,3X,F8,3,7H(DEG F)),8X,F8,3,7H(DEG C))	A2448

2150	FORMAT	(1H0,6X,14HOUTLET QUALITY,3X,F5.2,5H(PCT))	A2449
2160	FORMAT	(1H0,6X,14HCOND SAT TEMP,1X,F8.3,7H(DEG F),8X,F8.3,7H(DEG C	A2450
2170	FORMAT	(1H0,6X,14HCOND SAT TEMP,1X,F8.3,7H(DEG F),8X,F8.3,7H(DEG C)	A2451
2180	FORMAT	(1H0,6X,14HCOND SAT TEMP,1X,F8.3,7H(DEG F),8X,F8.3,7H(DEG C)	A2452
2190	FORMAT	(1H0,6X,14HCOND SAT TEMP,1X,F8.3,7H(DEG F),8X,F8.3,7H(DEG C)	A2453
2200	FORMAT	(1H0,6X,14HCOND SAT TEMP,1X,F8.3,7H(DEG F),8X,F8.3,7H(DEG C)	A2454
2210	FORMAT	(1H0,6X,14HCOND SAT TEMP,1X,F8.3,7H(DEG F),8X,F8.3,7H(DEG C)	A2455
2220	FORMAT	(1H0,6X,14HCOND SAT TEMP,1X,F8.3,7H(DEG F),8X,F8.3,7H(DEG C)	A2456
2230	FORMAT	(1H0,6X,14HCOND SAT TEMP,1X,F8.3,7H(DEG F),8X,F8.3,7H(DEG C)	A2457
2240	FORMAT	(1H0,6X,14HCOND SAT TEMP,1X,F8.3,7H(DEG F),8X,F8.3,7H(DEG C	A2458
2250	FORMAT	(1H0,6X,14HCOND SAT TEMP,1X,F8.3,7H(DEG F),8X,F8.3,7H(DEG C	A2459
2260	FORMAT	(1H0,6X,14HCOND SAT TEMP,1X,F8.3,7H(DEG F),8X,F8.3,7H(DEG C)	A2460
2270	FORMAT	(1H0,6X,14HCOND SAT TEMP,1X,F8.3,7H(DEG F),8X,F8.3,7H(DEG C)	A2461
2280	FORMAT	(1H0,6X,14HCOND SAT TEMP,1X,F8.3,7H(DEG F),8X,F8.3,7H(DEG C)	A2462
2290	FORMAT	(1H0,6X,14HCOND SAT TEMP,1X,F8.3,7H(DEG F),8X,F8.3,7H(DEG C)	A2463
2300	FORMAT	(1H0,6X,14HCOND SAT TEMP,1X,F8.3,7H(DEG F),8X,F8.3,7H(DEG C)	A2464
2310	FORMAT	(1H0,6X,14HCOND SAT TEMP,1X,F8.3,7H(DEG F),8X,F8.3,7H(DEG C)	A2465
2320	FORMAT	(1H0,6X,14HCOND SAT TEMP,1X,F8.3,7H(DEG F),8X,F8.3,7H(DEG C)	A2466
2330	FORMAT	(1H0,6X,14HCOND SAT TEMP,1X,F8.3,7H(DEG F),8X,F8.3,7H(DEG C)	A2467
2340	FORMAT	(1H0,6X,14HCOND SAT TEMP,1X,F8.3,7H(DEG F),8X,F8.3,7H(DEG C)	A2468
2350	FORMAT	(1H0,6X,14HCOND SAT TEMP,1X,F8.3,7H(DEG F),8X,F8.3,7H(DEG C)	A2469
2360	FORMAT	(1H0,6X,14HCOND SAT TEMP,1X,F8.3,7H(DEG F),8X,F8.3,7H(DEG C)	A2470
2370	FORMAT	(1H0,6X,14HCOND SAT TEMP,1X,F8.3,7H(DEG F),8X,F8.3,7H(DEG C)	A2471
2380	FORMAT	(1H0,6X,14HCOND SAT TEMP,1X,F8.3,7H(DEG F),8X,F8.3,7H(DEG C)	A2472
2390	FORMAT	(1H0,6X,14HCOND SAT TEMP,1X,F8.3,7H(DEG F),8X,F8.3,7H(DEG C)	A2473
2400	FORMAT	(1H0,6X,14HCOND SAT TEMP,1X,F8.3,7H(DEG F),8X,F8.3,7H(DEG C)	A2474
2410	FORMAT	(1H0,6X,14HCOND SAT TEMP,1X,F8.3,7H(DEG F),8X,F8.3,7H(DEG C)	A2475
2420	FORMAT	(1H0,6X,14HCOND SAT TEMP,1X,F8.3,7H(DEG F),8X,F8.3,7H(DEG C)	A2476
2430	FORMAT	(1H0,6X,14HCOND SAT TEMP,1X,F8.3,7H(DEG F),8X,F8.3,7H(DEG C)	A2477
2440	FORMAT	(1H0,6X,14HCOND SAT TEMP,1X,F8.3,7H(DEG F),8X,F8.3,7H(DEG C)	A2478
2450	FORMAT	(1H0,6X,14HCOND SAT TEMP,1X,F8.3,7H(DEG F),8X,F8.3,7H(DEG C)	A2479
2460	FORMAT	(1H0,6X,14HCOND SAT TEMP,1X,F8.3,7H(DEG F),8X,F8.3,7H(DEG C)	A2480
2470	FORMAT	(1H0,6X,14HCOND SAT TEMP,1X,F8.3,7H(DEG F),8X,F8.3,7H(DEG C)	A2481
2480	FORMAT	(1H0,6X,14HCOND SAT TEMP,1X,F8.3,7H(DEG F),8X,F8.3,7H(DEG C)	A2482
2490	FORMAT	(1H0,6X,14HCOND SAT TEMP,1X,F8.3,7H(DEG F),8X,F8.3,7H(DEG C)	A2483
2500	FORMAT	(1H0,6X,14HCOND SAT TEMP,1X,F8.3,7H(DEG F),8X,F8.3,7H(DEG C)	A2484
2510	FORMAT	(1H0,6X,14HCOND SAT TEMP,1X,F8.3,7H(DEG F),8X,F8.3,7H(DEG C)	A2485
2520	FORMAT	(1H0,6X,14HCOND SAT TEMP,1X,F8.3,7H(DEG F),8X,F8.3,7H(DEG C)	A2486


```

2900 FORMAT (1H0,4X,17HAMMONIA CIRC PUMP)
2910 FORMAT (1H0,6X,10HHEAD PRESS,4X,F8.3,4H(FT),11X,F8.3,3H(M))
2920 FORMAT (1H0,6X,8HCAPACITY,2X,F12.1,9H(GAL/MIN),2X,F12.1,9H(LIT/MIN)
1)
2930 FORMAT (1H0,6X,10HEFFICIENCY,1X,4HMECH,2X,F5.2,5H(PCT),7X,5HMOTOR,
11X,F5.2,5H(PCT))
2940 FORMAT (1H0,4X,20HAMMONIA RE-FLUX PUMP)
2950 FORMAT (1H0,6X,10HHEAD PRESS,4X,F8.3,4H(FT),11X,F8.3,3H(M))
2960 FORMAT (1H0,6X,8HCAPACITY,2X,F12.1,9H(GAL/MIN),2X,F12.1,9H(LIT/MIN)
1)
2970 FORMAT (1H0,6X,10HEFFICIENCY,1X,4HMECH,2X,F5.2,5H(PCT),7X,5HMOTOR,
11X,F5.2,5H(PCT))
2980 FORMAT (1H0,4X,21HGEN-TURB EFFICIENCIES)
2990 FORMAT (1H0,6X,14HGEN MECH&ELECT,4X,F5.2,5H(PCT))
3000 FORMAT (1H0,6X,9HTURB MECH,9X,F5.2,5H(PCT))
3010 FORMAT (1H0,6X,13HTURB INTERNAL,5X,F5.2,5H(PCT))
3020 FORMAT (1H0,4X,19HTURB OUTLET QUALITY,1X,F5.2,5H(PCT))
3030 FORMAT (1H1,2X,18HPOWER REQUIREMENTS)
3040 FORMAT (1H0,4X,14HTURB-GEN GROSS,10.3,4H(HPI),12X,F8.3,4H(MW))
3050 FORMAT (1H0,6X,17HEFFICIENCY LOSSES,21X,F8.3,4H(MW))
3060 FORMAT (1H0,4X,12HEVAP SW PUMP,4X,F8.3,4H(HPI),12X,F8.3,4H(MW))
3070 FORMAT (1H0,4X,12HCOND SW PUMP,4X,F8.3,4H(HPI),12X,F8.3,4H(MW))
3080 FORMAT (1H0,4X,13HNN3 CIRC PUMP,3X,F8.3,4H(HPI),12X,F8.3,4H(MW))
3090 FORMAT (1H0,4X,16HNN3 RE-FLUX PUMP,F8.3,4H(HPI),12X,F8.3,4H(MW))
3100 FORMAT (1H0,42X,10H)
3110 FORMAT (1H0,10X,16HNET POWER OUTPUT,18X,F8.3,4H(MW))
3120 FORMAT (1H0,2X,23HPERCENT PARASITIC POWER,10X,F5.2,5H(PCT))
3130 FORMAT (1H0,2X,29HTHE DYNAMIC CYCLE EFFICIENCY,4X,F5.2,5H(PCT))
3140 FORMAT (1H0,2X,18HCOST OF COMPONENTS)
3150 FORMAT (1H0,4X,10HEVAPORATOR,14X,F12.2,9H(DOLLARS))
3160 FORMAT (1H0,4X,9HCONDENSER,15X,F12.2,9H(DOLLARS))
3170 FORMAT (1H0,4X,11HGEN-TURBINE,13X,F12.2,9H(DOLLARS))
3180 FORMAT (1H0,4X,9HGENERATOR,15X,F12.2,9H(DOLLARS))
3190 FORMAT (1H0,4X,12HEVAP SW PUMP,12X,F12.2,9H(DOLLARS))
3200 FORMAT (1H0,4X,12HCOND SW PUMP,12X,F12.2,9H(DOLLARS))
3210 FORMAT (1H0,4X,13HNN3 CIRC PUMP,11X,F12.2,9H(DOLLARS))
3220 FORMAT (1H0,4X,16HNN3 RE-FLUX PUMP,8X,F12.2,9H(DOLLARS))
3230 FORMAT (1H0,28X,12H)
3240 FORMAT (1H0,10X,12HOPTIMUM COST,6X,F12.2,9H(DOLLARS))
3250 FORMAT (1H0,2X,22HCOST PER NET KW OUTPUT,4X,F12.2,17H(DOLLARS)
1)
END
C FUNCTION SUBROUTINES FOR SALT WATER AND AMMONIA
C
C FUNCTION RHO$W (I)
RHO$W=63.90152+.017512*T-5.684E-04*T**2+.6.336E-06*T**3-2.7949E-08*
T**4
1)

```

A2545
A2546
A2547
A2548
A2549
A2550
A2551
A2552
A2553
A2554
A2555
A2556
A2557
A2558
A2559
A2560
A2561
A2562
A2563
A2564
A2565
A2566
A2567
A2568
A2569
A2570
A2571
A2572
A2573
A2574
A2575
A2576
A2577
A2578
A2579
A2580
A2581
A2582
A2583
A2584
A2585
A2586
1
2
3
4
5
6
B
B
B
B
B
B
B

3 4 5 6-
1 2 3 4 5 6-
Y Y Y Y Z Z Z Z Z Z

FUNCTION AEC (D)
ACC=2.157473-5.206014*D+7.336678*D**2-3.656495*D**3+.7204888*D**4
RETURN
END
COND ALUMINUM TUBE COST/FT - LINDE-PROMOTER(\$/FT)
FUNCTION ACC (D)
ACC=1.799865-4.543195*D+6.56578*D**2-3.305876*D**3+.6622916*D**4
RETURN
END

C
C

LIST OF REFERENCES

1. Office of Technological Assessment, Renewable Ocean Energy Sources, Part 1 OTEC, p. 7, May 1978.
2. Claude, Georges, "Power from Tropical Sea," Mechanical Engineering, v. 52, No. 12, Dec. 1930.
3. Holman, J. P., Heat Transfer, 4th ed., p. 204-223, McGraw-Hill, 1976.
4. Tong, L. S., Boiling Heat Transfer and Two-Phase Flow, p. 76-79, Wiley, 1965.
5. Perry, J. H., and others, Chemical Engineers' Handbook, 4th ed., p. 18-82, 83, McGraw Hill, 1969.
6. Owens, W. L., "Correlation of Thin Film Evaporation Heat Transfer Coefficients for Horizontal Tubes," Proceedings of the Fifth Ocean Thermal Energy Conversion Conference, Vol 6 of 8, Miami Beach, Florida (February 20-22, 1978).
7. McAdams, W. H., Heat Transmission, 3rd ed., p. 325-343, McGraw-Hill, 1954.
8. Lorenz, J. J. and Yung, D., "Combined Boiling and Evaporation of Liquid Films on Horizontal Tubes," Proceedings of the Fifth Ocean Thermal Energy Conversion Conference, Vol 6 of 8, Miami Beach, Florida (February 20-22, 1978).
9. TRW Contract No. EG-77-C-03-1570, OTEC Power System Development Utilizing Advanced, High-Performance Heat Transfer Techniques, V. 2, p. 1-36, 30 Jan 78.
10. Streeter, V. L. and Wylie, E. B., Fluid Mechanics, 7th ed., p. 235-239, McGraw-Hill, 1979.
11. Baumeister, T., and others, Marks' Standard Handbook for Mechanical Engineers, 8th ed., p. 3-57, 58, McGraw Hill, 1978.
12. Metrek Division of the Mitre Corporation Contract No. ET-78-C-01-2854, OTEC Power System Performance Model, by H. Abelson, P. 74-81, August 1978.

13. Neuman, G. and Pierson, W. J., Jr., Principles of Physical Oceanography, Prentice-Hall, 1966.
14. Sverdrup, H. V., Johnson, M. W., and Fleming, R. H., The Oceans Their Physics, Chemistry, and General Biology, p. 1053, Prentice-Hall, 1949.
15. Westinghouse Electric Co. Contract No. EG-77-C-03-1569, Ocean Thermal Energy Conversion Power System, Phase 1: Preliminary Design, p. 9-9, 4 Dec 1978.
16. Kostors, C. H. and Vincent, S. P., "Performance Optimization of an OTEC Turbine," Proceedings of the Sixth Ocean Thermal Energy Conversion Conference, Vol 1 of 2, Washington, D.C. (June 19-22, 1979).
17. Olsen, H. L., and others, "Preliminary Considerations for the Selection of a Working Medium for the Solar Sea Power Plant," Proceedings, Solar Sea Power Plant Conference and Workshop, June 27-28, 1973.
18. Vanderplaats, G. N., COPES - A User's Manual prepared for a graduate course on "Automated Design Optimization" presented at the Naval Postgraduate School, Monterey, Calif., March-May 1977.
19. Vanderplaats, G. N., Numerical Optimization Techniques for Engineering Design, Class notes for a graduate course on "Automated Design Optimization" presented at the Naval Postgraduate School, Monterey, Calif., May 1978.
20. Vanderplaats, G. N., "The Computer for Design and Optimization," Computing in Applied Mechanics, AMD-Vol. 18, ASME Winter Annual Meeting, New York, Dec. 1976.
21. Vanderplaats, G. N., Method of Feasible Directions, Class notes for a graduate course on "Automated Design Optimization," presented at the Naval Postgraduate School, Monterey, Calif., July 1978.

INITIAL DISTRIBUTION LIST

	No. Copies
1. Defense Technical Information Center Cameron Station Alexandria, Virginia 22314	2
2. Library, Code 0142 Naval Postgraduate School Monterey, California 93940	2
3. Department Chairman, Code 69 Department of Mechanical Engineering Naval Postgraduate School Monterey, California 93940	1
4. Assoc. Professor R. H. Nunn, Code 69 Nn Department of Mechanical Engineering Naval Postgraduate School Monterey, California 93940	2
5. Asst. Professor G. H. Vanderplaats, Code 69 Me Department of Mechanical Engineering Naval Postgraduate School Monterey, California 93940	1
6. LCDR Raymond C. Schaubel 14673 Charter Oak Boulevard Salinas, California 93907	1
7. Dr. Harvey Abelson Argonne National Laboratory Washington Office Suite 185 400 N. Capitol Street, N.W. Washington, DC 20001	1
8. Mr. Gene Barsness OTEC Project Manager Westinghouse Electric Co. Lester Branch Box 9175 Philadelphia, PA 19113	1
9. Dr. James W. Connell Director, Thermal Sciences Energy Systems Division Alfa-Laval Thermal, Inc. South Deerfield, MA 01373	1

INITIAL DISTRIBUTION LIST (CONTINUED)

	No. Copies
10. Mr. Bruce E. Dawson Foster Wheeler Energy Corp. 110 South Orange Ave. Livingston, NJ 07039	1
11. Dr. Jeff Horowitz Dept. of Energy Chicago Operations Office Argonne National Laboratory 9700 South Cass Ave. Argonne, IL 60439	1
12. Mr. John Michel P.O. Box Y Bldg. 9204-1 Oak Ridge National Laboratory Oak Ridge, Tennessee 37830	1
13. Mr. Charles Rabidart Lockheed Missiles and Space Company 57-02 150 1 P.O. Box 504 Sunnyvale, CA 94088	1
14. Mr. Dan Rossard Westinghouse Electric Corp. Lester Branch Box 9175 Philadelphia, PA 19113	1
15. Mr. J. M. Shoji OTEC Project Engineer Rocketdyne, Dept. 545-113 6633 Canoga Avenue Canoga Park, CA 91304	1
16. Dr. J. E. Snyder OTEC Project Manager TRW Defense and Space Systems Group Mail Station 81/1538 One Space Park Redondo Beach, CA 90278	1
17. Dr. Jerry Taborek Heat Transfer Research, Inc. 1000 South Fremont Ave. Alhambra, CA 91802	1

INITIAL DISTRIBUTION LIST (CONTINUED)

	No. Copies
18. Mr. Lloyd Trimble OTEC Power System Development Project Manager Lockheed Missiles and Space Company 57-02 150 1 P.O. Box 504 Sunnyvale, CA 94088	1

**DAT
FILM**